9-14-2015

Understanding the Hydrological Impacts of Climate Variability and Climate Change based on Numerical Modeling and Observations

Dana Thomas Parr
University of Connecticut - Storrs, dtp08001@engr.uconn.edu

Understanding the Hydrological Impacts of Climate Variability and Climate Change based on Numerical Modeling and Observations

Dana Thomas Parr

University of Connecticut, 2015

The objective of this dissertation research is to better understand the hydrological impacts of climate variability and climate change. This objective is first addressed in a two-part study focusing on the Northeast US using the Connecticut River Basin as a case study. Changes to the hydrological cycle are investigated for the past several decades using precipitation and river discharge data from observations and soil moisture and evapotranspiration (ET) from the VIC hydrological model. From 1950-2011 a clear increase of precipitation intensity is identified, together with increasing precipitation amount, discharge, runoff ratios, and soil moisture. The ET trend is negligible. This study of the past is followed by projections of the future using the VIC model driven by a bias-corrected climate for the period of 2046-2065 from three climate models. The projected future changes that had not yet manifested in the past include enhanced ET for all four seasons and a change to the seasonality of snow melt and discharge. There are also indications of wetter winters, changing characteristics of flood events, and a consistently increasing mean intensity of precipitation which continues from the past analysis. Compared to the past, the future foods are projected to be less frequent but last longer.

Among all hydrological variable, ET is the most difficult to simulate. In this dissertation research, an innovative approach to improving the accuracy of ET estimations is developed,

which combines hydrological models with data derived from satellite remote sensing including leaf area index and ET. This model-data integration leads to a more accurate reconstruction of historic river flow and different future hydrological trends that include an increase of summer droughts.

This dissertation research also explores the mechanisms underlying the recently discovered decline of the ET trend in many regions focusing on the continental U.S. using the Community Land Model 4.5. Experimental simulations are conducted to isolate the effects of the most influential factors on ET. It is found that the changing characteristics of precipitation, precipitation amount in particular, are the primary cause of the ET trend decline. The roles of wind speed and temperature changes are found to be negligible.

Understanding the Hydrological Impacts of Climate Variability and Climate Change based on Numerical Modeling and Observations

Dana Parr

B.S., Wesleyan University, 2008

M.S., Yale University, 2009

A Dissertation

Submitted in Partial Fulfillment of the

Requirements for the Degree of

Doctor of Philosophy

at the

University of Connecticut

2015

APPROVAL PAGE

Doctor of Philosophy Dissertation

Understanding the Hydrological Impacts of Climate Variability and Climate Change based on Numerical Modeling and Observations

Presented by

Dana Parr, B.S., M.S.

Major Advisor_____

Guiling Wang

Associate Advisor_____

Emmanouil N. Anagnostou

Associate Advisor_____

Amvrossios C. Bagtzoglou

Associate Advisor_____

David Bjerklie

Associate Advisor_____

Christine Kirchhoff

University of Connecticut

2015

Acknowledgements

I would like to express my gratitude toward those who have helped and supported me in a variety of different manners during my time as a doctoral student at the University of Connecticut.

Firstly, I am deeply grateful to my advisor Guiling Wang. I am indebted to her for all that she has taught me and encouraged me to accomplish. She has been a tremendous help with continuous support and invaluable guidance in terms of my professional and personal development, and her dedication to scientific excellence has been an inspiration. I am also grateful to my committee members: Emmanouil Anagnoustou, Amvrossios Bagtzoglou, David Bjerklie, and Christine Kirchhoff for their comments, suggestions, and assistance with my dissertation research, and their various supports and being there for me when I needed them throughout different stages of my graduate study.

Secondly, I would like to thank my group members (Kazi Ahmed, Amir Erfanian, Congsheng Fu, Rui Mei, Miao Yu, Huanghe Gu, Shanshan Sun, Roop Saini, Zhenming Ji, Di Liu) as well as my other colleagues from the department in particular Yagmur Derin, Di Wu, and David Payne, all of my office mates throughout the years, the staff from the Department of Civil and Environmental Engineering, and all of my friends inside and out of UConn for all the help, support, and friendships that got me to where I am. I would not have been able to accomplish what I have without your assistance and encouragement, nor would my graduate life have been nearly as enjoyable or memorable.

Lastly, I would like to thank my family members: my parents Thomas and Deborah, my brothers Gary and Andrew, and my sister Alexis for always being there for me when things seemed too tough or when I needed encouragement or strength. I would not have made it this far without your unwavering love and support.

Contents

Figure Captions

Table Captions

Chapter 1

Introduction

1.1 Background and Motivation

While warming as the direct consequence of greenhouse gas enhancement is unequivocal at local, regional and global scales, the associated hydrological changes are subject to a large degree of uncertainty and remain poorly understood. Through past research, it has become evident that changes in hydrological conditions and extreme weather events that result from global warming have more profound adverse effects on human welfare than the warming itself. Therefore, understanding and quantifying how climate variability and changes may influence water resources and the terrestrial hydrological cycle is of critical importance for socioeconomic development, and remains a major challenge facing the field of hydrology. Hydrological models provide an important tool for re-constructing and understanding past hydrological variability, and for quantifying future hydrological changes. Both historical and future changes simulated by climate models depict a warmer world characterized by more extremes such as heavier rain and snow, and increased heat waves, droughts, and floods. However, due to the substantial spatial variability of climate, there is a high degree of regional dependence of responses to climate change.

An increase of precipitation intensity is the most definite and detectable hydrological consequence of a warmer climate and among all U.S. regions (Trenberth 1999, Shaw et al. 2001, Allen & Soden 2008), the Northeast has witnessed the strongest increase of extreme precipitation in the past five decades. Groisman et al. (2005) analyzed the increase in the amount of precipitation in the top 1% of extreme events from 1958 to 2007, based on NOAA's National

Climatic Data Center (NCDC) station data archives, and revealed that most areas of the continental U.S. have seen relative increases ranging from 5% to 37%, with the exception of U.S. Northeast, where the increase is 71% (Melillo et al. 2014). As precipitation acts as the main driver for extreme hydrologic events, this substaintial increase makes the Northeast U.S. an ideal location to investigate hydrological extremes such as floods (Karl et al. 2009). Previous studies have conjectured (Groisman et al. 2004, Collins et al. 2009) that in the late 20th century, regions in the U.S. with increased precipitation also experienced increased runoff and stream flow, and stream flow data suggests a large step increase in flood magnitudes in New England since the 1970's (Collins et a. 2009). Higher temperatures are likely be accompanied by a smaller proportion of winter precipitation falling as snow and these changes have been documented for New England leading to greater winter discharges and earlier peak discharges in the spring (Hodgkins et al. 2003; Wake & Markham 2005; Hayhoe et al. 2009). These recorded increases of precipitation intensity, the extent of hydrological changes, and the complexity of interactions served as motivation to investigate the Northeast U.S. region.

Many studies have examined future hydrological changes, of which several have focused on the Northeast. A number of studies have noted that as temperature increases, the increase of the atmospheric moisture holding capacity enhances the atmosphere's evaporative demand and therefore the global average of evapotranspiration (ET) (Trenberth 1999; Huntington 2006). Accompanying warming and ET increases are possible reductions of runoff, soil moisture, and a shifting seasonality of snowmelt. Huntington (2003) and Marshall and Randhir (2008) suggested that increasing temperatures could lead to an ET-driven runoff reductions and Hayhoe et al. (2006) found changes to the seasonality of runoff and discharge peaks. Hayhoe's simulation also showed reduced probability of winter low flows (10th percentile) and increased probability of

high flows (90^{th} percentile), which are intimately connected to flooding, as well as projections of drier, hotter summers and more frequent short and medium-term droughts. Sheffield & Wood (2008) support this potential for enhanced drought in the 21^{st} Century due to increased temperatures while also acknowledging the possibility that increasing precipitation may lead to positive soil moisture trends in this region. As a principle concern with climate change is how the dynamics of the water cycle and its associated energy fluxes will alter in the future, this dissertation research continues from the historic analysis exploring these possible future changes while examining whether the recent warming-induced hydrologic changes in the U.S. Northeast may continue in the future.

In many regions, studies of past hydrological variability are hampered by the lack of reliable river flow data. These include regions where no river gauge is maintained and regions where water diversion or a hydraulic structure has altered the natural flow. In these cases, the most reliable tools we have for reconstructing and evaluating hydrological processes are numerical models. However, a general underestimation of ET has been documented in several studies suing the VIC model including this dissertation research (e.g., Parr and Wang 2014; Xia et al. 2012, Vano et al. 2012, Sheffield et al. 2012). ET is an important component of the terrestrial hydrological cycle and pathway for land-atmosphere interactions as ET is at the core of the surface water, energy, and carbon fluxes (Xia et al. 2014). Although it is a critically influential factor, ET is a particularly difficult process to accurately measure or simulate (McKenney et al. 1993; Eitzinger et al. 2002; Lu et al. 2005; Helge 2011; Trambauer et al. 2014). The high spatial coverage, along with the high spatial resolution, of remote sensing makes it particularly useful in areas of spare ground based measurements; therefore, this research develops an innovative approach to improving the accuracy of ET estimation in hydrological models through the use of

remote sensing data. Remotely sensed vegetation parameters such and leaf area index (LAI) have previously been employed in land surface models (LSMs) to study impacts on the dynamics of the water cycle and investigate improvements to stream flow and soil moisture (Wattenbach et al. 2012; Tang et al. 2012; Zhang et al. 2011; Zhou et al. 2013; Ford and Quiring 2013). In addition to ET, inter-annually varying leaf area index data derived from satellite remote sensing is also incorporated into VIC with the ultimate goal of improving model performance in simulating stream flow and other hydrological processes and thereby also quantifying model related uncertainties.

Two fairly recent studies (Wang et al. 2010, Jung et al. 2010) discovered a global increase in annual mean ET around 7mm per year per decade from 1982 to the late 1990s. These results correspond with what is expected from an intensification of the hydrological cycle. However, from 1998-2008 this global trend was replaced with a decreasing trend of similar magnitude. More recently, Mueller et al. (2013) and Miralles et al. (2013) confirmed the overall positive mutli-decadal trend from the 1980's to the late 1990's and the declining trend occurring at the turn of the century. This poses an important question from a scientific standpoint, specifically, what is the driving mechanism behind this change in trend. Although there is still much uncertainty as to the spatial distribution of the global mean response to warming, all analyses have shown that ET has significant decadal variations whether it be regionally or globally. These themes inspired this research to expand to the national scale and investigate changing ET trends in the continental U.S. during this historic period while exploring interactions and the root causes of change.

The dissertation research facilitates a better understanding of how the hydrological processes, often focusing on the Northeast U.S., have changed in recent history and how they

may change in the near future under continued warming, and what issues and challenges this may or may not present to us. The research extends to explore novel techniques of incorporating remote sensing data into numerical models to enhance our capabilities of studying and understanding change, and expands the domain from the regional to the national scale examining land-surface interactions and inspecting possible root causes behind trends in our changing climate.

1.2 Objectives

The overall objective of this research is to better understand the impacts of climate change and climate variability on hydrological processes, using observations and numerical modeling. The specific research objectives are:

To determine how the hydrological cycle in the U.S. Northeast has responded to climate changes during the past several decades (1950-2011)

- Analyze precipitation data to examine whether the Connecticut River Basin (CRB) has undergone a similar substantial increase in precipitation intensity as referenced by previous studies, and if so, how it may alter the balance of the water budget variables or influence extreme hydrological events.
- Conduct a trend analysis of hydrological variables and ascertain what other effects warming may have on hydrological processes such as timing of snowmelt or seasonality and magnitude of discharge.

To explore whether or not recent hydrologic changes in the U.S. Northeast continue in the future while examining other potential warming-induced changes (2046-2065)

- Evaluate future precipitation characteristics, and investigate how the changing characteristics may influence other hydrological processes.
- Examine if the historic wetter trend of increasing precipitation, runoff, and soil moisture continues into the future and whether warming induced evapotranspiration increases alters these trends or influences drought risk.
- Identify changes or shifts in the seasonality and magnitude of snow pack and discharge, and determine how that may affect the seasonality and characteristics of flood events.

To assess the extent to which remote sensing data can help improve hydrological modeling

- Integrate inter-annual leaf area index data derived from satellite remote sensing and an ET bias adjustment based on remote sensing into a hydrologic model.
- Investigate the extent to which these incorporations may improve estimates of streamflow, soil moisture, and other hydrological variables; therefore helping to characterize model related uncertainties.
- Verify if the integration (bias correction algorithm) of the ET remote sensing data influences the projected future hydrological trends, and if so, how.

To Investigate recent changes in evapotranspiration across the continental U.S. and determine the driving mechanisms of change

- Examine recent historical changes in evapotranspiration trends across the continental U.S.
- Isolate and identify the primary drivers of change for various changing regional ET trends of different signs, and detect whether changing characteristics of precipitation influence these trends.

1.3 Thesis Structure

This thesis is composed of six chapters. Chapter 1 is the introduction. Chapter 2 investigates the recent historical hydrological changes in the Connecticut River Basin as a case study for the Northeast U.S. The study uses observational data and numerically modeled hydrological variables and the impacts of increasing precipitation intensity are analyzed. Chapter 3 continues this study exploring whether the recent warming-induced hydrologic changes in the U.S. Northeast will continue in the future and examines how future changes of precipitation characteristics may influence other hydrological processes. Chapter 4 assesses the extent to which remote sensing data can help improve hydrological modeling as well as how its incorporation may influence projected future hydrological trends. Chapter 5 studies recent historic changes in evapotranspiration trends across the continental U.S., while examining the driving mechanisms behind the changes. Chapter 6 presents a summary and conclusion.

Chapter 2

Modeling and Analysis of the Past

This Chapter has been published as:

Parr DT, Wang GL. 2014. Hydrological Changes in the U.S. Northeast Using the Connecticut River Basin as a Case Study: Part 1. Modeling and Analysis of the Past. *Global and Planetary Change*, 122, 208-222.

2.1 Introduction

Climate change due to accumulation of anthropogenic greenhouse gases in the atmosphere is a major threat for planet Earth. While warming as the direct consequence of greenhouse gas enhancement is unequivocal at local, regional and global scales, the associated hydrological changes are subject to a large degree of uncertainty and remain poorly understood. A major consequence of warming to the hydrological cycle is increases in extreme precipitation intensity (Trenberth 1999, Shaw et al. 2001, Allen & Soden 2008). According to the Clausius-Clapeyron (C-C) relation, the moisture holding capacity of the atmosphere increases by about 7% per degree of warming. As precipitation intensity is proportional to atmospheric moisture content and the maximum intensity precipitation tends to occur when the atmosphere is close to saturation, extreme precipitation events are expected to increase with the atmospheric moisture holding capacity and therefore increase with temperature.

Both historical and future changes simulated by climate models depict a warmer world characterized by heavier rain and snow, and increased heat waves, droughts, and floods (Tebaldi et al. 2006). Observed data already showed widespread increases of precipitation extremes. Groisman et al. (2005) analyzed the increases of the amount of precipitation in the top 1% of extreme events from 1958 to 2007, based on NOAA's National Climatic Data Center (NCDC) station data archives, and revealed that most areas of the continental U.S. have seen relative increases ranging from 5% to 37%, with the exception of U.S. Northeast, where the increase is 71% (Melillo et al. 2014). As precipitation acts as the main driver for extreme hydrologic events, this substaintial increase makes the Northeast U.S. an ideal location to investigate hydrological extremes such as floods (Karl et al. 2009). Globally, precipiation amount has to be balanced by evapotranspiration (ET), which according to results from global climate models increases by

about 2% per degree warming. Therefore, with the 7% increase of atmopsheric holdig capacity and precipitation intensity per degree of warming, it is expected that the frequency and duration of precipitation events on the global scale should decrease (Trenberth et al. 2006) and the frequency of consecutive dry days is expected to increase as it takes longer to replenish the atmosphere by ET. However, due to strong spatial heterogeneity in precipitation characteristics and their response, hydrological changes in any specific region can deviate sigificantly from the global mean signal. For instance, Marshall and Randhir (2008) noted that over the period of 1895-1999, annual precipitation averaged over New England increased by 3.7% while the change of annual precipitation for individual state in New England varied between -12% and 29.5 %. These changing precipitation characteristics directly influence other hydrological processes such as runoff, baseflow, evapotranspiration, and soil moisture.

Using the Connecticut River Basin (CRB) as an example, this study examines the importance of recent warming on hydrological processes in the U.S. Northeast, where some of the strongest increases of precipitation extremes have been observed. In accordance with the theme of increased precipitation extremes, it was conjectured (Groisman et al. 2004, Collins et al. 2009) that in the late 20^{th} century, regions in the U.S. with increased precipitation also experienced increased runoff and stream flow. Collins et al.'s study focused on 75 years of data until the year 2006 for 28 New England stream gages. Although it was found that 25 out of 28 of those gauges showed upward trends of instantaneous peak discharges, it was the annual minimum and median flows that showed the greatest increasing trends thus contradicting the concept that more extreme precipitation increases peak flows more (Collins et al. 2009). Collins' study also ventured that the pre-1970 era and the post-1970 era were "hydroclimatically distinct" as a large step increase in flood magnitudes was found in the post era.

Although many studies agree that there should be an increase in runoff and discharge accompanying the warming climate, others question this assertion. For example, Huntington (2003) found that a regression analysis for mean annual temperature versus evapotranspiration indicated an increase of annual ET at the rate of 2.85cm $^{0}C^{-1}$ increase in mean annual temperature and pointed out that this increase in ET could lead to a runoff reduction of 11-13%, especially in April and May, the wettest months in New England. On a much larger scale, Dai et al. (2009) analyzed gauge data for the Earth's largest 200 rivers, and found that 1/3 showed significant trends from 1948-2004, 45 downward and only 19 upward. This study concluded that the speculation that global discharge increases as the climate warms is unjustified. Marshall & Randhir (2008) used warming scenarios based on the IPCC's second report on emission scenarios to modify historical temperature observations and found that annual surface runoff decreased in the Connecticut Basin by 12-22% depending on the warming scenario.

In addition to the magnitude, timings of discharges are also important for this region due to the dependence of runoff on snowmelt. Higher temperatures should be accompanied by a smaller proportion of winter precipitation or snow. Changes can lead to greater winter discharges and earlier peak discharges in the spring. Wake & Markham (2005) analyzed the center of volume date for thirteen New England rivers, and found a significant change in the timing of this date. Center of volume is defined as the date at which half the yearly water budgets passes through a discharge station, and was considered a better indication of seasonal flow timing than peak discharge timing since it is less influenced by specific large events (Wake & Markham 2005). This study found a trend toward earlier discharge since 1970, with the center of volume date occurring earlier by ten days or more for some rivers, an indication of earlier snow melts and an earlier spring onset. While investigating 11 New England rivers (chosen based on their spring

flow's dependence on snowmelt), Hodgkins et al. (2003) found that the spring bulk flows had advanced by 1-2 weeks in the last 30 years of the 20th Century. Similar results involving increases in winter runoff with an earlier shift of peaks were found for future scenarios (2000-2099) using the VIC model in the U.S. Northeast in the study of Hayhoe et al. (2009).

Using the CRB as an example, this study focuses on how the terrestrial hydrological cycle in the U.S. Northeast responded to climate changes during the past several decades. In particular, our goal is to examine if the CRB has undergone a similar substantial increase in precipitation intensity, and if so, how it may alter the balance of the water budget variables or influence the magnitude of discharge and extreme hydrological events, in addition to analyzing other effects warming may have on hydrological processes such as timing of snowmelt or seasonality of discharge. CRB is one of the largest river basins in the U.S. Northeast where dramatic increase of precipitation extremes has been observed. The basin also spans a strong temperature gradient from north to south, and thus may offer indications on how hydrological response to warming might vary along a temperature gradient. In addition to data from observations, results from simulations run using a surface hydrological model are used to derive hydrological variables for which long-term observational data are not readily available. Section 2.2 of this paper describes the study area, the hydrological model used, as well as observational and forcing data sets. An overview of the model performance is presented in Section 2.3. Section 2.4 presents results on changes of precipitation extremes, trends of key water cycle variables, and discharge timings and magnitudes, and is followed by a discussion and conclusions in Section 2.5. A companion paper examines the projected future hydrological changes in this region based on results from the hydrological model driven with downscaled and bias-corrected future climate predictions.

2.2 Study Area, Model and Data Description

2.2.1 Connecticut River Basin

The Connecticut River Basin is situated within 4 New England states in the U.S. Northeast (*Figure 2.1*). With a total length of ~ 410 miles, the Connecticut River is the largest and longest river in New England. With its headwater from the Fourth Connecticut Lake in New Hampshire right near the Canadian border at Quebec, the river discharges into Long Island Sound near Old Saybrook on coastal Connecticut. The upper two thirds of the river runs through Vermont and New Hampshire defining the border between the two states. It bisects central and eastern Massachusetts and Connecticut in a north south direction. Vital to New England, the Connecticut River provides 70% of the fresh water that enters Long Island Sound with a drainage basin of approximately 11,000 square miles (or 28,489 km^2). Elevation of the basin ranges from sea level to 1,496 meters with an average of 354 meters.

The CRB is vital to life in New England. It drains 41% of Vermont, a third of New Hampshire and Massachusetts, and nearly a third of Connecticut for a total of about 1/6 of six New England states, making it one of New England's most important natural resources (Clay et al. 2006). Land cover in CRB is representative of the U.S. Northeast, with forest coverage reaching approximately 80%. Oriented in the north-south direction, the basin spans a large temperature gradient, encompassing potentially diverse responses to warming throughout the region. The basin therefore is characteristic of the U.S. Northeast and can be taken as a case study for other watersheds within the region. The CRB also provides New England with its most productive farmland which is of particular importance when investigating the possibility of droughts and floods.

2.2.2 Variable Infiltration Capacity (VIC) Model and Data

In addition to precipitation and runoff, other important variables of the terrestrial hydrological cycle include soil moisture and evapotranspiration, which is defined as the sum of evaporation and plant transpiration. Their variability and change with temperature are critically important for understanding and attributing the hydrological cycle changes. Unlike precipitation and discharge for which in-situ measurements or remote sensing data are abundant, observational data for soil moisture and ET are not readily available. A commonly used approach is to derive soil moisture and ET using hydrological models driven with meteorological forcing (e.g., Xia et al., 2011). Here the Variable Infiltration Capacity hydrologic model (VIC) is used.

VIC has been widely used (Liang et al. 1994, Xia et al. 2012, Park & Markus 2014, Zhang et al. 2014, Vano & Lettenmaier 2014) for water resources management, land-atmosphere interactions, and climate change. Although VIC can balance both water and energy budgets (in the water-and-energy mode, or the "full mode"), it can also be used in a "water-only" mode that only solves the water budget. The water-only mode does not solve the ground heat flux equations and related finite difference calculations. Instead, it estimates surface temperature based on air temperature (Gao et al. 2009). In this study, both approaches are implemented and compared. VIC calculates evapotranspiration as a function of net radiation, wind speed, vapor pressure deficit, and air temperature using the Penmen-Monteith equation. As much as 75% of the PET calculated by VIC can be explained by these four variables (Sheffield et al. 2012). The model is also suitable for application in cold environments, as cold season processes such as seasonal and permanently frozen soils and snowpack both on the ground and in the canopy are modeled.

A superior aspect of VIC that distinguishes it from other land surface models is its consideration for sub-grid variability: landcover, soil moisture storage capacity as a spatial

probability distribution (in estimating surface runoff), drainage between moisture zones, and modeling baseflow from the lowest soil layer as a non-linear regression curve (Gao et al. 2009). For example, in this study, the model was run at a 3km resolution, performing calculations for each 3km x 3km grid cell, but the data used for land cover in these experiments has a resolution of 1km. Rather than having to resample that land cover into a 3km resolution, VIC is able to subdivide each grid cell's land cover into whatever number of "tiles" is necessary. VIC only needs data on the fractions of each cell covered by each land cover, but the geographical locations of each land cover type within the grid cell is not tracked. The land class data in this study was taken from the University of Maryland's Global Land Cover Facility (*Figure 2.2*). VIC considers multiple soil layers at varying depths, with diffusion among layers. Each soil layer has a variable infiltration as well as non-linear baseflow and separate moisture holding capacities. For purposes of this study, three soil layers were used at depths of 0-10cm, 10-40cm, and 40-150cm, which are commonly used depths in VIC. The top-most layer allows for quick, bare soil evaporation, the second is most important in dynamic response to rainfall events, while the deepest layer contributes most to subsurface flows (Zhou et al. 2004). Soil data used, including soil type and texture, porosity, and bulk density are taken from Reynolds et al.'s (1990) data made available by the National Oceanic and Atmospheric Administration's (NOAA) National Geophysical Data Center (NGDC). Within the Connecticut River Basin, the first two soil layers share the same properties, which differ from the deepest soil layer.

Baseflow or subsurface runoff is a very important part of the VIC model, especially when it comes to calibration. Baseflow is calculated using the Arno Model, which varies depending on the level of saturation according to a nonlinear regression curve (Gao et al. 2009):

$$\begin{cases} \frac{D_s D_m}{W_s \theta_s} \theta_3, & 0 \le \theta_3 \le W_s \theta_s \\ \frac{D_s D_m}{W_s \theta_s} \theta_3 + \left(D_m - \frac{D_s D_m}{W_s} \right) \left(\frac{\theta_3 - W_s \theta_s}{\theta_s - W_s \theta_s} \right)^2, & \theta_3 \ge W_s \theta_s \end{cases}$$

Where: D_m-maximum subsurface flow (velocity); Θ_3-moisture in third soil layer; W_s-fraction of maximum soil moisture (porosity); Θ_s-saturated moisture in third layer; D_s-fraction of D_m where non- linear baseflow occurs

Higher values of "D_m" result in baseflow being greater in lower water content in the lowest soil layer, higher values of "W_s" will delay runoff peaks, and "D_m" is calculated as a function of saturated hydraulic conductivity and slope, but often requires adjustment (Gao et al. 2009). These are three of the five most commonly adjusted parameters for calibration of the VIC model (along with infiltration parameter and soil depths). For this study these parameters were estimated and then adjusted according to USGS observational records.

VIC is forced by meteorological data, and the data requirement depends on the mode of operation. For the water-only mode, the gridded data for daily precipitation, maximum and minimum temperatures, and wind speed were used from Maurer (2011). The data is at a 1/8° (~12 km) resolution and is available for the period 1950-1999. For the full mode, NASA's Land Data Assimilation Systems (NLDAS-2) forcing data are used, including hourly precipitation, air temperature, U-wind component, V-wind component, atmospheric pressure, specific humidity, surface downward longwave radiation, and surface downward shortwave radiation at a 1/8° resolution for 1980-2011.

The surface water (and energy) balances in VIC are performed at each grid cell. Interaction between cells is accounted for using a separate routing model. Flow accumulation, slope, and flow directions are derived from Digital Elevation Model (DEM) data, taken from the USGS: Earth Resources Observation and Science Center's Hydro 1k: Elevation Derivative Database.

Flow velocity was estimated using Manning's equation (Manning 1891) and adjusted during calibration. The routing model calculates discharges at station locations specified by the grid cell based on flow directions, velocity, and simulated surface runoff and baseflow. The main station used was the USGS #01184000 station at Thompsonville, CT, which had been used and judged as a reliable station in previous research (Bjerklie et al. 2011, Marshall & Randhir 2008). To make certain the routing path was accurate, discharge at another USGS station located north and upstream at West Lebanon, NH was also measured and then compared.

2.3 Model Performance

2.3.1 River Discharge

VIC was calibrated using the USGS river discharge observations at Thompsonville, CT for both the water-balance and water-and-energy-balance mode for the first 10 years of each simulation (1950-1960 and 1980-1990 respectively). It was then verified using data at both the Thompsonville, CT and West Lebanon, NH stations during the rest of the period where data is available. As an example, *Figure 2.3* shows the model performance for four years of the data sets' shared time period. The model captures the temporal variability of observed discharge well, with a correlation coefficient at the bi-weekly time scale reaching ~0.9. The model captures the timing of high and low flows as well as the general seasonality. *Figure 2.4* documents the performance of the model during 1980-1999, the overlap period between the two modes of simulation. Both modes tend to overestimate the discharge in summer, and this bias persists with different calibration parameters and meteorological data. The main differences in representation of seasonality are the spring peak discharges and winter discharge: the water mode tends to overestimate flow in the spring melting season and underestimate in winter when the energy

mode offers a more accurate representation. The additional radiation forcing data used in the full mode leads to more realistic representation of the energy fluxes related to snowpack accumulation and melting that dominate the energy budget in winter.

In all time periods examined, simulations in the water-only mode overestimates total accumulated discharge at Thompsonville by ~5% due mostly to overestimation in the melting season, when discharges are greatest (*Table 2.1*). The full mode tends to overestimate the summer discharge, when water is more limited at the surface. The most noticeable difference between the water fluxes of the two modes is that ET in the full mode is much lower than in the water-only mode, which is consistent with its higher discharge. Overall, the overestimation of discharge magnitude is consistent with documented VIC behavior in previous studies which point out its larger runoff ratios compared to other land surface models (Xia et al. 2012, Vano et al. 2012, Sheffield et al. 2012).

Figure 2.5 presents the inter-annual variability of the river discharge at both stations for 4 seasons simulated using the energy mode. Despite considerable overestimation in the magnitude in the JJA & SON seasons, the model captures the inter-annual variation of discharge in all four seasons extremely well, with correlation coefficients ranging between 0.87 and 0.96. Although the bias is greatest in the summer and fall months, the correlation is also the strongest.

Taken as a whole, despite some model biases in specific seasons, VIC captures the overall seasonal patterns, and the inter-annual variability of river discharge, as well as the timings of the high and low flows quite precisely.

2.3.2 Soil Moisture and Evapotranspiration

Here we compare the model soil moisture with remote sensing data from the European Space Agency's (ESA) Essential Climate Variable (ECV) surface soil moisture product (Naeimi et al. 2009, Dorigo et al. 2010, Liu et al. 2012). This product is a merged data set from both active and passive microwave measurements, and has a spatial resolution of 0.25 degrees. Since VIC simulates soil moisture in each layer, and the ESA data was for surface soil moisture only, the output from VIC's topmost (and also the thinnest) layer is used for the comparison (*Figure 2.6)*. In most cases, VIC slightly underestimates soil moisture. More importantly, VIC's spatial distribution matches well with the remote sensing data, with coefficients of spatial correlation ranging from 0.7 in DJF to 0.92 in MAM.

To compare the evapotranspiration data provided by Dr. Fischer from the NASA Jet Propulsion Laboratory at 0.5 degree resolution (Fisher and Tu 2008), VIC data was resampled and scaled up to the same resolution. VIC represents ET reasonably well, but underestimates year round, particularly in the summer months (*Figure 2.7*). This is consistent with earlier findings that compared to other land surface models (LSMs), VIC produces generally larger runoff ratios and/or lower estimates of ET (Xia et al. 2012, Vano et al. 2012, Sheffield et al. 2012).

Overall, although model biases do exist in certain seasons, VIC sufficiently captures the inter-annual variability, seasonality, and spatial variation of important hydrological variables in the CRB. The calibrated parameters may be used for studying past trends and future changes.

2.3.3 Comparison of two datasets and two modes of simulation

To facilitate comparison between the two modes of simulations and between the two different datasets the NLDAS forcing data was aggregated to daily temporal resolution and used

to drive a VIC simulation in the water-only mode. Results from this simulation are then compared with the full-mode simulation driven by hourly NLDAS data to quantify differences due to the simulation mode, and compared with the water-only mode simulation driven by the gridded daily Ed Maurer (E.M.) data (2011) to quantify the impact of the difference between the two datasets. A comparison of seasonal discharge for all three simulations during their overlap period can be found in *Figure 2.8.* It is apparent that the modes have greatest discrepancies during winter months. When compared to the observed values, the coefficients of correlation are 0.7974 and 0.9294 for the NLDAS water-only and full modes respectively. Throughout the other seasons, the two modes produce almost identical results in terms of inter-annual variation as shown by their correlations in *Figure 2.8*. The water-only mode performs best when water, rather than radiation, is the limiting factor and has the highest correlation with observations in summer months, particularly June. The situation is more complex in winter, and to a lesser extent spring, due to stress on the ground heat flux equations to accurately represent frozen soil, snowpack, snow melting amount and timing. The full mode with its more robust treatment of surface radiation budget produces a more accurate simulation in these snow dominated seasons. Although the simulation for winter months appears inaccurate, it is not unprecedented. Bjerklie et al. (2011) modeled all river basins with discharge into Long Island Sound, including the Connecticut River Basin, and found the largest errors in simulating discharge occurred as an underestimation during the winter months. Inter-annual mean values of water flux variables including evapotranspiration, surface runoff, baseflow, and soil moisture are also compared for various sections of the basin and for each season. There are some differences in magnitude. Most notably, ET was consistently higher in the full mode. The winter season sees the lowest correlation between ET simulated by the two modes, since winter ET averages to less than

0.5mm/day, it is not as influential to the rest of the water budget. Compensating for the larger ET values, the water-only mode simulates wetter soil than the full mode. Despite the model biases, temporal variations throughout the time period in all seasons and sections of the basin are consistent between the two modes.

Figure 2.9 compares between the two modes the simulated timing of discharge as represented by center of volume date and extreme amounts of discharge as represented by peak discharge and amount of surface runoff over the 95 percentile, and compared with observational data as well. Both modes of the model produced similar inter-annual variation and 32-year trends for the hydrological extreme indicators examined. The center of volume date for the observational data is significantly earlier than either of the simulated data sets, due to relatively lower winter and greater summer discharge in the model. However all data sets show a similar increasing delay in timing throughout the thirty-two years. We conclude that the water-only mode driven with daily forcing data is sufficient to capture inter-annual variations of critical water fluxes as well as hydrological extremes at daily or coarser resolution.

From *Figure 2.8* it can be found that results from the water-only mode simulations driven with the two different datasets are more similar than the results from the two different modes of simulations driven with the same dataset, indicating a high level of consistency between the two datasets. The precipitation forcing data are nearly identical throughout the overlapping time period, and the inter-annual variation of the simulated hydrological variables closely follows each other. Evapotranspiration is slightly lower for the Ed Maurer data, but inter-annual variation is still very similar (results not shown). Overall, the two separate data sets simulate the seasonal cycle consistently, and their inter-annual variations are well correlated. Both the forcing data and the model output in the water-only mode driven with the two datasets can therefore be

merged to form a longer data record (spanning 1950-2011) for trend analysis. To merge the two data sets, a linear relationship between the two is established based on their overlap period of 1980-1999, and this relationship is then used to extend the Ed Maurer data set to 2011 based on the NLDAS daily data during 2000-2011.

2.4 Results

2.4.1 Precipitation Extremes

Four indicators of extreme precipitation were analyzed. Three of the indicators were adopted from Frich et al. (2002): number of days with greater than or equal to 10mm (R10), maximum number of consecutive dry days of less than 1mm (CDD), and the simple daily intensity index, defined by the annual total amount divided by the number of days with greater than or equal to 1mm (SDII). Simple daily intensity gives us insight into changes of the average intensity of precipitation rather than just extreme precipitation events. These three indicators are estimated based on averages over 20-year periods, using 1950-1969 as the reference period and using 1970-89 and 1990-2009 to examine changes from the reference. The fourth indicator is the annual accumulated amount of precipitation that falls on days above the 99^{th} percentile of daily precipitation defined based on the reference period of 1950-1999.

Our analysis of R10, SDII, and CDD support the theory that extreme precipitation events are becoming more common in a warming world (*Figure 2.10*). From 1950-1969 to 1970-89 there was a basin average increase of R10 by 4.5 days, a 14.4% increase. The increases from 1950-1969 to 1990-2009 were more substantial, with 6.5 more R10 days, a 20.3% increase. Similarly, the basin average SDII increased by 8.2% from 1950-1969 to 1970-1989 and by 20.4% to 1990-2009. Results show a clear increase in precipitation intensity for the Connecticut River Basin in

the latter half of the 20th Century and early 21st Century. It is interesting to note that although the intensity of precipitation has increased, there is no similar trend for consecutive dry days. As precipitation intensity increases, frequency of precipitation is likely to decrease. This however is not always the case. The basin-averaged change in CDD from 1950-1969 are -2.4 days for 1970-1990 and -1.7 for the period 1990-2009.

To be consistent with the approach of Karl et al. (2009) and Groisman et al. (2005) in representing changes of extreme precipitation, *Figure 2.11* (left panel) plots the relative change from 1950 to 2011 in the amount of precipitation falling on days with precipitation exceeding the 99th percentile of daily precipitation, where the 99th percentile is estimated using 1950-1999 as the reference period. This change is based on the value for 1950 and 2011 derived from linear regression with time, instead of the actual value in these two years. The basin average change is approximately 240%, which is much higher than the 67% for the whole U.S. Northeast as presented in Karl et al. (2009). There are several factors that contribute to the difference between these two estimates: region of focus (Connecticut River Basin in this study vs. the whole Northeast), precipitation data (gridded data in this study vs. station-based), reference period (1950-1999 in this study vs. 1961-1990), and period of changes (1950-2011 in this study vs. 1958-2007). To put the relative changes in perspective, *Figure 2.11* also plots the time series of the basin-averaged amount of precipitation exceeding the 99th percentile, as well as the absolute change from 1950 to 2011 of the extreme precipitation amount as a fraction of the total precipitation which increased by an average of 0.146. While the increasing trend is clear through the whole period, the large values found in the 21st Century are highly influential. The increasing weight of extreme precipitation as shown in *Figure 2.11* (right panel) indicates that

the increase of extreme precipitation took place at the expense of light and moderate precipitation events.

It is clear that the changes in intensity are the greatest after the turn of the new century. In fact during 2001-2011 the relative increase in the amount over the 99th percentile is 11% per year. Out of all the indicators examined here, the amount over the 99th percentile is by far the most restricted by the amount of water the atmosphere is capable of holding. It is for this reason that the most extreme precipitation events are expected to continue to increase and change the surface water budgets as the warming continues.

Precipitation is the most important driver for surface hydrological processes. Several different hydrological changes may result from the increasing intensity of precipitation. During heavy rain events, infiltration rates cannot keep up with the rain rate, which leads to larger runoff ratios and possibly flooding. Intense winter storms can produce large snow packs, creating large winter runoff events and a greater spring peak discharge when the snow melts. Indeed, in many analyses of discharge measurements around the globe there have been findings (Labat et al. 2004, Nohara et al. 2006, Oki & Kanae 2006) of increasing annual or peak discharge. For example, Gerten et al (2008) reported a 7.7% increase in global runoff during 1901-2002. The greatest increases are often found in areas with increased precipitation intensity (Groisman et al. 2001). In fact, strong correlations have been found between the frequency of very heavy precipitation and the frequency of very high stream flow based on observational data in the eastern United States (Groisman et al. 2004). It has been noted that areas of the United States that have experienced increased wetness or flooding coincide with increases to intense precipitation events and long term increases to mean precipitation (Easterling et al. 2000). Meanwhile, since moderate to light rains will occur less frequently, without compensating

increases to mean precipitation, drought conditions may be exacerbated (Easterling et al. 2000). However, this does not seem to be the case in the Connecticut River Basin, as indicated by the slight decrease of consecutive dry days. Also, with less water infiltrating to the soil, soil moisture may be diminished. However, as soil and topography differ, the response might be region specific. In the following we analyze the past trend and changes of other hydrological variables to gain a better understanding of hydrological response and impact.

2.4.2 Trends

The trend analysis here is based on the merged data and model output that span the period 1950-2011. The trend for each variable is calculated as the slope of a linear regression between that variable and time. The precipitation trends are positive throughout the whole basin except during the winter season when precipitation decreased over some portions of the basin (*Figure 2.12*). The basin average trends for each season and annual averages are summarized in *Table 2.2*. Despite strong warming and predominantly increase of precipitation and soil moisture, no consistent increase of ET is found. Summer is the only season when ET increased in more than half of the basin; in the other three seasons, ET signal is mixed. Basin average of evapotranspiration showed a downward trend in three of the seasons, but the large increase in the summer season accounts for a small positive trend on the annual scale. Correlations between ET and net radiation are strong with values of 0.659 for the water-only mode and 0.798 for full mode, at the daily time scale. Correlations between ET and soil moisture are not nearly as substantial at 0.228 and 0.453 also at the daily time scale for water and full modes respectively. This indicates that ET is often limited by the amount of radiation at the surface rather than by available water. Soil moisture has a slight increasing trend throughout all seasons.

The most significant changes to the hydrologic cycle have been in surface runoff and baseflow, which are combined in *Figure 2.12* and *Table 2.2*. A large portion of the precipitation increases is accounted for by increase of discharge. The trend for each are consistent for all seasons. Although baseflow has greater trends, VIC simulated larger values of baseflow than surface runoff throughout most of the year, and it accounts for more than 50% of total discharge. In fact, the increased precipitation is almost entirely accounted for by runoff. This is not surprising due to the large changes in intensity of rainfall.

To examine the potential difference of hydrological response between cold upper basin in the north and the relatively warmer part in the south, the basin was divided into three sections (upper, middle, and lower) and the spatial average of hydrological variables over each section was examined. Despite strong gradient in the temperature change and in snow-vs-rain partition in the precipitation regime (Bjerklie et al., 2011), no qualitative difference in annual average hydrological response was found between different sections of the basin. *Figure 2.13* shows the trend of annual averages and the time series averaged over the middle section is shown as an example for temporal variation. As mentioned by Collins et al. (2009), the pre and post-1970's eras appear to be fairly distinct. The 1960's were classified as a drier period, and the 1950's to late 60's show a clear downward trend for all variables across every part of the basin. With the exception of ET, all other variables examined show upward trends throughout most of the 1970's, and trends appear to be particularly strong for the period post 2000. According to this historic analysis, the Connecticut River Basin entered a wetter regime at this time, distinguished by a greater amount of and more intensive rainfall resulting in greater amounts of discharge and slight increases to soil moisture storage.

Consistent with the increase of intense precipitation, there is a change to runoff ratios. With runoff and base flow trends increasing at a greater rate than ET, the runoff ratio increases throughout the basin (*Figure 2.14*). It basin average increased by 0.0552 for the period of 1950-2011, equivalent to ~10% relative increase.

2.4.3 Discharge Extremes and Floods

It is evident that runoff for the Connecticut River Basin has an upward trend similar to many other rivers across the globe and in the U.S. Northeast in particular (Groisman et al. 2004, Collins et al. 2009). In order to determine whether the Connecticut River Basin responds similarly to other changing properties of stream flow found in previous studies such as earlier spring melt and discharge timing, an analysis of discharge taken from the Thompsonville station for 1950-1999 was conducted (*Figure 2.15*). Another question that arises is whether more intense precipitation has resulted in larger peak flows, or whether possible changes to precipitation frequency have resulted in lower minimum flows.

Peak discharge values indicate a slight decrease. Minimum discharge values, on the other hand, have increased at a rate of 40cfs/yr from 1950-2011. This is similar to the Collins et al. 2009 analysis for which New England rivers indicate an increase in discharge with the periods of low flow showing the greatest change. Similar to the analysis showing a decrease to maximum number of consecutive dry days, rising minimum flows may also be an indication that frequency of precipitation has not been altered as greatly as precipitation intensity. Contrary to the study mentioned previously which investigated 13 New England rivers from 1970-2000 (Wake & Markham 2005), there is no change to an earlier center of volume date for the Connecticut River Basin but rather a delayed date. For this historical period, there is no apparent earlier shift to

peak timings as was simulated for the future in the Northeast by VIC in Hayhoe et al. (2006). In that study, it was found that winter runoff was increasing while spring runoff was decreasing; however, for this historical period, trends are greater for the spring season than the winter partly because the winter season showed a downward precipitation trend.

2.5 Conclusions and Discussion

Comparison between VIC's two modes of operation shows that the full mode does a better job of simulating cold season fluxes and discharge due to its more robust treatment of energy budget allowing for a better simulation of snow pack and melting. However, both the full and water-only modes perform well in reproducing the observed inter-annual variation of the hydrological variables, and closely match each other. As such, VIC in the water-only mode driven with daily atmospheric forcing data is considered sufficient for analyzing past variability, changes, and trend of hydrological processes in the Connecticut River Basin. The change and trend analysis is based on a long record of 62 years (1950-2011) derived from merging two gridded datasets.

It was found that the Connecticut River Basin experienced an increasingly wet regime during the recent historical period including the latter part of the 20th century through the year 2011, and with significant increase in precipitation extremes. Compared with the 1950-1969 time span, the 1990-2009 period had an average of 6.5 more days per year with at least 10mm of precipitation and a 20.4% increase in simple daily intensity index. The relative increase during 1950-2011 in the amount of precipitation falling as extremes (i.e. with daily precipitation exceeding the 99th percentile) was approximately 240%, and the amount of extreme precipitation as a fraction of the total precipitation increased by 0.146. Note that the 240%

relative increase of extreme precipitation is much higher than the previously reported 67% for the Northeast region as a whole. Much of the difference is related to the use of a different dataset, a different reference period to define the 99th percentile and a different period over which the change is calculated. The increases of average precipitation intensity, as represented by SDII, for the period of 1990-2009 was more than double that of 1970-1989. The number of consecutive dry days showed a decrease of drought conditions as did increases to minimum discharge values. These conditions suggest the basin has become more susceptible to flood conditions rather than to drought conditions.

Together with the increase of precipitation extremes, precipitation amount increased by more than 3mm/year/year with the strongest signals occurring during the summer and fall seasons in the central and southern portion of the basin. The mean annual evapotranspiration trend is much weaker indicating only slight increases. ET is most likely limited by available energy. This suggests that the acceleration of the hydrologic cycle, especially the increase of precipitation rate derives primarily from increased large-scale moisture convergence over the basin instead of local ET acceleration. The increase of moisture convergence is likely related to increased evaporation rates in the nearby Atlantic Ocean. Runoff and baseflow are the parts of the water budget which seem to be most significantly affected by increasing precipitation trends, all of which are strongest during the summer and fall. Soil moisture trends also rise most during these seasons, meaning the summer and fall months are most affected by the wetter regime. Runoff ratios indicate a larger share of precipitation being partitioned to discharge. Similar to most investigations, this study confirms that discharge is indeed on an upward trend in the Connecticut River Basin, but response of extremes and timings differ from findings in previous studies.

Contrary to suggestions by prior work (Lettenmaier et al. 1993, Hodgkins et al. 2003, Wake & Markham 2005, Hayhoe et al. 2009), VIC simulations in this study produced no sign of an earlier snow melt season or timing of peak discharge; in fact, a slight delay in the timing of center of volume was found. Although there were increases to minimum discharge as well as amount of extreme runoff over the 95% threshold, these changes are embedded within considerable inter-annual variability. Of note, however, positive trends of mean precipitation, runoff, and to a lesser extent, soil moisture, appear to be particularly strong toward the end of the simulation period, especially from the year 2000 forward as does the extreme precipitation. While the strength of discharge changes does not appear to be as significant as those previously cited, there is also the possibility that these changes are in early stages and have just begun to manifest. Previous simulations have suggested that changes to the frequency of dry and wet day extremes are unlikely to be statistically significant before the mid-21st century (Singh et al 2013). The response of the basin to warming may become more significant or discernible in other ways in the near future.

Overall, the response of the Connecticut River Basin shows indications of change toward more extreme precipitation, increasing discharge, an increasing runoff ratio wetter soil conditions, and negligible trend in ET. These recent historic changes have very likely manifested in other river basins in the U.S. Northeast. The causal-effect relations among different aspects of the changes and the mechanisms underlying the interactions among different hydrological processes are likely to hold as well. Beyond the Northeast, this study can provide insight for other forested watersheds in the mid-latitudes where increases to mean and extreme precipitation have been documented. Part 2 of this study examines how hydrological processes in the Connecticut River Basin may change in the future, using the VIC model forced by bias-

corrected and downscaled future climate projections. The two parts combined together facilitate a better understanding on how greenhouse gases and warming may influence the surface energy and water cycles in the U.S. Northeast both in the past and in the future.

	Thomps. USGS	Thomps. VIC	W. Lebn. USGS	W. Lebn. VIC
1980-1999 (water mode)	129.38	136.99	52.87	59.32
1980-1999 (energy mode)		148.91		65.18
1950-1999 (water mode)	292.97	311.61	121.65	135.12
1980-2011 (energy mode)	217.91	249.24	89.87	110.09

Table 2.1: Accumulated discharge (10^6 cfs) at Thompsonville & West Lebanon discharge stations for observational data (USGS) and simulated (VIC- water balance only mode "water mode" and full water-and-energy balance mode "energy mode")

1950-2011 Trends - Basin Mean				
Season	Precipitation	Evapotranspiration	Runoff	Soil Moisture
DJF	-0.00977 mm/day/yr	-0.000069 mm/day/yr	0.00153 mm/day/yr	$3.67*10^{-5}$ vol. fraction/yr
MAM	0.00539 mm/day/yr	-0.000227 mm/day/yr	0.00363 mm/day/yr	$5.36*10^{-5}$ vol. fraction/yr
JJA	0.01621 mm/day/yr	0.000581 mm/day/yr	0.01228 mm/day/yr	$1.86*10^{-4}$ vol. fraction/yr
SON	0.01297 mm/day/yr	-0.000188 mm/day/yr	0.01238 mm/day/yr	$1.82*10^{-4}$ vol. fraction/yr
Annual	3.06529 mm/yr/yr	0.04297 mm/yr/yr	2.71428 mm/yr/yr	$1.15*10^{-4}$ vol. fraction/yr

Table 2.2: Basin mean of water variable trends shown in *Fig. 2.12*

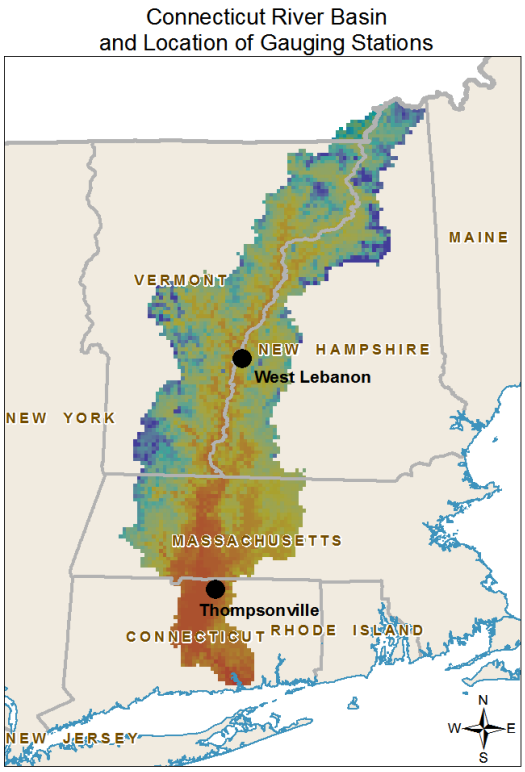

Fig. 2.1: Elevation and location of Connecticut River Basin & gauging stations

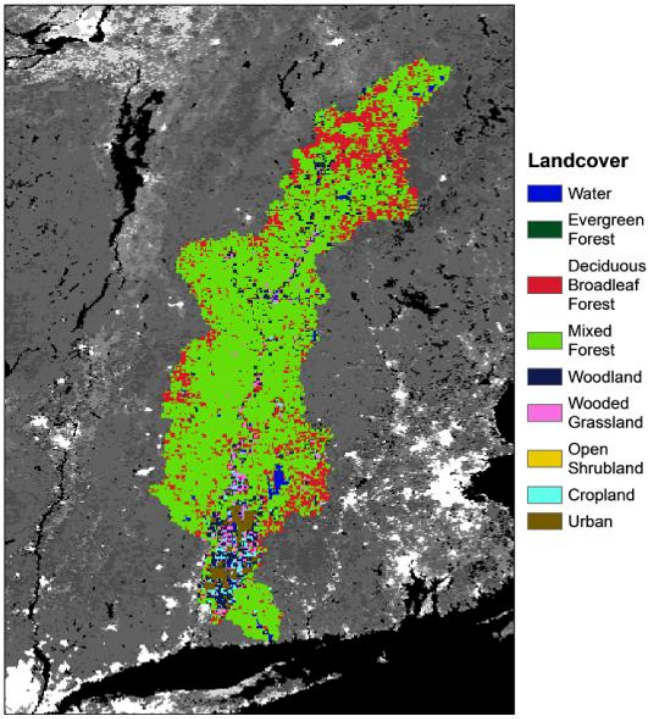

Fig. 2.2: Land cover classes raster data (left) and legend (right). Data is taken from the University of Maryland's Global Land Cover Facility. Data is at ~1km resolution

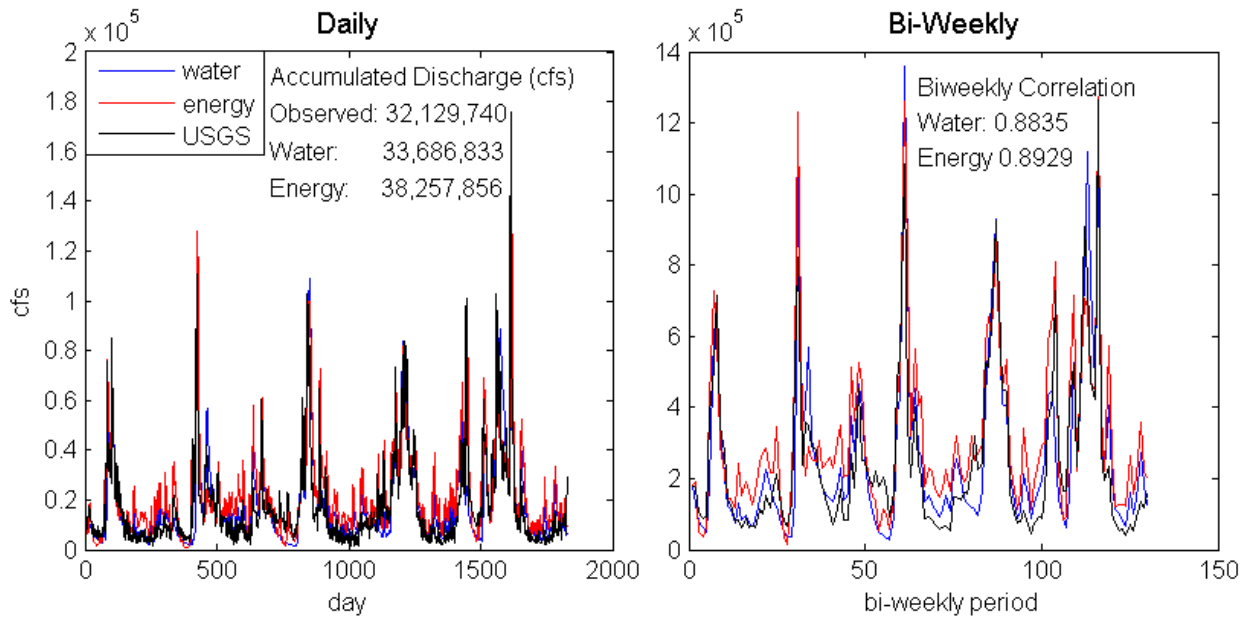

Fig. 2.3: 1980-1984 snapshot of simulated (for water balance ("water") and water-and-energy balance ("energy") mode) versus USGS observed discharge data at Thompsonville, CT station, plotted as: a) Daily accumulation b) Bi-weekly accumulation.

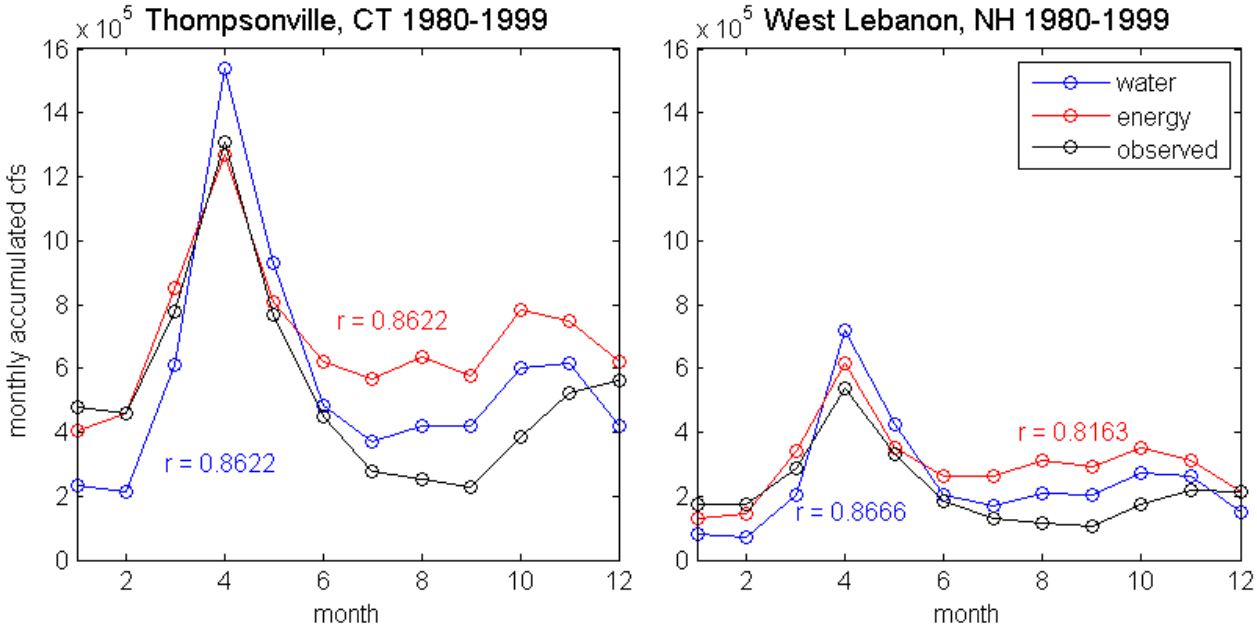

Fig. 2.4: Average monthly accumulated discharge for both the simulated and the observational data sets at Thompsonville station (shared time period for both data sets: 1980-1999).

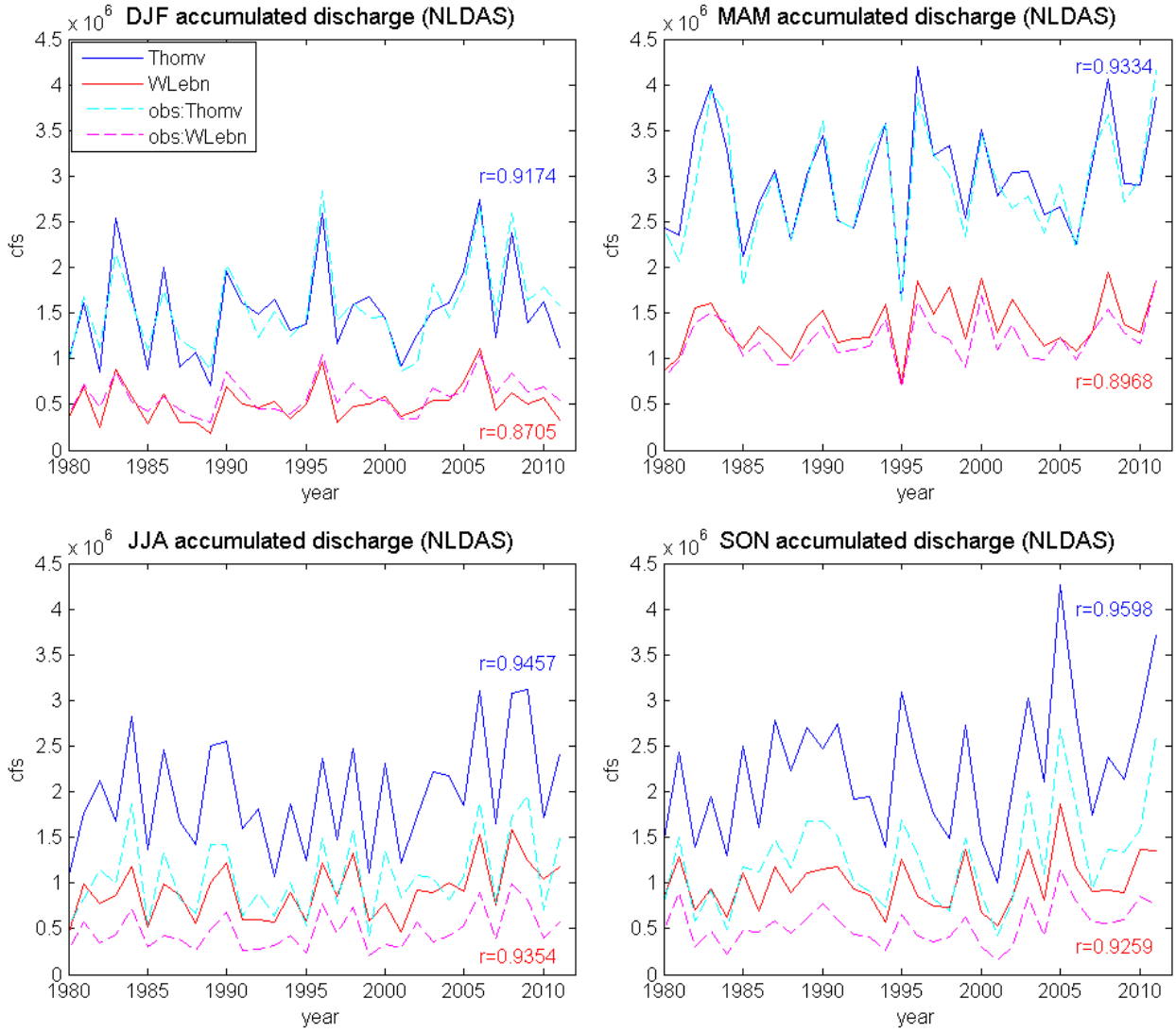

Fig. 2.5: VIC water-and-energy balance mode & USGS Seasonal accumulated discharge at Thompsonville & West Lebanon stations (1980-2011). Correlation coefficients are also included.

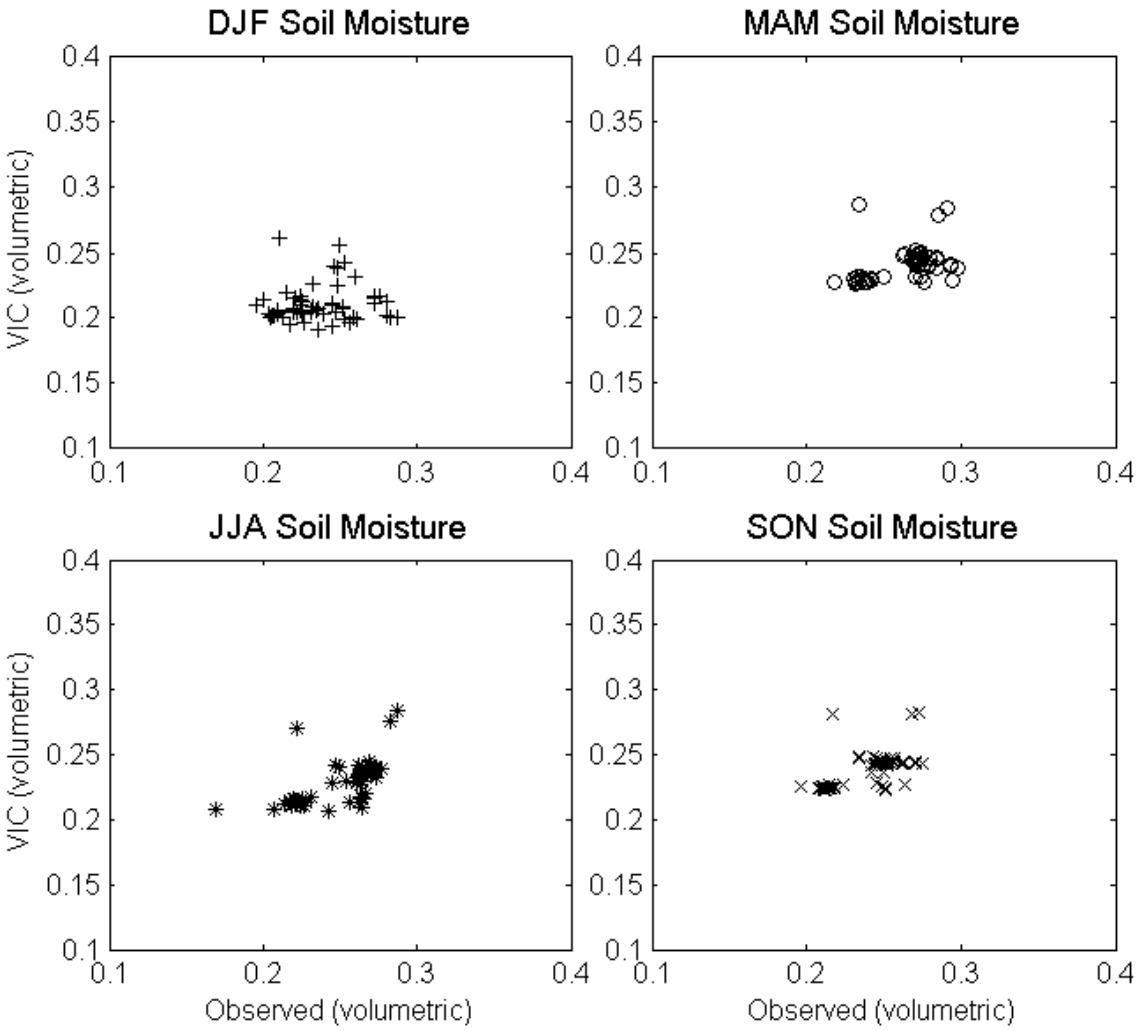

Fig. 2.6: Soil moisture comparison for VIC water mode versus ECV observation- each point is a particular grid cell average for 1980-1999. The simulated soil moisture data was scaled up to 0.25° resolution.

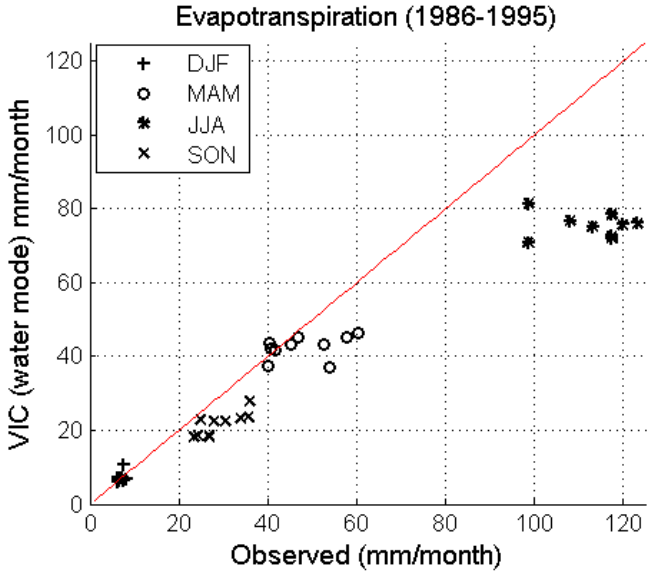

Fig. 2.7: Seasonal average evapotranspiration for VIC water mode versus Landflux observation. Each point is a particular grid cell average for 1986-1995. The simulated ET data was scaled up to 0.5° resolution.

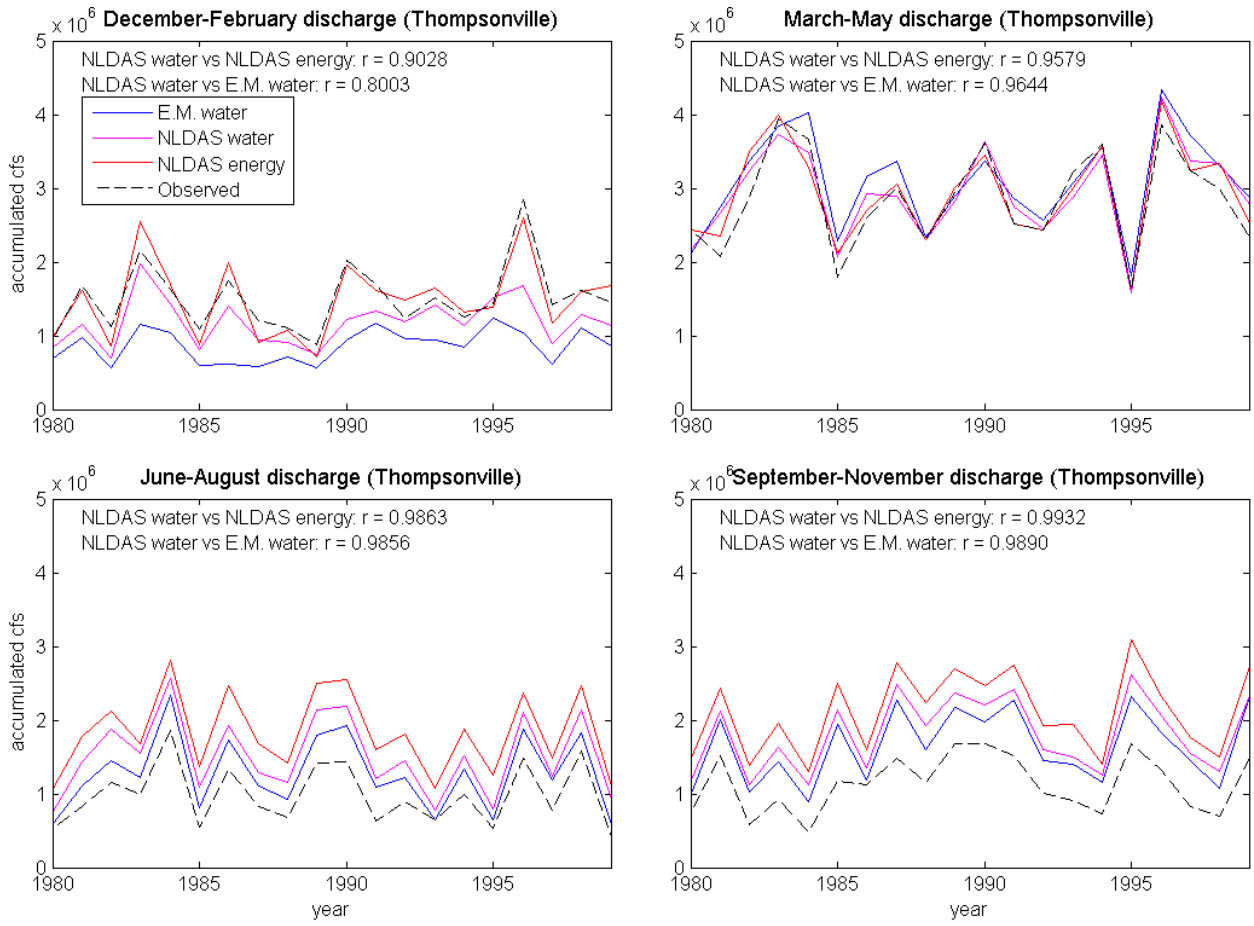

Fig. 2.8: Seasonal discharge comparison between modes of operation (water balance mode: "water" and full water-and-energy mode: "energy") and between data sets (NASA's Land Data Assimilation Systems phase 2 forcing: "NLDAS" and Ed Maurer's gridded observed meteorological data: "E.M.").

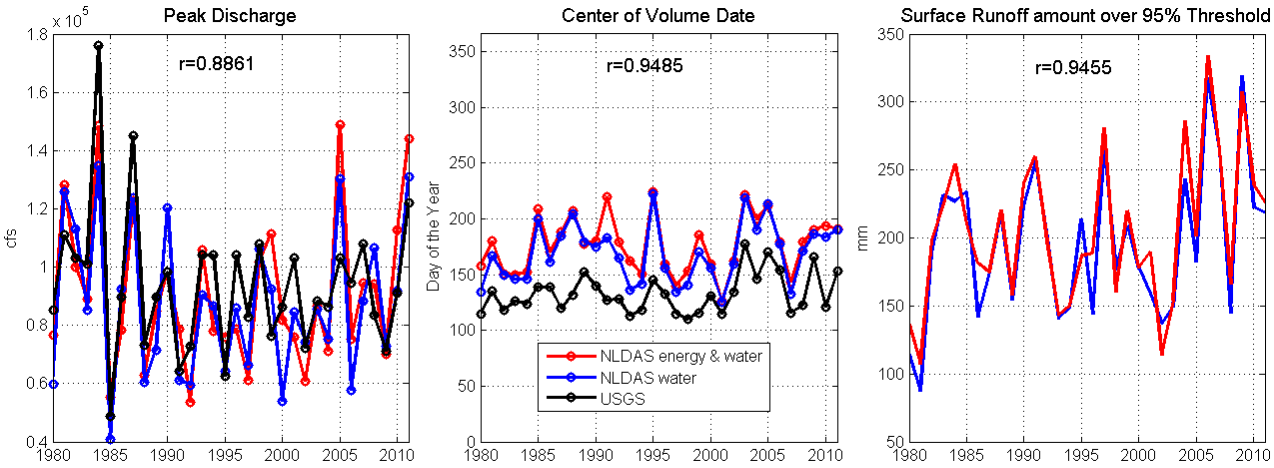

Fig. 2.9: Analysis of extreme discharge/runoff indicators compared for VIC water vs. energy mode using the same NLDAS forcing data. Left is magnitude of annual peak discharge, center is day of year where half of discharge passes the Thompsonville station, right is grid cell average surface runoff over threshold of 95th percentile with a reference period of 1980-2011. Correlations shown are for the two simulations.

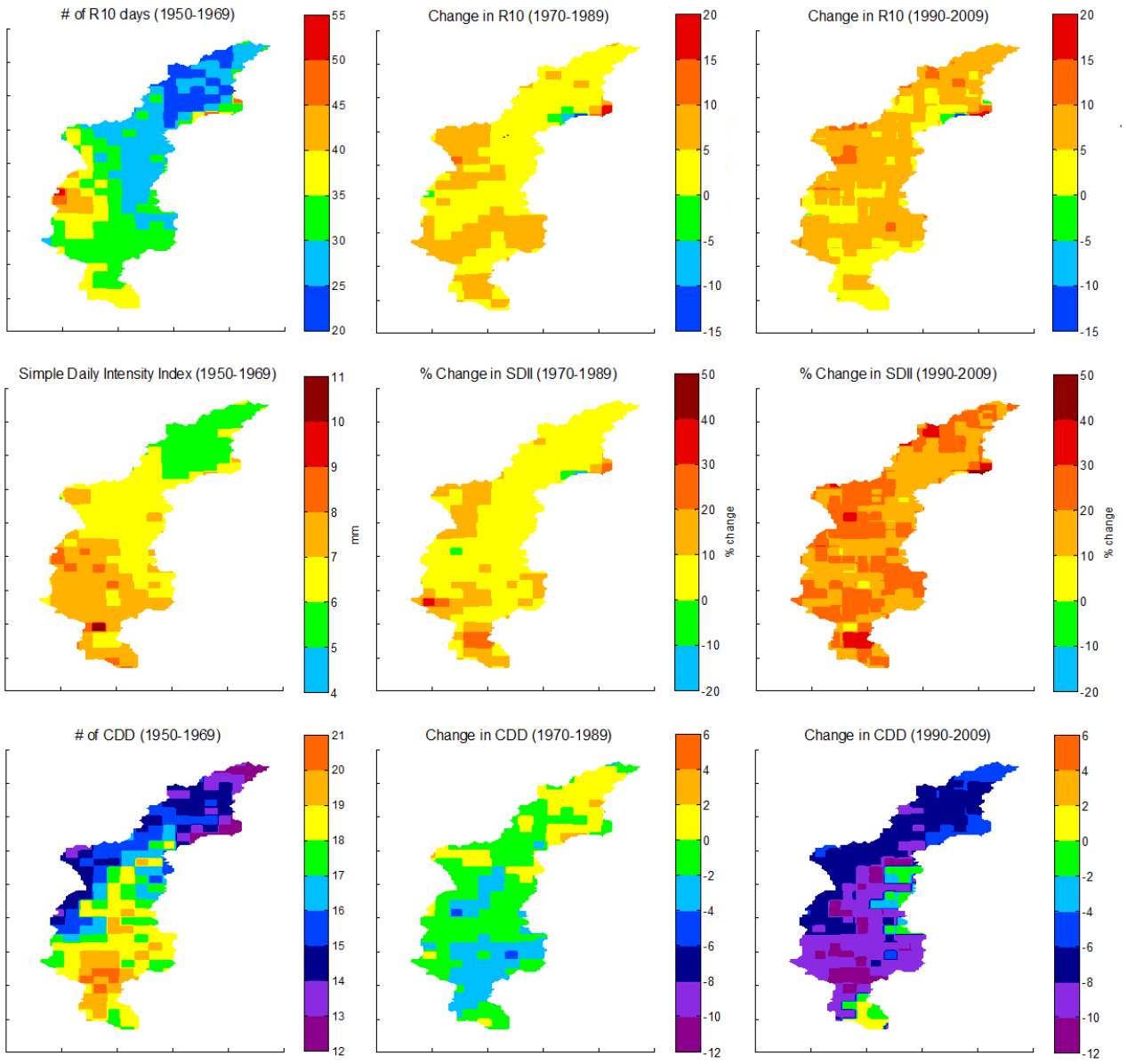

Fig. 2.10: Precipitation extreme indicators (R10 top, SDII middle, CDD bottom): for the reference period 1950-1969 and their changes in two periods 1970-1989 and 1990-2009. Units are mean number of days per year for R10 and CDD and relative change in percent for SDII.

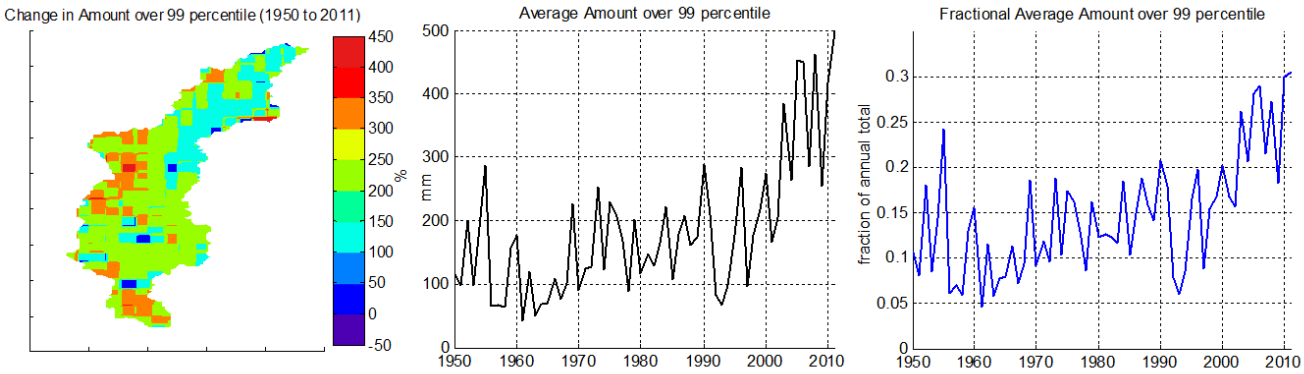

Fig. 2.11: Precipitation extreme analysis: Change in the amount over 99th percentile from 1950 to 2011 based on a regression with the threshold defined by the reference period of 1950-1999 (left). Annual basin average precipitation amount over the 99th percentile threshold (center). Annual basin average fractional amount of precipitation over the 99th percentile (right). Data comes from the merged data set.

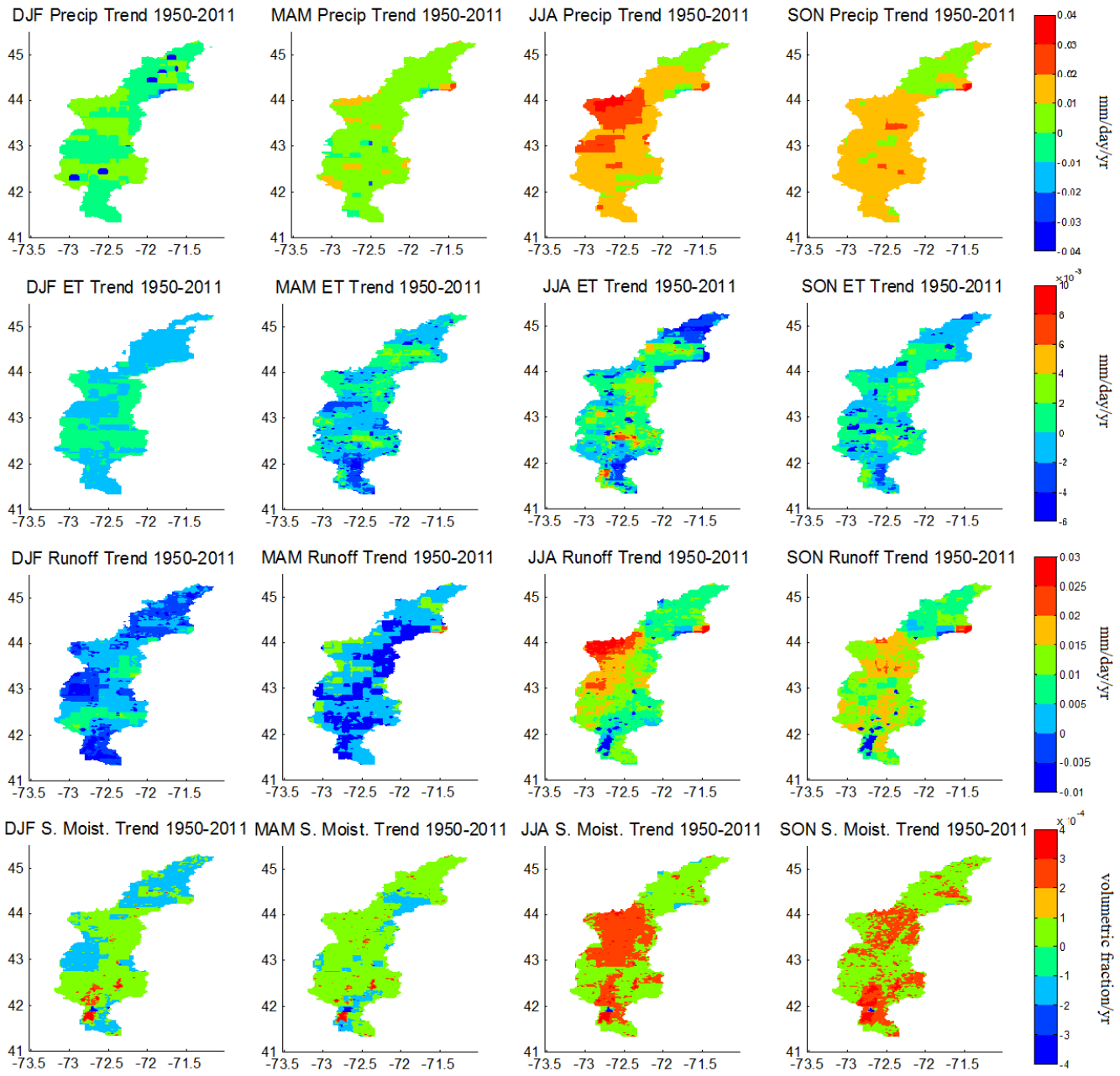

Fig. 2.12: Seasonal trends of water cycle variables for 1950-2011: includes precipitation (Precip), evapotranspiration (ET), surface runoff and baseflow (Runoff), & soil moisture (S. Moist.) for change in daily average values per year (mm/day/year) (volumetric fraction/year for soil moisture). Data comes from the merged data set.

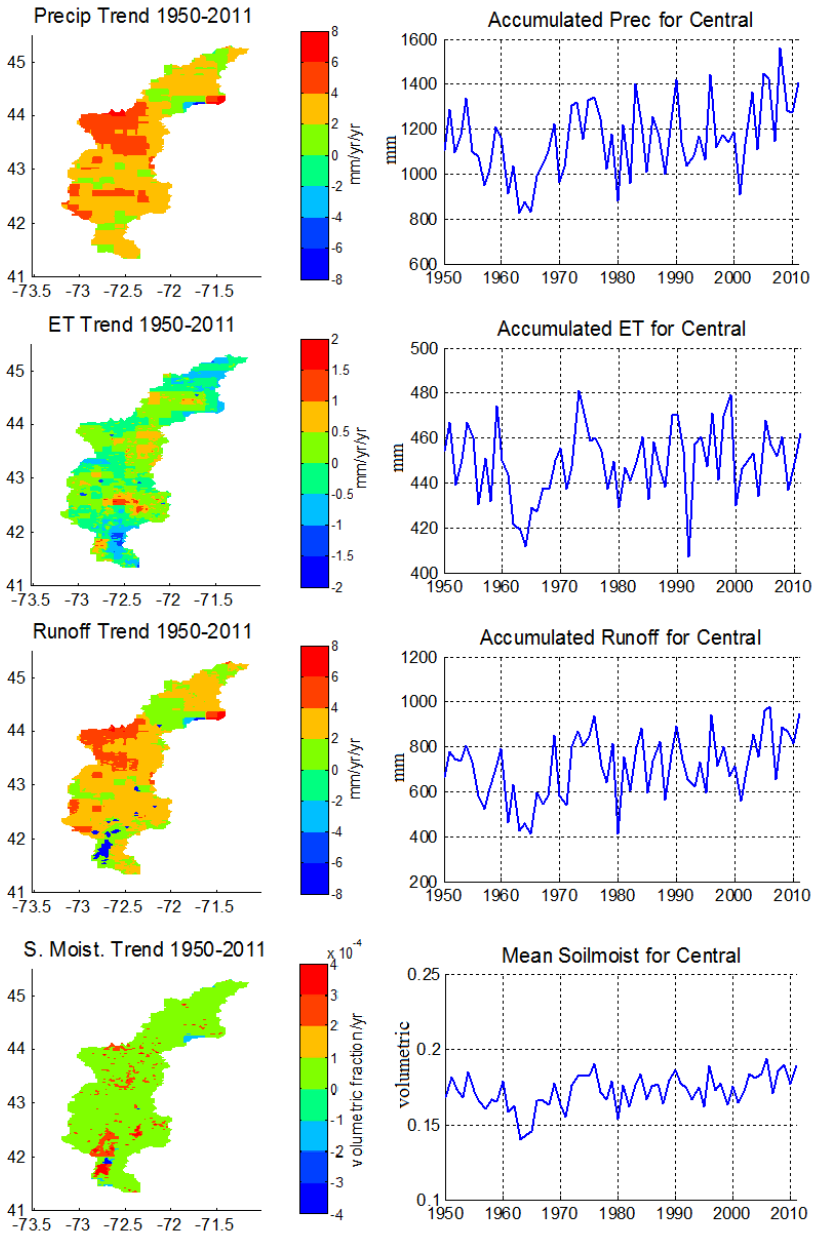

Fig. 2.13: Annual trends of water cycle variables for 1950-2011 in mm/year/year and volumetric fraction/year for soil moisture (left) and annual time series for the central part of basin (right). Data comes from the merged data set.

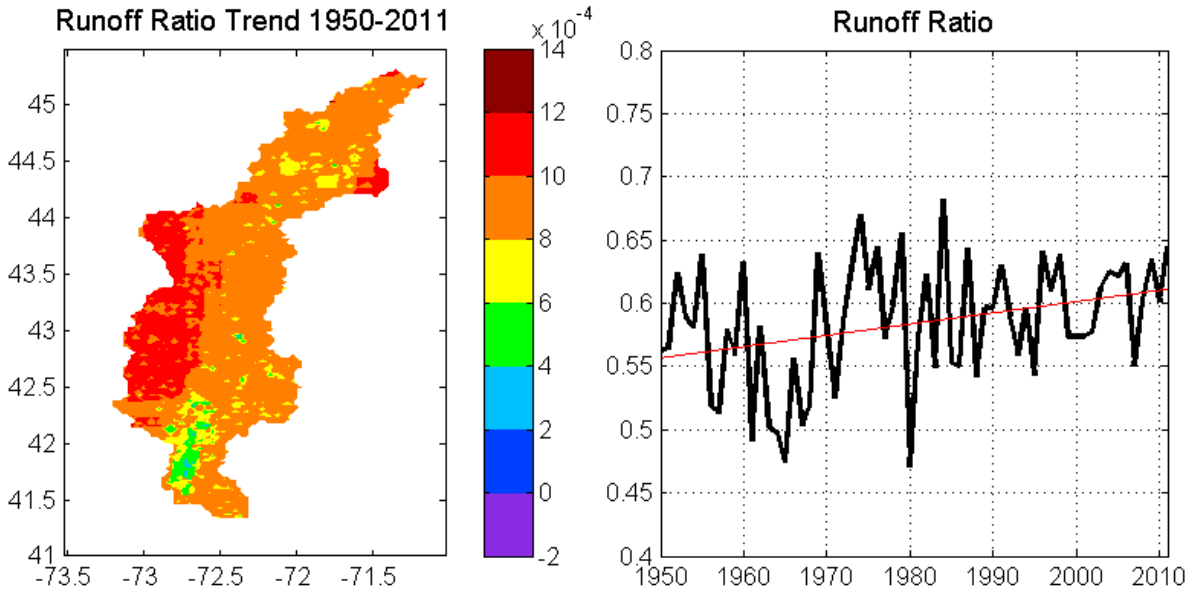

Fig. 2.14: Annual trend for the runoff ratio fraction/year - includes surface runoff & baseflow (left) and annual basin average runoff ratio and linear regression (right). The data comes from merged data set and describes fraction of precipitation resulting in runoff. The linear regression indicates an increase of 0.0552 over 62 yrs.

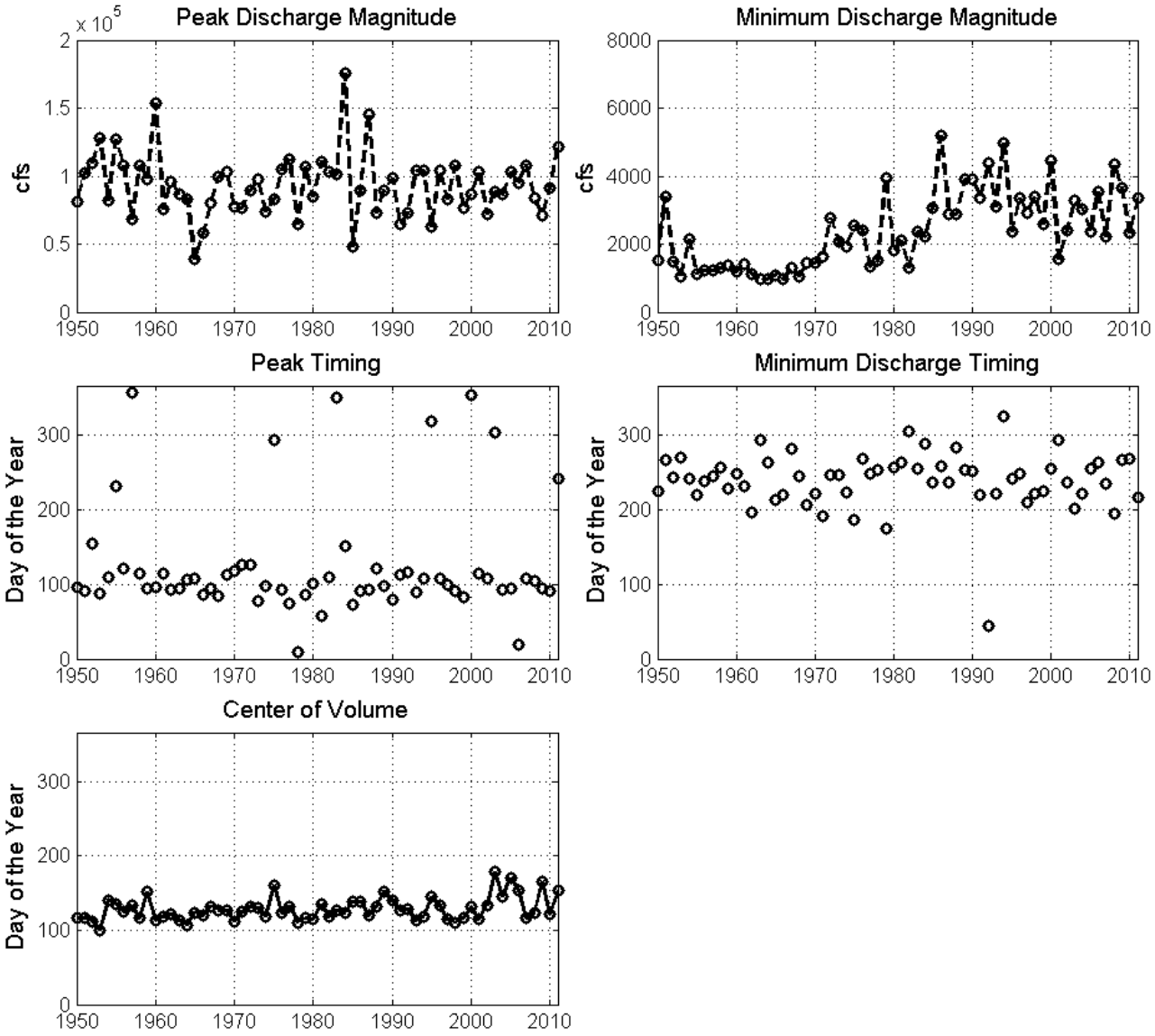

Fig. 2.15: Analysis of magnitudes and timings of USGS observational discharge: includes peak magnitude and timing (top), minimum magnitude and timing (center), and center of volume.

Chapter 3

Projections of the Future

This Chapter has been accepted for publication and is currently available online:

Parr DT, Wang GL, Ahmed, KF. 2015. Hydrological changes in the U.S. Northeast using the Connecticut River Basin as a case study: Part 2. Projections of the Future. *Global and Planetary Change*, doi:10.1016/j.gloplacha.2015.08.011.

3.1 Introduction

According to the Intergovernmental Panel on Climate Change (IPCC)'s 4th Assessment Report (AR4), warming of the climate is unequivocal and long term temperature changes have been observed at all spatial scales. Increasing temperatures have major effects on the hydrologic cycle and the surface energy budget. One such possible impact to the hydrological cycle is an increase in precipitation intensity. More specifically, atmospheric moisture holding capacity increases exponentially with temperature which can lead to more intense heavy precipitation (Trenberth 1999; Shaw et al. 2001; Allen & Soden 2008). The warming-induced changes to evapotranspiration (ET), characteristics of precipitation, and the seasonality of snow melt and stream flow peaks could all substantially increase flood and drought risks (e.g., Sheffield & Wood 2007). Climate models project a warmer future world characterized by heavier rain and snow, increased heat waves, droughts, and floods (Tebaldi et al. 2006). Extreme events like droughts and floods account for a large proportion of climate-related damages.

Due to the substantial spatial variability of climate, there is a high degree of regional dependence of responses to climate change. This study focuses on the U.S. Northeast, a region where a strong increase of precipitation extremes has been observed in the past several decades. Based on NOAA's National Climatic Data Center (NCDC) station data archives, Groisman et al. (2005) analyzed the increases of the amount of precipitation in the top 1% of extreme events from 1958 to 2007, and found that within the U.S. these increases range from 9% in the Southwest to 67% in the Northeast. The U.S. Northeast is therefore a critical place to investigate extremes (Karl et al. 2009). In studying climate changes impact on hydrological processes in the Connecticut River Basin (CRB) of the U.S. Northeast during the period 1950-2011, Parr and Wang (2014) found significant increases in simple daily intensity of precipitation and the

number of days with 10mm or more of precipitation. They also found that the total amount of precipitation from the upper 1% of daily precipitation increased by 240% during 1950-2011 in CRB, and the weight of extreme precipitation is the greatest after the turn of the century, with extreme precipitation accounting for about 10.6% of total precipitation in the 1950s to 30.4% in the 2000s.

It has been shown previously that runoff and stream flow have been increasing in the greater Northeast region of New England (Groisman et al. 2004; Collins et al. 2009), and peak discharges are on the rise in the entire Northeast (Collins et al. 2009). Wake & Markham (2005) and Hayhoe et al. (2006) documented greater winter discharge and an earlier shift of peak flows. Part 1 of this study (Parr & Wang, 2014) found that the hydrological cycle has changed towards greater discharge and runoff ratios, primarily as a result of increasing mean precipitation and increasing precipitation intensities combined. Increases to precipitation are almost entirely accounted for by increases to runoff, with negligible trend in ET despite a strong warming trend. However, Parr and Wang (2014) found no discernable earlier shift in the timing of peak discharges and snowmelt season, and no increase of winter discharge. It was suggested that the basin is entering a wetter regime more subject to meteorological flood conditions than to drought conditions. This current study focuses on how the hydrologic cycle might be affected by continued warming in the future and whether the responses and trends found in the historical period will continue in the future.

Many studies have examined future hydrological changes of which several have focused on the Northeast. A number of studies have noted that as temperature increases, the increase of the atmospheric moisture holding capacity enhances the atmosphere's evaporative demand and therefore the global average of evapotranspiration (Trenberth 1999; Huntington 2006).

Huntington (2003) suggested that increasing temperatures could lead to an ET-driven runoff reduction of 11-13%, especially in April and May, the wettest months in New England. Using the VIC model driven with future climate projections, Hayhoe et al. (2006) found increases in winter runoff but decreases in spring runoff with an earlier shift of peaks for the Northeast for the period 2000-2099. Hayhoe's simulation also showed reduced probability of winter low flows (10^{th} percentile) and increased probability of high flows (90^{th} percentile) with significantly higher flows across much of the northern part of the Northeast as well as projections of drier, hotter summers and more frequent short and medium-term droughts. Similar to these prior results, another study using the SWAT model in the Connecticut Watershed found annual surface runoff decreases of 12-22% (depending on CO2 emission scenarios) for the period 2060-2100, and these decreases take place primarily during the early spring to fall seasons (Marshall & Randhir 2008). Higher temperatures could lead to a smaller proportion of winter precipitation falling as snow, which could lead to greater winter discharges and earlier peak discharges in the spring.

Sheffield & Wood (2008) stated that although increasing precipitation may lead to positive soil moisture trends in many parts of North America, increasing temperatures present the potential for enhanced drought in the 21^{st} Century. Warming has major effects on the surface energy budget, and influences evapotranspiration (Teuling et al. 2009). The focus of this part of our study is on whether the recent warming-induced changes in precipitation characteristics will continue in the future and how future changes of precipitation characteristics may influence other hydrological processes in the CRB. In the following, Section 3.2 provides a description of the data sets and methods of analysis used, including the use of the Variable Infiltration Capacity (VIC) hydrological model. Section 3.3 describes the results of the study in regards to future

changes, including mean hydrological changes, extreme precipitation, snow pack and discharge seasonality changes, and an in depth analysis of changing flood risk and drought risks respectively. Section 3.4 presents conclusions and discussion.

3.2 Data and Methods

3.2.1 VIC Model and Data

The VIC hydrological model was calibrated based on observational river discharge on the Connecticut River during Part 1 of this study. The same model parameters are used here, including land cover data from University of Maryland's Global Land Cover Facility and soil data (type, texture, porosity, and bulk density) from Reynolds et al. (1990) made available by the National Oceanic and Atmospheric Administration's (NOAA) National Geophysical Data Center (NGDC). The same soil layers are used at depths of 0-10cm, 10-40cm, and 40-150cm. To simulate the future hydrological conditions in the Connecticut River Basin, both present-day (1971-1995) and projected A1B scenario future (2046-2065) climate from the North American Regional Climate Change Assessment Program (NARCCAP) models are used to derive the meteorological forcing for the VIC model, including daily precipitation, surface air temperature, and wind speed. Note that VIC can be run in two different modes of operation, with the "water balance mode" requiring daily meteorological forcing and the "water and energy balance mode" requiring hourly forcing (Gao et al. 2009). Here the "water balance mode" is utilized for consistency with the availability of downscaled and bias-corrected future driving forcing for VIC.

To account for inter-model variability of future projections, data from three NARCCAP RCMs are used, including the Regional Climate Model version 3 (RegCM3; Giorgi et al.

1993a,b; Pal et al. 2000, 2007) driven with lateral boundary conditions (LBCs) from the Canadian Climate Centre Coupled General Circulation Model version 3 (CGCM3; Scinocca and McFarlane 2004; Flato 2005) (REGCM-CGCM), RegCM3 driven with LBCs from the Geophysical Fluid Dynamics Labortory Climate Model ((GFDL; GFDL Global Atmospheric Model Development Team 2004) (REGCM-GFDL), and the Canadian RCM (CRCM; Caya and LaPrise 1999) driven with LBCs from CGCM3 (CRCM-CGCM). The future daily meteorological forcing from each RCM-GCM combination was first downscaled to 1/8 degree resolution and bias-corrected using the methodology of Ahmed et al. (2013). Specifically, parameters for a quantile mapping methodology were derived by comparing the present-day climate from each model with the present-day observational data, and were then applied to the future climate projection from the same model to correct the model bias. The resulting downscaled and bias-corrected meteorological forcing data is then used to drive VIC for future hydrological projections.

Although data from additional NARCCAP models exist, they have been shown to predict very similar future changes (Ahmed et al., 2013). In addition, in terms of hydrological variables and indicators, downscaling and bias correction was shown to produce very similar hydrological results between different models in past studies (Wood et al., 2002, 2004). Within this study, the three different GCM-RCM combinations experimented produce extremely similar mean and variability of stream flow and concur in signal for almost every hydrological analysis conducted. Among the ten RCMs and GCMs for which output were downscaled and bias-corrected for the domain of this study (Ahmed et al., 2013), the projected precipitation changes by the three models used in this study are within one standard deviation from the multi-model ensemble mean in most of the months, and none of the models stands out as an outlier. More importantly, in any

specific month, of the three models used, some are above the ensemble mean and some are below. Therefore, results from our study should be representative of the larger ensemble behavior and should not contain systematic biases. We therefore consider the three combinations used here sufficient for studying changes in hydrological processes. Although the NARCCAP models have been shown to underestimate extreme precipitation in the U.S. East (Mishra et al. 2012), the quantile mapping approach corrects both mean and variability based on the Cumulative Distribution Functions (CDF), and thus has been shown to adjust for more frequent heavy precipitation events in this region (Ahmed et al. 2013) potentially correcting these underestimations.

3.2.2 Methods of Analysis

In the extreme precipitation analysis, for each grid cell the 99th percentile daily precipitation was derived based on the reference period 1950-1999. This value was then used as a threshold for both the past and future analyses in defining extreme precipitation. The amount of extreme precipitation for each year was defined as the accumulation of daily precipitation exceeding this threshold, and the weight of extreme precipitation was derived as the fraction of the total annual precipitation accounted for by extreme precipitation. Additionally, the number of days with more than or equal to 10mm of precipitation (R10) and the simple daily intensity index (SDII) follow the definition of Frich et al. (2002).

A future flood risk analysis is conducted in this study based on river discharge. First a rating curve was derived based on past observational discharge and gauge height for the Thompsonville, CT station from data provided by USGS. Second, the correspondence between observational and VIC simulated discharge was derived from the past climate. Assuming that

both relationships are stationary as climate changes in the future, any simulated discharge for the future climate can be converted to a corresponding gauge height. The derived future gauge height data were then used to analyze the flooding risks with reference to the "action level" gauge height for this station provided by the National Weather Service Advanced Hydrologic Prediction Service from NOAA. The "action level" height refers to the height at which flooding becomes a risk and actions should be taken. Here the flood risks analysis examines the number of days when the gauge height exceeds the action level, and the duration and frequency of flooding events for each year of the simulations.

The future drought risks were analyzed using two methods. The first is based on consecutive dry days (CDD), a simple measurement of meteorological drought. Daily precipitation of less than 1mm defines a dry day. The second method of drought analysis makes use of soil moisture data. For each grid cell in the basin, a month-specific 20^{th} percentile daily soil moisture threshold was identified based on historic data. If 20 or more of the days in a specific month were under the threshold, it was considered a drought month for that specific grid cell. The mean duration of droughts and the number of short (4-6 months), medium (7-11 months), and long (≥12 months) term droughts, were then identified. This analysis method was adapted from a similar one conducted by Sheffield & Wood (2007) where the percentile was based on monthly rather than daily data.

3.3 Results

3.3.1 Mean Hydrological Changes

In the previous historic analysis for years 1950-2011 mean precipitation, runoff, and soil moisture all displayed increasing trends. Due to large increases in extreme precipitation in this

region toward the end of the time period, the increases to precipitation were almost entirely accounted for by increases to runoff; however, no significant trend for ET was found. Mean precipitation for future years 2046-2065 shows a negligible change during summer, significant ($p \leq 0.05$) increases during spring and winter, and a slight decrease during autumn (*Figure 3.1*). An increase of 0.37mm/day during the winter was accompanied by a substantial significant ($p \leq 0.05$) increase of 0.787mm/day to daily mean winter runoff, which may be affected by seasonality changes to snowmelt more so than any changes to mean precipitation. Despite the precipitation increases in spring, runoff actually decreases by ~0.1mm/day. This is likely a result of spring SWE decrease, an indication of earlier melting as detailed in section 3.3. Also, soil moisture displays large increases in winter and appears to follow a near linear relationship. Furthermore, the precipitation decrease of 0.05mm/day in autumn is accompanied by a fairly significant decrease to soil moisture (*Figure 3.2*). Soil moisture is perhaps most crucial in the spring and summer seasons for this region due to flooding and drought events. However, soil moisture shows the least change in future simulations for these two seasons although summer soil moisture is slightly decreased. Only the increase in winter soil moisture is found to be significant.

Other than these significant changes during winter, by far the most critical change to water cycle variables is to evapotranspiration. As ET is strongly dependent on available energy and the surface radiation budget, it is not surprising that as temperature rises, so does ET as long as moisture is available. The negligible ET trend found in the historic analysis is replaced here by a universal significant ($p \leq 0.05$) increase throughout all four seasons in the future (*Table 3.1*). Therefore, in response to precipitation increases under future warming conditions, the

Connecticut River Basin will likely experience an acceleration of ET and a slowing down of the increasing runoff trend compared with the past.

3.3.2 Extreme Precipitation

In our historic analysis for the U.S. Northeast, we found a large increase in the number of days with more than or equal to 10mm of precipitation (R10) as well as increases to the simple daily intensity index (SDII). These indicators were estimated based on averages over 20-year periods, using 1950-1969 as a reference period and then 1970-89 and 1990-2009 to examine changes. The latter period 1990-2009 had the largest increases, including an increase of 6.5 R10 days (20.3%) and on average a 20.4% increase to the simple daily intensity index. Comparing the 2046-2065 data to the same reference period, we see a change similar as for the 1990-2009 period (*Figure 3.3*), although the degree of spatial variation of the changes is greater in the 2046-2065 period.

Another indicator we examined is the amount over the 99th percentile for daily values, which are most restricted by the amount of water the atmosphere can hold. Historical data showed a basin average change of approximately 240% (Parr & Wang, 2014), much higher than the 67% for the entire Northeast found by Karl et al. (2009). In the historical record, the amount of extreme precipitation is the greatest for the years after the turn of the century (*Figure 3.4*). Compared to these years, despite continued warming, the mean of future annual extreme precipitation amount decreases by over 100mm/year. However, when compared with the whole historical record or the pre-2000 period, the future projected change is an increase, by ~31mm/year when compared to the average over the 1950-2011 period, and by 85.85 when compared to the average over the 1950-1999 period (*Figure 3.4*).

It is apparent that the strong increase of extreme precipitation amount at the beginning of the 21st century is likely a reflection of a positive phase of natural decadal fluctuations superimposed to milder increases related to continuous climate changes. For a more detailed analysis, we also examined changes of the number of extreme precipitation days. It was found that the basin mean number of extreme days is significantly greater in the early 21st Century than in the mid-century (*Figure 3.4*). There were, on average, 4.353, 4.492, and 4.300 days recorded for the three future data sets (REGCM-CGCM, REGCM-GFDL, CRCM-CGCM respectively) in 2045-2065 as opposed 6.523 days throughout 2001-2011. However, the precipitation intensity averaged over extreme days continues to increase in the future, as indicated by the time series in *Figure 3.4*, which shows a fairly consistent increase from the beginning of the historic study though the conclusion of the future projections despite large inter-annual variability.

3.3.3 Snow Pack and Discharge Seasonality Changes

One of the biggest consequences of warming for a temperate climate such as that of the U.S. Northeast is its effect on the rate and timing of snow melting. The Northeast has undergone changes including greater winter discharge and an earlier shift of peak flows (Wake & Markham 2005; Hayhoe et al. 2006). Our simulations portray decreases to snow water equivalent (SWE) throughout the cold season which is attributed to warming. Along with substantial increases to winter precipitation, the smaller winter snow pack indicates greater winter melting contributes to an increased winter runoff ratio. There is also an earlier shift in the timing of peak SWE (*Table 3.2*), accompanied by an earlier shift in peak flow. *Table 3.2* provides the historic and future SWE statistics on peak magnitude and timing as well as the timing of complete melting and the melting rate. Although the peak magnitude has decreased, our simulations suggest a faster

melting in the spring. The timing of the peak SWE has advanced, but the first snow-free day has advanced even more, indicating not only earlier but also faster melting. This shift in seasonality of snow melt has implications towards the seasonality of discharge as the monthly accumulated discharge at the gauging station shows a decrease in April (and to a less extent in May) and increases in December-March *(Figure 3.5).* April still contains the majority of the annual peak flows; however, this peak is highly influenced by snow melt occurring earlier in the year and contributing more to winter runoff. The winter runoff ratio displays a relative increase of 53% accompanied by a significant ($p \leq 0.5$) 18% relative decrease in runoff ratio during the spring. In the simulations of past variations, the winter season contained the vast majority of the lowest flow events, however, the magnitude of the lowest flows in the winter are not as severe by the mid Century.

3.3.4 Flood Risk Analysis

Intensification of extreme precipitation due to climate change is expected to increase flood risks, which is of great concern for our modern infrastructure and society. *Figure 3.6* presents historic and future flood risk at the Thompsonville, CT gauging station using NOAA's defined "action level" gauge height to indicate when flooding becomes a risk. It is clear that inter-annual variability is greater for future simulated data. In specific years, such as 2058 for the REGCM-CGCM and REGCM-GFDL data sets, there are far more days with flood risk than in the past. However, the number of years with floods is projected to decrease, making the overall annual mean of days with flood risk statistically similar for both periods. Flood events are projected to become less frequent in the mid-21st century; when a flood event does occur, it will persist for a much longer duration. Thus, individual flood event may have more damaging effects

due to its longer duration and thus severity. The large majority of these events in both past and future occur during the spring particularly when of a significant duration, although winter floods also have significantly longer durations in the future.

To better understand the projected changes in flood characteristics, an analysis on the rate and timing of snow melting was conducted. *Figure 3.7* shows the past, future, and change in SWE as well as each NARCCAP model's individual mean compared to a year with the longest duration flood event. Despite a decrease in future snowpack, the quicker melting rates contribute to the longer events. Atop the increases to mean future melting rate, 2/3 of the most extreme years show even faster snow melting and a much greater amount of melting due to a large snowpack. Therefore, majority of the major events can be attributed to melting. In addition to the faster melting rates, meteorological changes could potentially also contribute to these changing flood characteristics. As the mean duration of past flood events was typically below five days and many future events longer than five days are projected, the 5-day maximum precipitation was also examined. All three future simulations projected an increase of the 5-day maximum over almost the entire river basin, with a basin-average increase of 16.04mm when compared to historic data.

One potential area of concern when using bias correction techniques is that the patterns and signals of climate extremes may be altered, which may propagate to the hydrological extremes. As a sensitivity test, several of the same analyses were repeated based on raw data from the REGCM-GFDL model for the 1971-1995 historical period and the 2046-65 future data. As an example, *Figure 3.8* shows that the 5-day maximum precipitations, spatial patterns of change as well as general magnitudes of change are statistically similar. Both analyses indicate an increase in 5-day maximum precipitation as well as an increase to the average length of flood events, and

decreases to frequency. We also used this data to examine peak and minimum discharge and timings. From our findings there were no indications that bias correction and downscaling techniques altered the nature of our results.

3.3.5 Drought Risk Analysis

The U.S. Northeast has not historically suffered frequent or long term droughts. However, it is uncertain whether this will continue to be the case in the future, especially since ET is projected to increase as shown in Section 3.1. Droughts can be categorized as, meteorological, hydrological, and agricultural, depending on whether the detection of drought is based on precipitation, river flow, or soil moisture. Consecutive dry days can be used as an indicator for extreme precipitation in regard to intensity and frequency, and it can also be used as an indicator of meteorological drought. The number of consecutive dry days has significantly decreased in all three future simulations (*Figure 3.9*). The past mean is 15.63 days/year while the future means are: 12.42 (REGCM_CMCG), 13.17 (REGCM_GFDL), and 11.82 days/year (CRCM_CGCM). For the Connecticut River Basin, mean precipitation consistently increases, and intensity of the most severe precipitation events decreases in our future data. Frequency of rainfall is relatively stable thus displaying fewer consecutive days with little to no precipitation.

Although precipitation is the major driver of drought, soil moisture is perhaps more indicative of the dryness of the land surface and the extent to which water is available for agricultural purposes. All categories of droughts defined based on soil moisture, including short-term, medium term, and long-term drought, were found to decrease in the CRB. The basin average mean duration of droughts fell from 1.74 months in 1950-2011 to 1.57 months in 2046-2065. As the Northeast is not a region particularly plagued by frequent or persistent drought,

there are a number of cells which display little to no signal of drought. The southern section of the basin indicates the greatest drought threat and it is this area that shows the greatest decreases over time. The number of short term droughts per twenty years indicates a 26.6% relative decrease and medium and long term droughts both indicate even greater decreases surpassing 50%.

3.4 Conclusions and Discussion

This study provides a comparison between historic and future hydrological conditions in the U.S. Northeast using the Connecticut River Basin as a case study. For the historic period, results show the Connecticut River Basin experienced an increasingly wet regime with significant increases to extreme precipitation, increasing runoff ratios, wetter soil conditions, no signs of earlier snow melt, and a negligible trend in ET. Our future projections show wetter winters with significantly greater runoff and soil moisture, slight decreases to runoff during the rest of the year, enhanced ET for all four seasons, and an earlier and faster snow melting. Soil moisture increases in winter and spring, the two seasons with the most significant precipitation increases, and deceases in autumn and summer when ET increases are the greatest. Significant changes are projected for the characteristics of flooding as there is a large increase in the average duration of individual flood events, accompanied by a similar decrease to frequency of these events, which combined, accounts for a statistically similar number of days with flood risk.

The most significant change and perhaps critical change in future climate as compared to past climate is the increase to ET. A negligible trend in the past is replaced by universally significant increases throughout four seasons. The greatest is a 0.2mm/day increase to the summer ET daily mean, but relative increases indicate on average a 14% increase with the

greatest relative increase occurring during winter when the values are lowest. With warming, the surface energy budget is increased allowing more heat to be partitioned to latent heat. As long as water is available in the soil, ET is expected to increase along with temperature and net radiation, consistent with the theoretical prediction for an accelerated hydrological cycle (Trenberth 1999; Huntington 2006).

We found that the number of days with ≥10mm of precipitation and the simple daily intensity index were both statistically similar to results from the early 21st century while the amount of precipitation above the 99th percentile significantly decreases by more than 100mm/year on average across the three future data sets. However, relative to the more consistent second half of the 20th Century, the amount, frequency, and intensity of these very heavy precipitation events have all significantly increased as have R10 days and SDII. The decreased amount relative to the early 21st Century is due to a reduction in frequency of about 33%.

Other major indicators of hydrological change as a response to warming are changes to snow pack and discharge characteristics and timing. Increased temperatures have led to decreased snow pack, and the peak timing of both SWE and discharge has shifted to an earlier date. Despite the decreases in the amount of snow melting in spring, there are indications of a faster spring melting. Some of the longest lasting floods in the model occur due to melting in years with considerably greater snowpack occurring later than the advancing mean. The much larger buildup of snow pack in these specific years does not correlate strongly with colder temperatures but is due to anomalously large precipitation. The combination of increasing winter precipitation and less winter snow pack has led to significantly increased winter runoff in all three future simulations. In the historic analysis, the majority of low flow events occurred in

either the winter or summer seasons, but in the future scenarios, the lowest winter flow is significantly higher. Any change to the seasonality of snow melt, and therefore discharge, could cause complications with water availability, as it would change the magnitude and timing of the flow available for diversion or other use during other times of the year. Although similar results were found for much of the Northeast for historic data and simulations (Wake & Markham 2005, Hayhoe et al. 2006), throughout our historic VIC simulations, there were no sign of earlier peak discharge or earlier center of volume as defined by the date at which half the annual stream flow is discharged, or any indications of earlier or faster snow melt in the Connecticut River Basin. It is possible that these changes were already in early stages but had not yet manifested.

Results from this study indicate that some characteristics of floods will be changing in this region. During 2046-2065, it appears that flood events will be less frequent but each event will last longer. Projections driven by meteorological forcing derived from all three models (REGCM_CGCM, REGCM_GFDL, and CRCM_CGCM) are consistent in changes of floods characteristics. Despite the increases in winter runoff, the majority of extreme discharge events still occur during the spring. Also, a decrease of runoff during the most flood-prone season of spring may have helped alleviate flood risk to some extent. Despite the projected increase of ET, enhanced drought risk does not appear to be as relevant of a threat as flooding for the Connecticut River Basin by mid-century.

This study has facilitated a better understanding of how the hydrological processes in the Northeast may change in the near future under continued warming, and what issues and challenges this may or may not present to us. We expect an enhancement of ET, along with a shift in the seasonality of snowmelt. The decreased frequency but increased duration/intensity of the flood and very heavy precipitation events respectively suggests that these potentially

calamitous events will be rarer but potentially more economically and ecologically damaging. Although droughts do not appear an immediate concern by the mid-21st Century, the increased ET and drier summer soil moisture indicates that greater drought risk may manifest in a more distant future.

Mean Daily Evapotranspiration (mm)		
	Past (1950-2011)	**Future (2046-2065)**
DJF	0.3409	0.4491
MAM	1.4065	1.4992
JJA	2.5022	2.7048
SON	1.0405	1.1579

Table 3.1: The basin mean of daily evapotranspiration (mm/day) for all seasons in both the past (1950-2011) and future (2046-2065).

Snow Pack Magnitude, Timings, and Melting Rate				
	Historic (1950-2011)	**Regcm_Cgcm** (2046-2065)	**Regcm_Gfdl** (2046-2065)	**Crcm_Cgcm** (2046-2065)
Peak Magnitude (mm)	155.33	112.96	113.39	115.32
Peak Timing (day of the year)	62.37 (Mar. 3rd)	54.45 (Feb. 23rd)	55.30 (Feb. 24th)	52.70 (Feb. 21st)
Timing of Zero Snow Pack Remaining (day of the year)	132.15 (May 12th)	96.60 (April 6th)	99.25 (April 9th)	98.10 (April 8th)
Rate of Melting from Peak to Zero (mm/day)	2.23	2.68	2.58	2.54

Table 3.2: Basin average statistics for magnitude of snow pack, the mean date at which snow pack is at a peak magnitude, the date at which snow pack is first completely absent in the entirety of the basin, and the rate of melting from the peak time to the time of zero snow pack. Snow pack includes both ground and canopy.

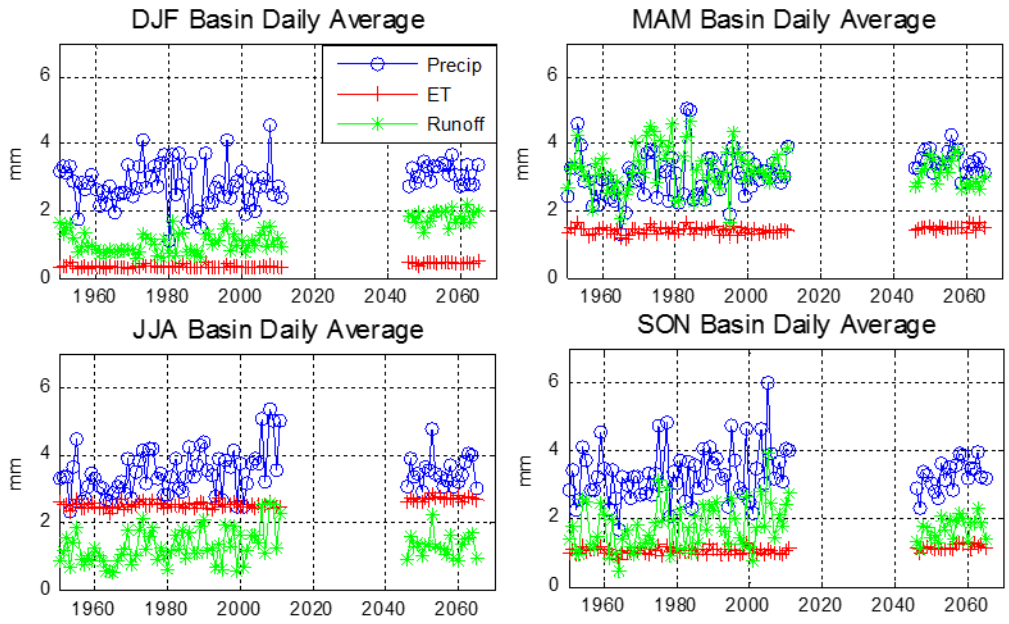

Fig. 3.1: Basin average of daily mean precipitation, evapotranspiration, and surface and subsurface runoff for all four seasons. The future results for 2046-2065 are the mean ensemble of the regcm_cgcm, regcm_gfdl, and crcm_cgcm future data sets.

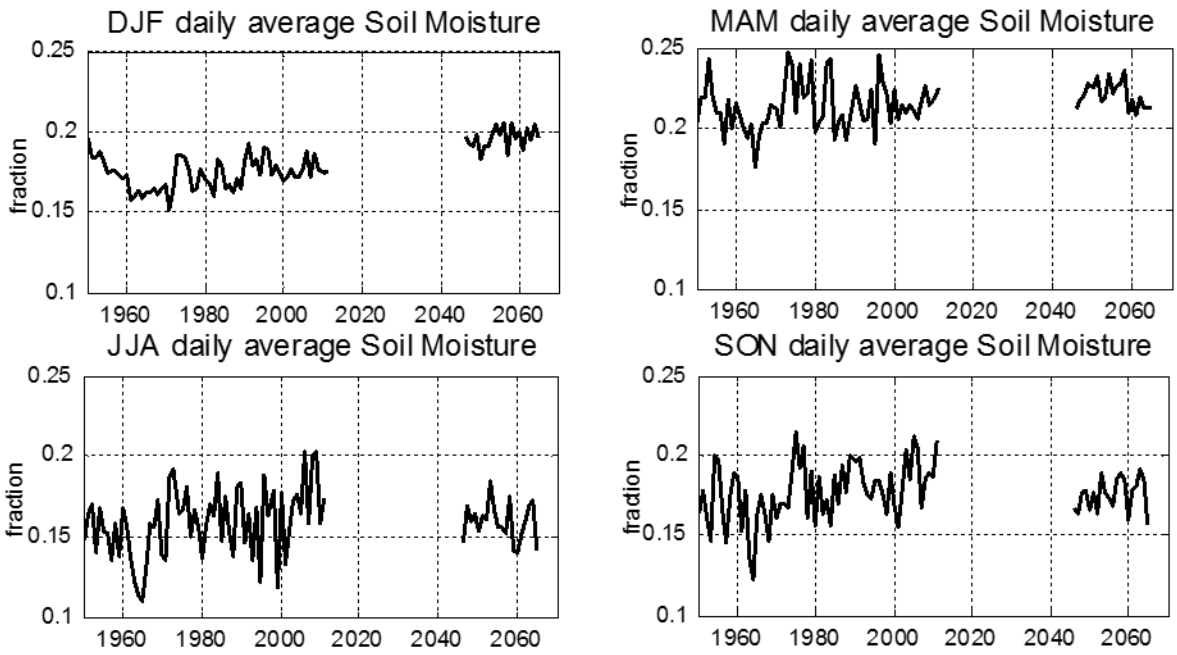

Fig. 3.2: Basin average volumetric fraction of soil moisture for each season. The future results for 2046-2065 are the mean ensemble of the regcm_cgcm, regcm_gfdl, and crcm_cgcm future data sets.

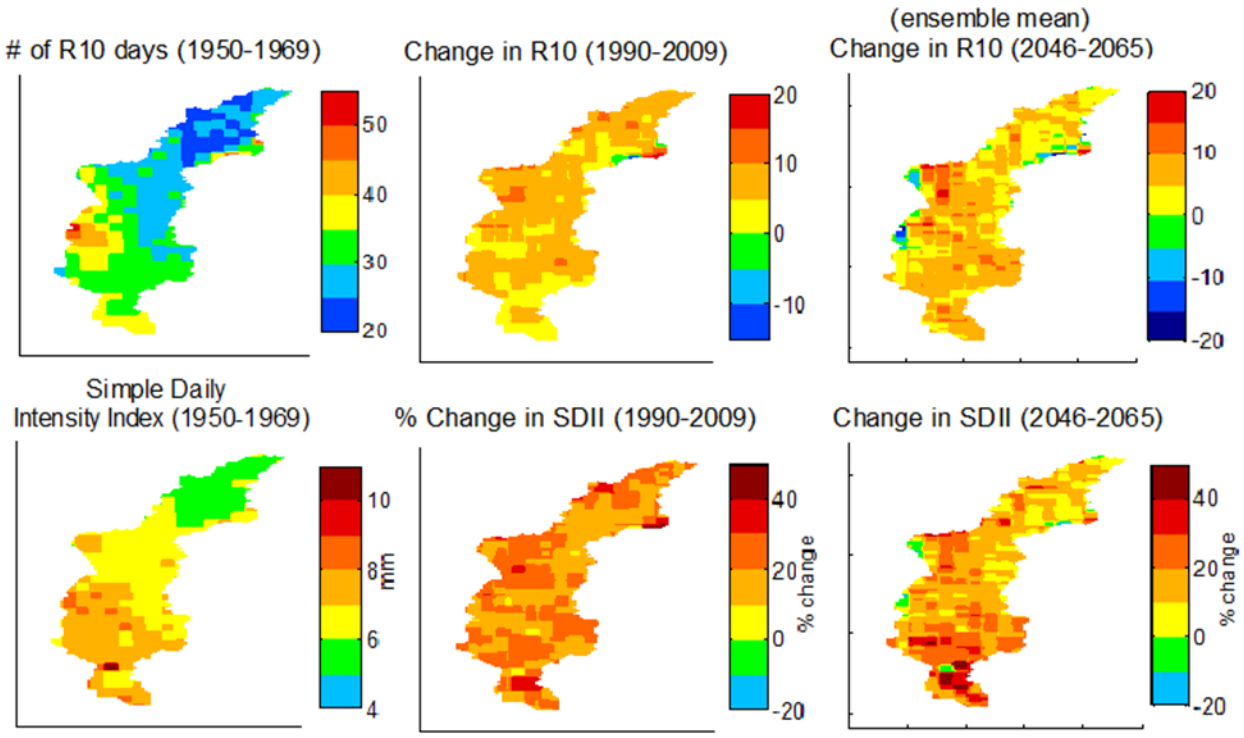

Fig. 3.3: Number of R10 days (1950-69) and change in R10 days for 1990-2009 and 2046-65, SDII (1950-69) and change in SDII days for 1990-2009 and 2046-65.

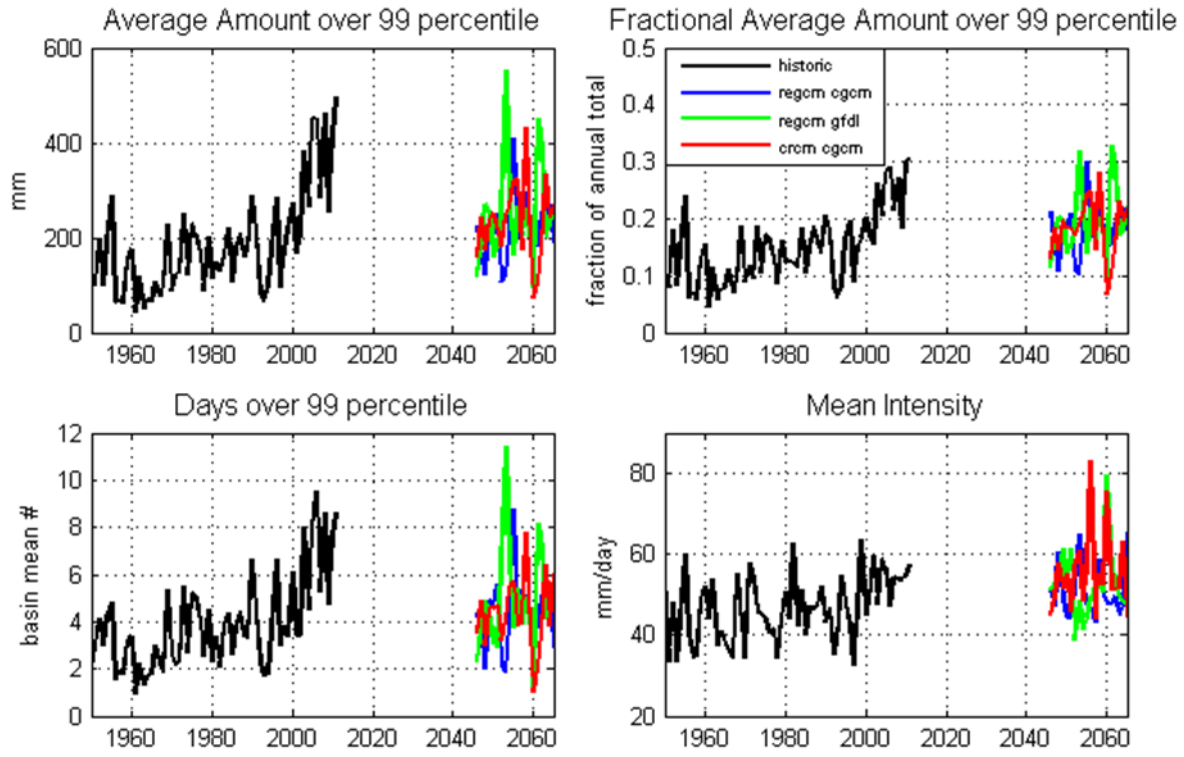

Fig. 3.4: Annual accumulated amount, fractional average amount of yearly total, basin mean number of days, and mean intensity for precipitation falling over the 99th percentile.

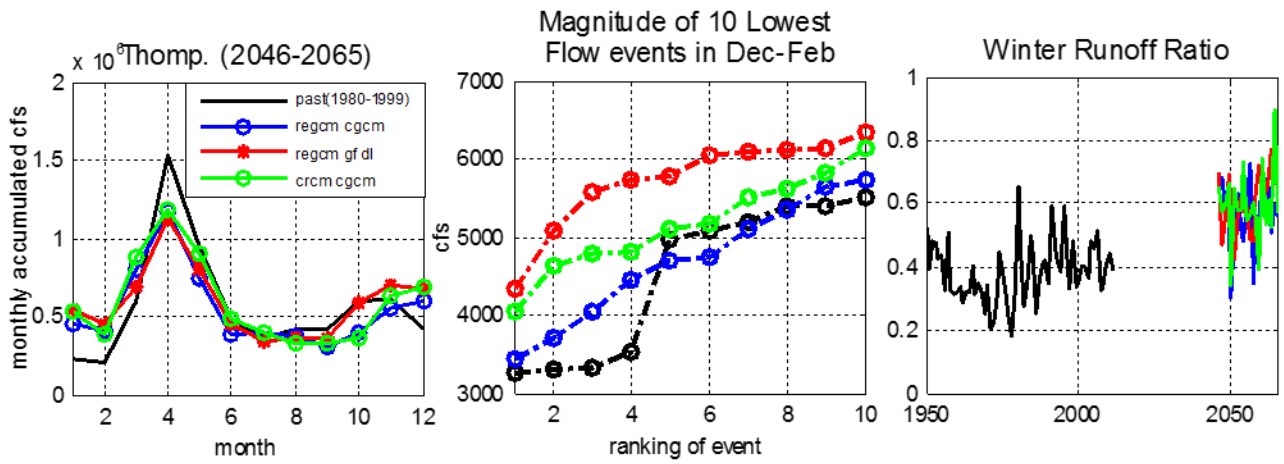

Fig. 3.5: The monthly accumulated discharge at Thompsonville station for each simulation showing the changing of seasonality of runoff (left), the magnitude of daily discharge (cfs) of the lowest 10 daily flows in the winter by ranking of event for 1992-2011 and 2046-2065 (middle), And the annual winter runoff ratio including surface and subsurface runoff (right).

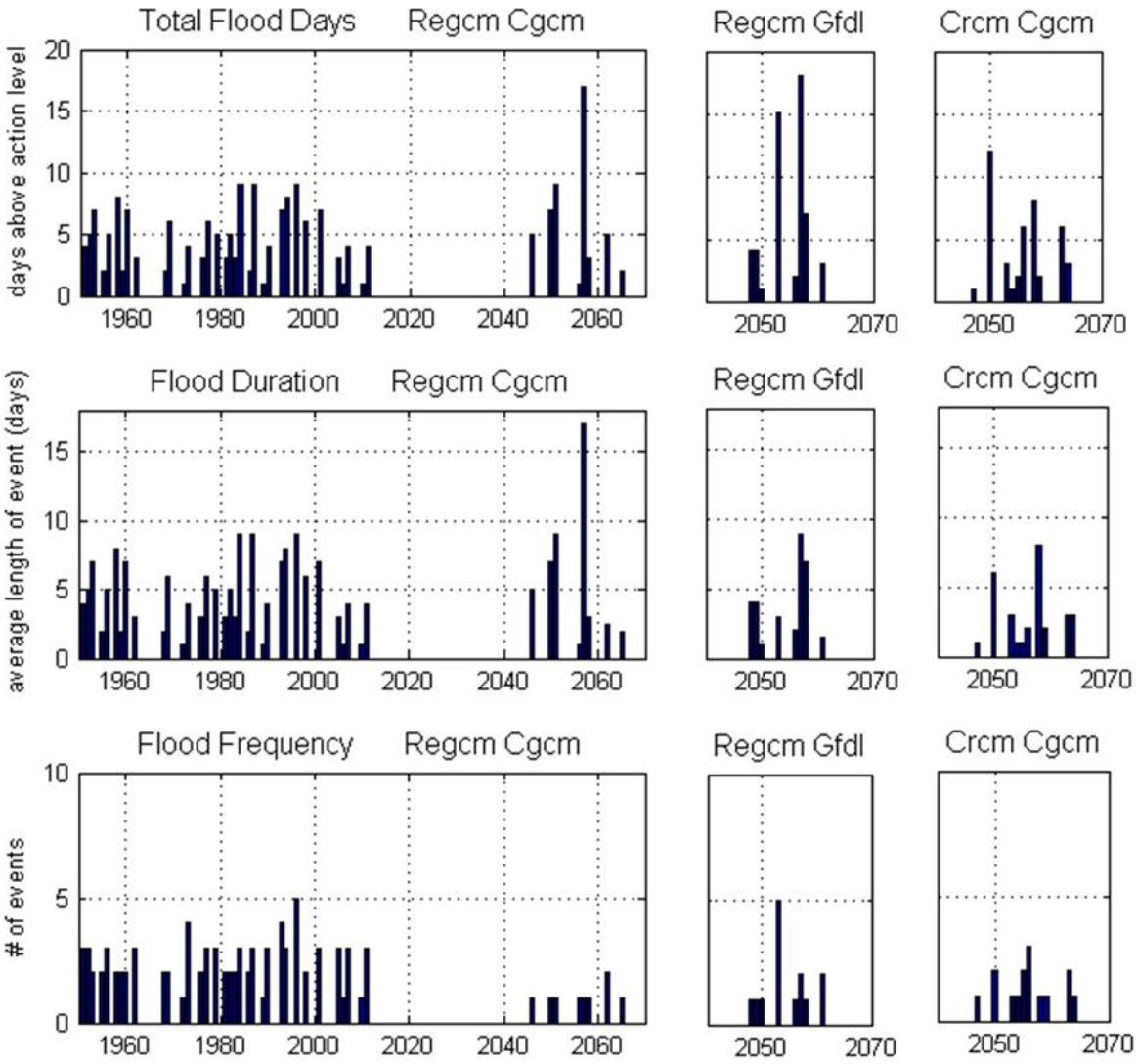

Fig. 3.6: The total flood days (top) describes the number of days each year in which the gauge height is above the "action level". The flood duration analysis (middle) shows the mean duration of events in each year, and the flood risk frequency (bottom) shows the number of events each year.

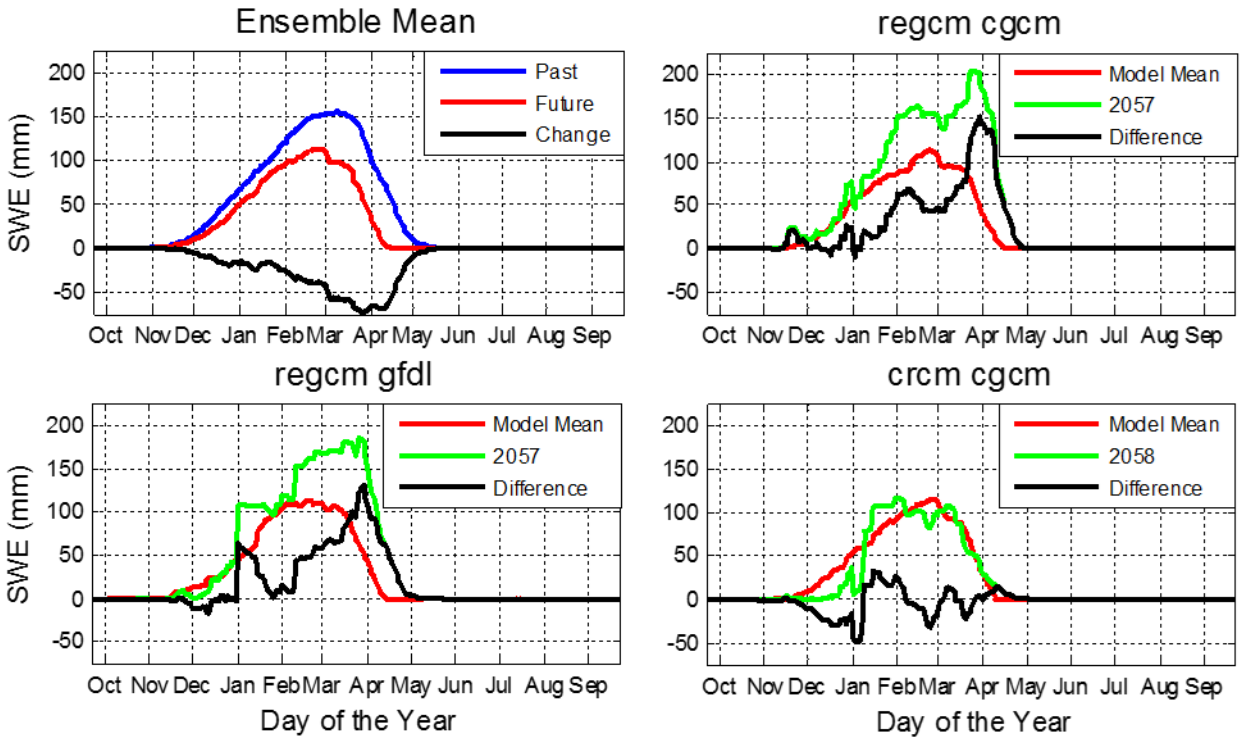

Fig. 3.7: The ensemble mean of the Past, Future, and Change in snow water equivalent (SWE) within the basin including snow pack on both the ground and canopy (top left); the mean SWE, the SWE in a specific year which showed a strong signal of flood risk duration, and their differences from hydrological simulations corresponding to forcing from the three NARCCAP models.

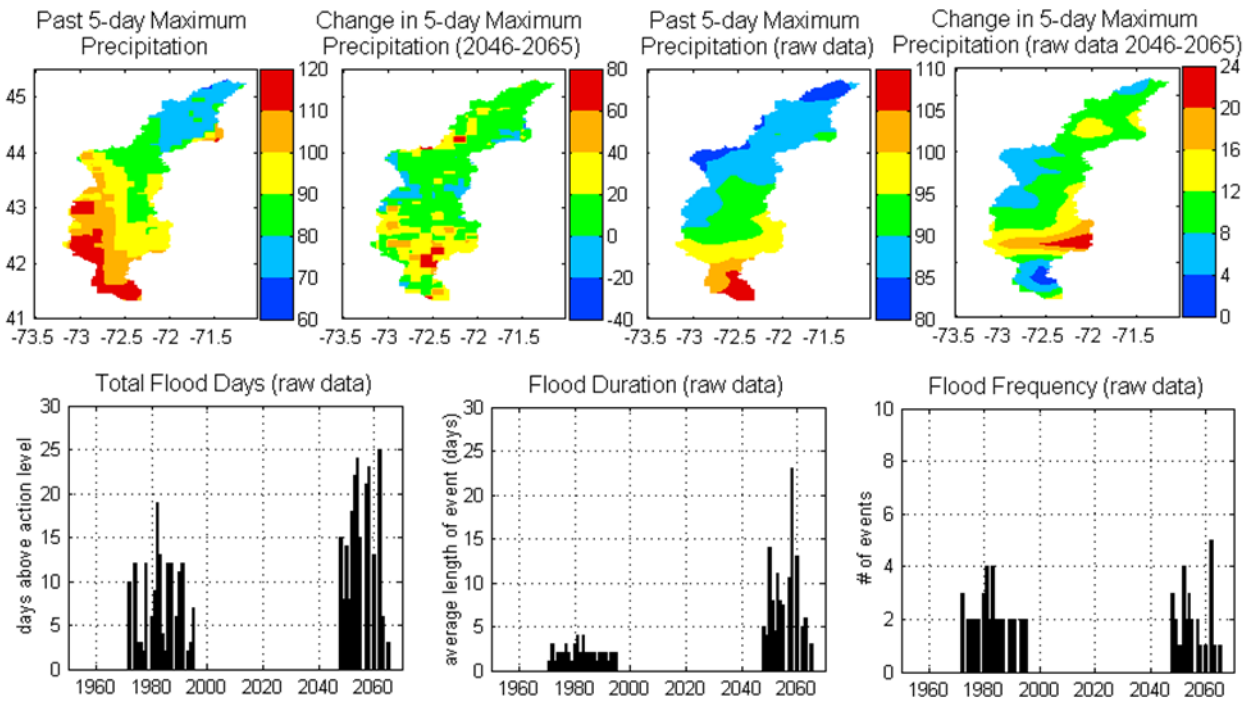

Fig. 3.8: The annual average of maximum 5-day accumulated precipitation (mm) in both the historic precipitation data and the change in the future, based on the downscaled and bias corrected data (top left) and the raw data from the GFDL model (top right); results from a flood risk analysis similar to those shown in Figure 3.6 but using the raw GFDL data without any bias correction or downscaling (bottom).

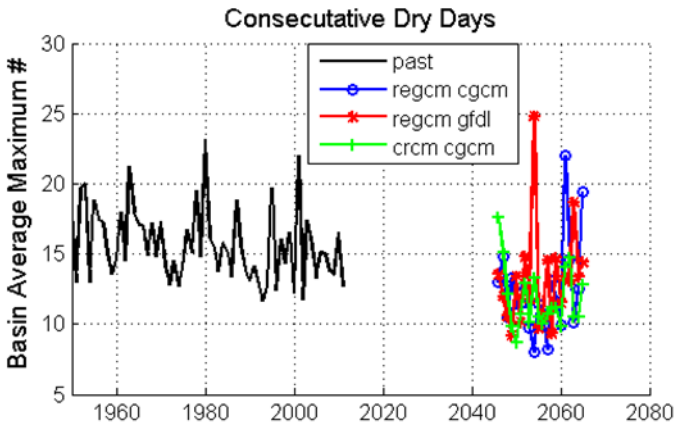

Fig. 3.9: The basin average of the maximum number of consecutive dry days in each year. A dry day is defined as a day with less than 1mm of daily precipitation.

Chapter 4

Integrating Remote Sensing Data with Hydrological Modeling

This Chapter has been accepted for publication and is currently available online:

Parr DT, Wang GL, Bjerklie, D. 2015. Integrating Remote Sensing Data on Evapotranspiration and Leaf Area Index with Hydrological Modeling: Impacts on Model Performance and Future Predictions. *Journal of Hydrometeorology,* doi: http://dx.doi.org/10.1175/JHM-D-15-0009.1

4.1 Introduction

Understanding and quantifying how climate variability and changes may influence water resources and the terrestrial hydrological cycle is of critical importance for socioeconomic development, and remains a major challenge facing the field of hydrology. In many regions, studies of past hydrological variability are hampered by the lack of reliable river flow data. These include regions where no river gauge is maintained and regions where water diversion or hydraulic structure has altered the natural flow. Hydrological models provide an important tool for re-constructing and understanding past hydrological variability, and for quantifying future hydrological changes.

Evapotranspiration (ET) is an important component of the terrestrial hydrological cycle. As an important pathway for land-atmosphere interactions, ET influences the surface water, energy, and carbon fluxes (Xia et al. 2014). However, ET is a particularly difficult process to accurately measure or simulate. In the study of Kite and Droogers (2000) using eight different methods of estimating actual evaporation and transpiration including field data, hydrological models, and the early generation of satellite data, a wide range of ET estimates emerged from the various methods, and no method is evidently better than others. Another study (Weiß, M and Menzel 2008) compared four different equations for potential ET to assess their impact on stream flow simulation, and found that results based on each equation differ substantially from one another. Together with many others on this topic (McKenney et al. 1993; Eitzinger et al. 2002; Lu et al. 2005; Helge 2011; Trambauer et al. 2014), these studies highlighted the need to explore innovative approaches to improving the accuracy of ET estimation in hydrological models.

In a recent study on hydrological modeling for the Connecticut River Basin using the Variable Infiltration Capacity (VIC) model (Parr and Wang 2014), model ET was compared

against the ET data derived from Advanced Very High Resolution Radiometer (AVHRR) and the International Satellite Land Surface Climatology Project Initiative II (ISLSCP-II) (Fisher et al. 2008), and a significant underestimation of ET (especially in summer) was identified. The summer (June, July, and August) underestimation of ET by the VIC model identified by Parr and Wang (2014) ranged from 20 to 30 percent as compared to Fisher et al. (2008). It is not clear whether the underestimation of ET by VIC results from the estimation of potential evaporation by the Penman-Monteith equation used in the model (which requires several parameters difficult to characterize) or due to limiting soil moisture storage. A general underestimation of ET (and therefore overestimation of runoff ratio) was also documented in several other studies using the VIC model (e.g., Xia et al. 2014, Vano et al. 2012, Sheffield et al. 2012). Recently, Xia et al. (2014) based on NLDAS-2 output compared the output of four land surface models including VIC to eddy covariance data at 46 AmeriFlux tower sites, and found that VIC had the lowest ET of all the models and was less than observation for most of the year, but particularly in the summer.

Given the model bias in simulating ET in the past, future hydrological predictions (e.g., Parr et al., 2015a) may also be subject to similar model biases, leading to substantial uncertainties in the model-generated future hydrological trend. In particular, a major challenge and uncertainty in modeling stream flow is related to the difficulty in realistically modeling the ET process. Although ET is biased low, VIC stream flow has been shown to be more accurate than the Noah or Mosaic Models (Xia et al. 2012) using the same NLDAS-2 forcing data. In this study, we integrate ET remote sensing data with hydrological modeling using VIC, and examine how more accurate ET in the model may influence model performance in simulating other hydrological processes.

Vegetation is an important land surface state variable that profoundly affects both the long term and seasonal dynamics of all components of the water cycle (Wattenbach et al. 2012). There are a number of vegetation parameters within the VIC model, including roughness length, displacement height, architectural resistance, minimum stomata resistance, and rooting depth. However, leaf area index (LAI) has the greatest influence on hydrologic simulations in VIC (Ford and Quiring 2013). In this study we replace the model's typical system of using a climatological or static LAI with an inter-annually varying dynamic LAI in order to improve the model simulation of inter-annual variability of hydrological processes.

A large number of past studies have applied remote sensing data to hydrological models. Dynamic vegetation parameters have previously been employed in land surface models (LSMs) typically in the form of LAI acting as a model input parameter for purposes such as investigating the impacts on long term and seasonal dynamics of the water cycle (Wattenbach et al. 2012), on the predictability of ET patterns (Tang et al. 2012), on potential improvements of stream flow (Zhang et al. 2011; Zhou et al. 2013), and on soil moisture (Ford and Quiring 2013). Soil moisture has been employed in hydrological models as a forcing to improve estimates of actual ET (e.g., Ottle and Vidal-Madjar 1994), and to improve runoff estimates and regional model calibration (e.g., Zhang et al. 2011). Remote sensing-based ET data has been used in past hydrological modeling, but primarily for model calibration purpose in identifying the model parameters that best reproduce the ET data (e.g. Immerzeel and Bold 2008).

Here, we propose a new approach to improve hydrological modeling and prediction using ET remote sensing data, in which the data is used to support a bias-correction procedure that can be applied to the model for any time period. Using the Connecticut River Basin as an example, this study assesses the extent to which remote sensing data can help improve hydrological

modeling and how it may influence future hydrological trends. In the following, section 4.2 provides a description of the data sets utilized, and our experimental design. Section 4.3 describes the results including both model improvements and the impact on hydrological trends with a focus on extremes such as flood and drought risks. Section 4.4 provides a summary considering model-related uncertainty and the sensitivity of the model results to the choice of the ET dataset, as well as a discussion based upon the results found.

4.2 Data and Methodology

4.2.1 Data Sets

The model used is the Variable Infiltration Capacity (VIC) Model v.4.1.2.g (Liang et al 1994). In earlier studies, we have applied VIC to the Connecticut River Basin for past simulation and future projections. The simulation for the past was driven by the NASA Land Data Assimilation System phase-2 (NLDAS-2) forcing data for the period 1980-2011 (Parr and Wang, 2014), and future projections for the period 2046-2065 were driven by downscaled and bias-corrected output from three North American Regional Climate Change Assessment Program (NARCCAP) models. The NARCCAP models (Mearns et al., 2012) from which the three future forcing was derived include the Regional Climate Model version 3 (RegCM3; Pal et al. 2007) driven with lateral boundary conditions (LBCs) from the Canadian Climate Centre Coupled General Circulation Model version 3 (CGCM3) (REGCM-CGCM), RegCM3 driven with LBCs from the Geophysical Fluid Dynamics Laboratory Climate Model (GFDL) (REGCM-GFDL), and the Canadian RCM (CRCM; Caya and LaPrise 1999) driven with LBCs from CGCM3 (CRCM-CGCM). The future daily meteorological forcing from each RCM-GCM combination was first downscaled to 1/8 degree resolution and bias-corrected using the methodology of

Ahmed et al. (2013). Based on quantile mapping between the cumulative distribution function (CDF) of a model present day climate and that of observations, the downscaling and bias correction algorithm of Ahmed et al. (2013) was developed based on the bias correction and downscaling method in Wood et al. (2002, 2004), but with modifications for application to daily model output and modifications to the procedure to take full advantage of the fine resolution observational data. While the metrological forcing is at 1/8-degree resolution, the model simulations are run at a 0.025 degree resolution in order to incorporate fine-resolution topographical data and land cover data. Therefore, all 25 grid cells within each 1/8-degree box share the same meteorological forcing. The surface water (and energy) balances in VIC are solved at each 0.025-degree grid cell.

The land cover data in this study was taken from the University of Maryland's Global Land Cover Facility, DEM was taken from the USGS HYDRO1k project, and soil data including soil type and texture, porosity, and bulk density were taken from National Oceanic and Atmospheric Administration's (NOAA) National Geophysical Data Center (NGDC) (Reynolds et al. 1990). The vegetation data used is the leaf area index (LAI) data derived from Moderate Resolution Imaging Spectroradiometer (MODIS) sensors aboard the polar-orbiting Terra and Aqua satellites. The LAI data has an 8 day temporal resolution from which a monthly average is derived and a 1km spatial resolution matching our land cover data set. The ET data, spanning 1986-1995, was from Fisher et al. (2008) with monthly and 0.5-degree spatial resolutions. As ET flux cannot be remotely sensed, it is estimated according to a surface radiation budget algorithm with net radiation, air temperature and water vapor pressure taken from the ISLSCP-II and visible spectrum reflectance and near-infrared spectrum reflectance gathered with AVHRR. This ET product has been validated over 36 FLUXNET towers sites, with an R^2 value of 0.90 and a

7% bias (Fischer et al. 2008; Fisher et al. 2009). As eddy flux sites generally achieve about 90% closure for an energy balance with 10% of the variation unexplained, for a product like this we would not expect any R^2 value much greater than 0.90 (Fisher et al.2008). Vinukollu et al. (2011) compared three remote sensing ET products (including the Fisher et al. 2008 product used here) and VIC and ERA interim reanalysis estimates. It was found that the product used in this study had the lowest bias of annual ET over 26 basins and the highest correlations of monthly mean latent heat flux compared with tower observations.

For discharge simulation and analysis, the USGS #01184000 station at Thompsonville (CT) is used, which had been identified as a reliable station in previous research (Bjerklie et al. 2011, Marshall and Randhir 2008). Also used is the station #01144500 located north and upstream at West Lebanon (NH). Remote sensing data from the European Space Agency's (ESA) Essential Climate Variable (ECV) surface soil moisture product is also utilized to compare potential model improvements. This product (Naeimi et al. 2009, Dorigo et al. 2010, Liu et al. 2012) is a merged data set from both active and passive microwave measurements, and has a spatial resolution of 0.25 degrees.

4.2.2 Experimental Design

Several different types of simulations are conducted. One uses the default VIC model calibrated for the CRB (Parr and Wang 2014), referred to as "VIC". VIC was calibrated using the USGS river discharge observations at Thompsonville, CT for the first 10 years of each simulation (1950-1960 and 1980-1990 respectively). The suggested calibration parameters such as the variable infiltration parameter ("b_infilt"), the soil parameter controlling when non-linear baseflow occurs ("D_s"), the fraction of maximum soil moisture where non-linear baseflow occurs

("W_s"), maximum baseflow velocity ("D_{smax}"), and soil layer depth were adjusted such that discharge best matched USGS observation in terms of both magnitude and variation on a variety of different timescales (Parr and Wang 2014). The model was then verified using discharge data at both the Thompsonville (CT) and West Lebanon (NH) stations for the rest of the simulation period as well as remotely sensed ET and soil moisture. A more descriptive explanation of the default VIC model and its calibration and validation process for the Connecticut River Basin can be found in Parr and Wang (2014).

The VIC model requires LAI data as model input; however, it uses the climatological LAI with a seasonal cycle, and does not include inter-annual variation. This type of LAI condition is referred to as "static vegetation" hereafter. In a second type of simulations ("VICVEG"), for more realistic representation of vegetation, the MODIS LAI data is used as model input. The MODIS LAI includes not only seasonal but also inter-annual variations of vegetation captured by the remote sensing data. This type of vegetation condition is referred to as "dynamic vegetation" hereafter. In simulations with dynamic vegetation, the model was adjusted to read in different seasonal LAI data sets for each year of a simulation (*Figure 4.1*), although the fraction of various land covers does not change. Within the model, LAI quantifies canopy cover and influences the maximum amount of water intercepted by the canopy, canopy resistance and root water uptake and therefore evapotranspiration rates (Liang et al 1994). The use of the MODIS-derived LAI can therefore potentially improve the simulated seasonal and inter-annual variability of the surface water budget. It should be noted that since the climatological LAI is from a different source, the evaluation of performance and potential improvements will focus on temporal variations rather than the magnitude, particularly at the inter-annual timescale.

In another type of simulation, the model-simulated ET components were overwritten to correct the ET bias identified based on the comparison of ET from a default model simulation with ET data derived from remote sensing. This procedure therefore involves a pair of simulations. The default VIC calculates the potential ET based on atmospheric forcing using the Penmen-Monteith equation and then derives the actual ET based upon water availability. The model calculates each of the five components of ET (canopy evaporation, transpiration, bare ground evaporation, canopy sublimation, and surface sublimation) separately, at daily or hourly time steps, while the ET data is monthly. In this study, the monthly average of model ET from a default run is compared with the "observational" ET (from remote sensing data) during 1986-1995 to calibrate a ratio between the two, and this was done for each grid cell for each of the 12 months. The resulting ratio, which varies spatially and seasonally, is then used to scale the model-simulated five ET components (at the model native resolutions both spatially and temporally) for any period of interest assuming stationarity of the model-observation relationship. As the remote sensing-based ET data cannot distinguish the five different components of ET, all five are scaled equally, and this scaling ratio is specific to a grid cell and a particular month. The resulting data for the five ET components (referred to as the corrected ET components) are then used to overwrite the model simulated values in a re-run of the simulation, and this type of simulation is referred to as "VICET". As such, in the VICET simulation, the use of ET data prevents the inaccuracy of ET parameterization from propagating to other hydrological variables (including for example runoff and soil moisture) thus correcting the bias of the model hydrological processes caused by inaccurate ET parameterization. *Figure 4.2* provides a schematic diagram describing the procedure of implementing the ET bias correction algorithm into hydrological modeling.

Note that overwriting a model variable with a prescribed value often causes violation of mass and/or energy conservation. When a violation does occur, depending on specific processes related to such violation, a corresponding procedure will be triggered in the model to adjust the values of related variables (including the overwritten variable itself) so to conserve mass and energy thus maintaining physical realism. For example, if in a given time step the prescribed canopy evaporation amount is greater than the current storage of the canopy, it will be reduced back to the value of the canopy storage. Likewise, ground evaporation cannot exceed what is currently stored at the surface, and transpiration will not deplete soil moisture past the wilting point. As VIC derives its estimates of soil moisture and runoff after ET estimates, mass balance is compensated for primarily through these variables, and there are mass checks within the model which will reiterate a time step adjusting physically unrealistic values. As a result, water imbalance in the VICET simulations, when present, remains minimal. The remote sensing-based observation, default model simulation (VIC) and the simulation including ET bias correction (VICET) are compared in *Figure 4.3*. The VICET simulation was run over the period 1980-2011, which is the span of the NLDAS-2 forcing data.

Lastly, a combination model (VICET+VEG) was also run for the time period with LAI data available, in which LAI has minimal effect on ET due to the use of prescribed ET. LAI's effects are more limited, but still alters potential canopy storage, interception, infiltration, and root uptake. The VICVEG and VICET+VEG model simulations are run for the period 2003-2011 due to the more limiting availability of LAI data. *Table 4.1* summarizes the four different experiments and the acronyms used to describe them.

It is expected that after incorporating these data, the data-enhanced model will perform significantly better in simulating river discharge, its magnitude, seasonality, timing, soil moisture

and its temporal variation as well as long-term trend. This will facilitate a more accurate understanding and attribution of past hydrological variability/changes. In addition, the difference between the default model results and the data-enhanced model results will help characterize the range of model-related uncertainties. To quantify the model improvement in simulating river flow attributed to the use of remote sensing data, a significance test was done to determine whether the correlation coefficient between model and observed river flow in an experiment is significantly different/higher than that in the default VIC run. The null hypothesis here is that the correlations are not different from one another, and the Fisher's test is used to determine the significance of the differences.

Assuming that the relationship between the remote sensing ET data and the default model simulation stays stationary, future simulations for both the default model (VIC) and the data-enhanced model VICET can be run for a future period 2046-2065 using meteorological forcing derived from the NARCCAP models output. This allows for an examination of the impact of the ET bias correction on the simulated long term trends of hydrological processes. Those of interest include hydrological extremes such as peak and minimum discharge magnitude and timing, floods, as well as water cycle fluxes and drought.

4.3 Results

4.3.1 Model Improvements

Due to data availability, the primary method for determining the model simulated improvements is by comparing the various simulated discharges to observation. The river flow was simulated using the default model (VIC) as well as each data-enhanced version (VICET, VICVEG, VICET+VEG). Due to the nature of the alterations made to the various model

versions, the impact on model results is expected to manifest at different temporal scales. The prescribed ET is devised off of month-specific relationships between observation and simulation, and the relationships do not vary from year to year, whereas the MODIS LAI incorporated into the model is specifically designed to introduce inter-annual variations into the model. Our analyses are therefore conducted at several temporal scales, ranging from daily to inter-annual.

Compared to the default VIC simulation, the seasonal cycle of discharge in VICET (*Figure 4.4*) shows great improvement. This specific analysis excludes the calibration period in which observational data was used to calibrate the observation-model ET relationship. The results therefore indicate how the relationships hold and whether they are capable of improving the model performance for time periods when observational data is not available. *Figure 4.4* clearly displays that the dominant improvements made to the seasonal discharge occurs during the summer and, to a lesser extent, the fall months. This is due to the greatest changes in ET between the default and VICET model occurring during these months. As the default model did best at estimating ET in the winter and spring months, there is not much room to further improve runoff simulations in those season. The correlations for *Figure 4.4* as well as correlation improvements on the daily, bi-weekly, and monthly timescale can be found in *Table 4.2*. Due to the nature of the enhancements made to VICET, improvements were intended to manifest particularly on the seasonal scope, but the summer and fall months match observation accurately in both magnitude and variation. There are also substantial significant improvements on the monthly, bi-weekly and the even finer daily timescale.

When comparing the improvements of all four model versions in a single graph (*Figure 4.5*) it is clear that the VICVEG model does not show any marked improvement on the seasonal cycle timescale. In the summer months, when the impact of the ET bias correction is greatest, the

dynamic LAI is lower on average than the climatological LAI used in the default model (*Figure 4.1*). It is due to this reason that ET is decreased during these months, providing a greater overestimation of stream flow than with the default model. Perhaps more important than magnitude, the dynamic LAI does not appear to better capture the average seasonal variations. The results for the VICET+VEG combination model also very closely resemble those of the VICET model on the seasonal scale. In addition to improvement at the seasonal timescale, improvements on the bi-weekly timescale were also achieved *(Figure 4.6*) for both the VICET and VICET+VEG models. *Table 4.3* contains the correlations, and root mean square errors for every model version for the period of 2003-2011. Whereas the daily, biweekly, and monthly time series are simply the accumulated values in each period, the seasonal cycle is the long term average of each month's accumulated discharge, and the inter-annual variability is computed based on the normalized anomalies of discharge in each month to remove the impact of seasonal cycle (i.e, subtracting the long-term mean of each month from the discharge time series, and normalizing the anomalies with the standard deviation of that corresponding month). *Table 4.3* exhibits just how important the timescale analyzed is towards the impact of data enhancement on improving stream flow estimates. Although the VICVEG model does not show any improvements on the finer timescales, it is more capable of enhancing the accuracy of stream flow on the inter-annual timescale (*Figure 4.6* and *Table 4.3*) due to the introduction of the inter-annually varying LAI.

The combination model (VICET+VEG) shows improved stream flow estimates on every timescale analyzed, achieving the strongest correlations on the daily, bi-weekly, monthly, and seasonal cycle timescales. In addition to the inter-annual monthly analysis, the inter-annual variability of each season was examined separately (*Table 4.4*). The VICVEG model better

captures variability particularly in the winter and spring and not as much in the fall or in the summer months, despite many of the dynamic variations in LAI occurring in the winter and summer months.

The improvement of model performance in simulating runoff and river flow indicates that the model performance in simulating soil moisture must have been improved too. The combination model VICET+VEG does indeed produce a seasonal cycle of soil moisture which better matches the variations of the observational seasonal cycle including the summer season decrease (which is not as well captured by the default model). This is consistent with the improved seasonal cycle of discharge. However, there is disparity in terms of magnitude between simulation and remotely sensed soil moisture, as the model top soil layer is 10cm thick while remote sensing soil moisture pertains to the top 2-3cm of soil surface. Further comparisons are therefore not presented here as they are subject to larger uncertainties due to the depth scale mismatch.

4.3.2 Hydrological Changes and Trends

After establishing that the data-enhanced models are capable of more accurately reconstructing past variability and magnitude of stream flow, it is important to examine whether the historic and future hydrological changes and long term trends produced by the data-enhanced model may differ from those produced by the default model. This is especially the case for the VICET model since the impact of the ET data enhancement is not limited to the period when ET data are available and is therefore applicable to future predictions. Interestingly, it was found that the VICET model future predictions differ greatly from the default model in not only the

magnitude, but also in some cases, the direction of changes of water cycle variables including some extreme indicators.

Daily peak and minimum discharge were analyzed in terms of both magnitude and timing for the Thompsonville, CT station. Although there was minimal difference in the peak flow changes between the two models, the minimum discharge analysis shows drastic changes. Between our historic (1980-2011) and future (2046-2065) simulations, the default model displays a change in the multi-year mean of the annual minimum daily flow from 2,734 to 3,443 cfs, equivalent to an average increase of 12 cfs/year. However, the VICET model produces a changing mean from 1,592 to just 607cfs, equivalent to an average decrease of 13 cfs/year. To provide some context, the default model daily mean flow decreased from 21,336 to 18,094 cfs between historic and future periods, a 15.2% relative decrease, and VICET daily mean flow decreased from 16,843 to 14,016 cfs, a 16.8% relative decrease. In addition to the opposite trends of the minimum flow magnitude, the mean timing of the daily minimums (which typically occurs in summer or fall) was delayed 22 days from September 16th to October 8th for VICET and only delayed 14 days from August 23rd to September 6th for the default model. *Figure 4.7* shows the 5 day minimum discharge as well as the center of volume defined as the date at which half the discharge passes through the discharge station as an indication of seasonal timing. The 5 day minimum discharge has a similar trend to the absolute minimum discharge in each of the model simulations, with the two simulations producing opposite trends. The center of volume, which does not change much between past and future in the default model, shows an earlier date in VICET.

The future flood risk analysis conducted in this study is based on river discharge using the same methodology of Parr and Wang (2014). The analysis compares past and future simulations

by adjusting VIC simulated discharge based on the correspondence found between observational and VIC simulated discharge derived from the past climate and a rating curve derived from observational data. Specifically, a rating curve was first derived based on past observational discharge and gauge height for the Thompsonville, CT station from data provided by USGS. Second, the correspondence between observational and VIC simulated discharge was derived from the past climate. The derived gauge height data were then used to analyze the flooding risks with reference to the "action level" gauge height (the height at which flooding becomes a risk and actions should be taken) for Thompsonville determined by the National Weather Service Advanced Hydrologic Prediction Service from NOAA. The flood analysis showed a fairly dramatic future change in characteristics when analyzed based on output from the default VIC model (Parr and Wang, 2014). The changes include an increasing duration of floods with a decreasing frequency, leading to a similar number of total flood days. Output from the ET-enhanced model produces the same change characteristics, with no qualitative difference in the future change signal between VIC and VICET (*Figure 4.8*).

A drought analysis was also conducted which measures the change in drought signals between the future and historic scenarios for both model versions. It is adapted from a similar one conducted by Sheffield and Wood (2007) where their percentile was based on monthly rather than daily data. In this study, for each grid cell in the basin, a month-specific 20^{th} percentile daily soil moisture threshold was identified based on historic (1980-2011) data. If soil moisture was below this threshold for 15 or more days in a specific month, it was considered a drought month for that specific grid cell. The mean duration of droughts and the number of short (4-6 months), medium (7-11 months), and long (≥12 months) term droughts, were then identified. *Figure 4.9* displays a clear and fairly drastic difference in trends between the two model versions. The

default VIC model produces little to no change in drought for any of the categories, but VICET predicts universal increases. The influence of model version is evident when comparing the difference in trends shown in the right-most column. The future increase of the mean drought duration changes from 0.21 months for the default VIC model to 4.48 months for VICET. The future increase in the quantity of the droughts changes from 0.72 for the default VIC model to 12.66 for VICET for the number of short term droughts per 20 years, from 0.80 to 5.12 for the number of medium term droughts per 20 years, and from 0.54 to 1.80 for the number of long term droughts per 20 years. The VICET future scenario is capable of having such a large number of drought hits due to the percentile threshold used to define droughts being taken from the default historic scenario. Due to an increase of ET in VICET compared with VIC and an increase of ET in the future scenarios, the soil moisture is substantially less in the VICET future than in the VIC historic scenario which the drought threshold was based upon.

To understand the results shown in *Figures 4.7* and *4.9*, the differences between the two model versions in water cycle variables and their change between the historic and future scenarios (*Figure 4.10*) are explored. There exists no observable difference between the two model versions in seasonal trends from the past to future for direct surface runoff or subsurface runoff, including groundwater and interflow. However, as one might expect from the response of drought characteristics, a larger magnitude of increase in future ET is produced by the VICET model specifically in the summer season when droughts are most likely to occur, and a decrease of summer soil moisture in VICET is not simulated in the default VIC model.

4.4 Summary and Discussion

Incorporating remote sensing data into the VIC model has made a measureable improvement towards recreating historic river flow estimates in the Connecticut River Basin. The improvements indicate that incorporation of remote sensing information into hydrologic models can improve model accuracy and insight into current and future hydrologic processes, and help characterize the model-related uncertainties in hydrological predictions.

Hydrologic modeling can be affected by four main sources of uncertainty (Renard et al. 2010), including input uncertainty arising from sampling or measurement errors, output uncertainty related to analysis such as with rating curves, model uncertainties arising from the oversimplification or representation of hydrological processes, and existing parametric uncertainty reflecting the inability to specify exact values of model parameters for a variety of reasons (Renard et al. 2010). In this study we have attempted to minimize the input uncertainty involved in LAI with more accurate and specific data, and replaced model uncertainty in representing the ET process with input uncertainties related to ET data. Remote sensing data is chosen for this study due to its high spatial coverage as the ultimate goal is to improve model estimates within basins without accurate stream flow or ground based measurements. Potential uncertainties related to the choice of the ET data can be examined based on the relationship between the simulated and observed data sets at the grid cell level. This relationship is very similar between the Landflux dataset used in the study and the MODIS ET dataset of Mu et al. (2007). The Landflux data was chosen for use here over the MODIS ET data for better spatial coverage, as the MODIS ET data is missing for some grid cells within our model domain. The relationship between the default VIC model ET and remote sensing ET data applied in this study is based on a simple ratio bias adjustment. The bias correction algorithm based on this month and grid cell specific ratio leads to adjustment to both the mean and variance of the model ET, but

majority of the differences in model performance and in future projections are due to adjustment of the mean ET. As such, the use of an alternative, more sophisticated bias correction approach is not expected to result in qualitative changes in the results of this study. As any gridded meteorological forcing data contains a certain degree of biases, the ET bias correction implemented here corrects for not only model bias but also potential forcing errors. This may contribute to uncertainties in the application of the methodology to future predictions.

As for the choice of LAI data sets, the MODIS data provides the most accurate estimates available with good spatial coverage and fine spatial resolution, and was used in the majority of similar studies examining the impact of including dynamic LAI (Wattenbach et al. 2012; Tang et al. 2012; Zhou et al. 2013; Ford and Quiring 2013). For the LAI and FPAR data retrievals, there have been algorithm refinements targeted to be consistent with field measurements over every type of biome but with particular focus on woody vegetation which is the most prominent biome found in the Connecticut River Basin.

In conclusion, the incorporation of the remotely sensed data is capable of creating statistically measureable model improvements particularly towards the estimations of river flow. Due to the nature of the alterations made to the various model versions, improvements manifest on different temporal scales. As the prescribed ET is devised off of monthly relationships of daily ET at the grid cell level between observation and simulation, it is the seasonal signal that shows the greatest improvements in stream flow. The MODIS LAI incorporated into the model is specifically designed to introduce inter-annual variations into the model, so it is not surprising that it is on this particular scale that we see its performance enhanced the most. However, more notable are the VICET model version improvements which occur on a variety of time scales, including improved estimates of stream flow variations on the finer daily and biweekly scales.

The observational soil moisture data set from the ESA which uses active and passive microwave data is only able to capture the top 10cm of the soil. The difficulty to retrieve soil moisture from remote sensing likely also contributes to the differences between simulations and observation.

Another interesting finding from this study was how the VICET+VEG combination model was able to find a balance between the other two enhanced versions displaying the most significant increases on the seasonal, monthly, bi-weekly, and daily scales, as well as still slightly improving the performance at the inter-annual timescale. As it incorporates the prescribed ET, it was possible that the effects of the dynamic LAI would be marginalized as one of LAI's greatest impacts is on transpiration and the surface energy budget.

The VICVEG model better captures variability particularly in the winter and spring and not as much in the fall or in the summer months. The spring season improvements could be accounted for by changing greening onset dates which are particularly important to the hydrology of this region during these months, and the winter seasons display some of the greatest variations from year to year in terms of LAI; however so do the summer months, so this lack of improvement is difficult to account for, but may be due to ET being more restricted by water availability and thus less dependent on the effects LAI would have on transpiration.

The ET ratio is applied to all 5 components of ET equally and it is possible this may result in changes where and when such changes are not needed. For example if PET is estimated reasonably well, the canopy evaporation may be accurate in VIC, and only the transpiration may need adjustment because of limiting soil moisture. Similarly, the summer ET needs correcting in VIC, but winter and spring ET may not. These types of issues may be playing a role in why the revised ET reduces discharge magnitude accuracy in spring, but improves in the summer. It is

possible that the seasonal ET errors in VIC are associated with limiting soil water rather than PET estimation.

In the application of the ET bias correction to future predictions, compared with the default model, VICET produces a very different signal of future changes in soil moisture drought and minimum discharge; little difference is found in flooding characteristics or maximum discharge. This is due to the extent to which ET is altered in the months these extremes occur, and may be region-dependent. The analyses from both the default and VICET model versions point towards the future of the Connecticut River Basin being characterized by fewer but also longer flood events. Note that the VIC model is not designed to predict floods so these conclusions are based upon an observational rating curve, a stage height threshold, and an adjustment of simulated discharge according to a linear relationship with observation (Parr et al., 2015a), and as such may be tenuous. The main point here is that there is no observable difference between model versions in the predicted future flooding risks. However, when compared to VIC, VICET does simulate more frequent and longer droughts. This drought signal was detected in soil moisture, as well as the absolute minimum and 5-day minimum stream flows.

Although VICET simulated more accurate historic streamflow, it cannot be said conclusively that the predictions of the enhanced model are more accurate in all respects. However, since the enhanced model produces stream flow with improved accuracy during time periods without ET observational data available, it is reasonable to expect that the ET enhancement may improve future predictions in the same manner.

Although this study focuses solely on the Connecticut River Basin, the methodology developed to incorporate remote sensing data into physically based hydrological models is applicable to other regions for the same model and to other hydrological or land surface models as well. In

fact, high spatial coverage is one of the greatest advantages of remote sensing data along with its high spatial resolution, which makes remotely sensed data particularly useful in areas of spare ground based measurements. In the case of stream flow, this occurs when river gauges are not maintained, in regions where water is anthropogenically diverted, or where the natural flow has been altered. Depending on the deficiencies any particular model may have in a particular region, the incorporation of remote sensing data could provide a variety of different kinds of improvements. Similar techniques could be useful in more complex models, or if applied by systems like NLDAS and GLDAS, could help to better improve our understanding of climatic or hydrologic change and perhaps even improve upon our future predictions.

Summary of Experiments and Acronyms	
Acronym	**Experiment**
VIC	Default VIC 4.1.2.g model with no remote sensing enhancement
VICET	VIC with a evapotranspiration bias correction applied based on a product derived from remote sensing
VICVEG	VIC with inter-annually varying MODIS Leaf Area Index data
VICET + VEG	A combination of both the VICVEG and VICET enhancements

Table 4.1: Summary of experimental simulations and the acronyms used to describe each.

Stream flow Comparison 1980-1985 and 1996-2011 (for period without observational ET data)				
	Correlation (r)		**RMSE (cfs*10^4)**	
	VIC	**VICET**	**VIC**	**VICET**
Daily	0.7538	**0.8091**	1.212	1.057
Bi-weekly	0.8504	**0.9052**	11.91	9.451
Monthly	0.8640	**0.9277**	22.81	16.40
Seasonal Cycle (Monthly)	0.8495	**0.9759**	17.53	9.570

Table 4.2: Comparison of stream flow for period of simulation excluding the availability of ET data. Includes correlation and root mean square error for Thompsonville, CT. Bold signifies significantly improved correlations at p=0.05 in comparison to default model.

Stream Flow Comparison (2003-2011)									
		Correlation (r)				RMSE (cfs*10^4)			
Time scale	**Station**	**VIC**	**VICET**	**VICVEG**	**VICET +VEG**	**VIC**	**VICET**	**VICVEG**	**VICET +VEG**
Daily	Thomps.	0.729	**0.795**	0.727	**0.811**	1.268	1.073	1.297	1.015
	W. Lebn.	0.709	**0.763**	0.702	**0.772**	0.6515	0.5527	0.6679	0.5311
Bi-weekly	Thomps.	0.808	**0.8783**	0.8123	**0.910**	13.39	10.91	13.45	9.14
	W. Lebn.	0.796	**0.855**	0.795	**0.876**	7.365	6.108	7.320	5.317
Monthly	Thomps.	0.829	**0.922**	0.823	**0.946**	0.5948	0.8079	0.5432	0.8740
	W. Lebn.	0.818	**0.900**	0.811	**0.918**	0.3650	0.6704	0.3070	0.7522
Seasonal Cycle (Monthly)	Thomps.	0.798	**0.969**	0.759	**0.982**	19.30	10.12	22.02	7.22
	W. Lebn.	0.820	**0.968**	0.782	**0.975**	10.35	6.00	11.30	4.62
Inter-annual Variability (Monthly)	Thomps.	0.862	0.861	0.898	0.895	0.4928	0.4989	0.4262	0.4333
	W. Lebn.	0.809	0.804	0.838	0.835	0.5853	0.5919	0.5377	0.5438

Table 4.3: Comparison of stream flow for the period of simulation shared by all model versions. Includes correlation and root mean square error for both discharge stations. Bold signifies significantly improved correlations at p=0.05 in comparison to default model.

Seasonal Inter-annual Stream Flow (2003-2011)						
	Correlation (r)			RMSE (cfs*10^4)		
	VIC	VICVEG	VICET+VEG	VIC	VICVEG	VICET+VEG
DJF	0.782	0.826	0.802	45.34	34.10	42.29
MAM	0.768	0.828	0.837	37.67	33.25	34.16
JJA	0.955	0.960	0.899	70.01	88.16	15.01
SON	0.979	0.9803	0.977	77.29	92.41	16.68

Table 4.4: Comparison of the seasonal inter-annual variability of stream flow for 2003-2011 for Thompsonville, CT.

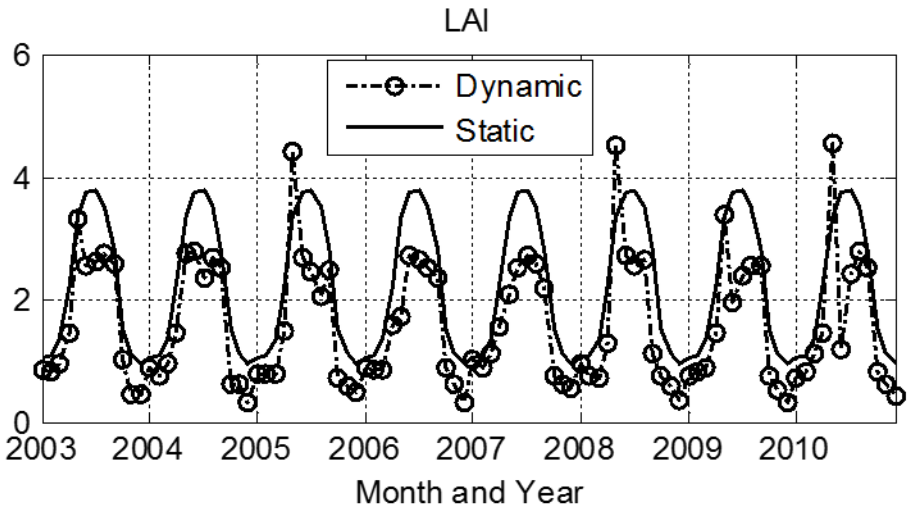

Fig. 4.1: Seasonal comparison between the dynamic LAI used in VICVEG and the static LAI used in the default VIC model.

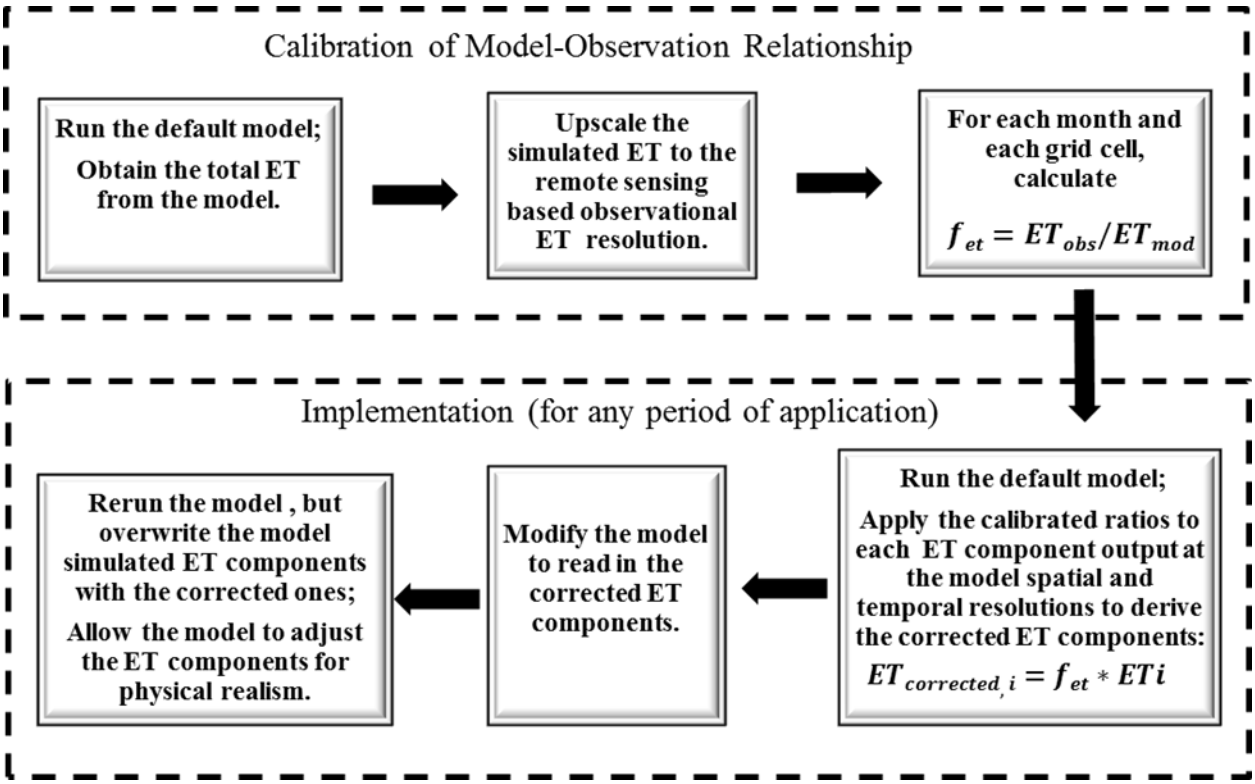

Fig. 4.2: A flow chart of the calibration and application of the ET bias-correction process utilized. Where f_{et} represents the month and grid cell specific relationship between model and observation, ET_{obs} represents the remote sensing ET and ET_{mod} represents the total model simulated ET both for the time period with remote sensing data available, and ET_i represents each of the five ET components simulated in each time step by the default model over the application period of interest.

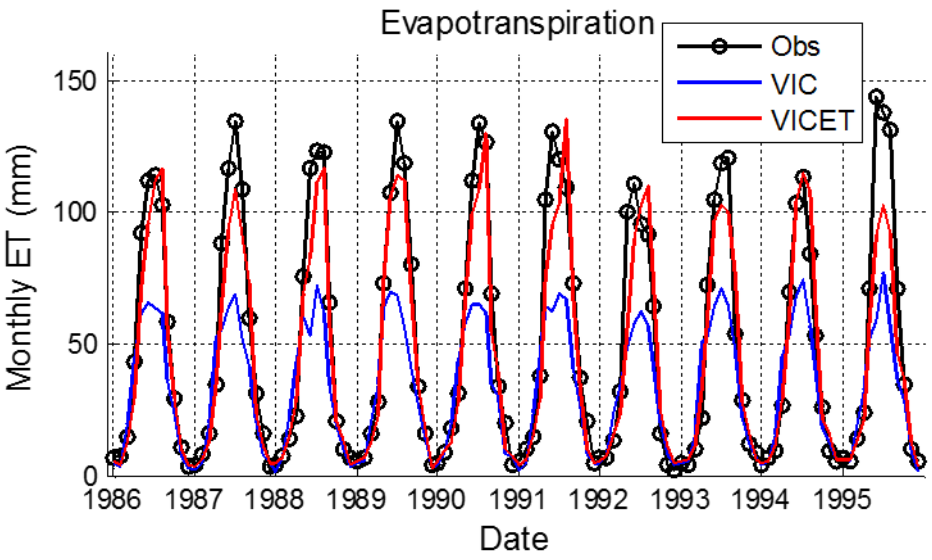

Fig. 4.3: Comparison of Landflux remotely sensed ET (Obs), default model ET (VIC), and bias corrected ET used to force the ET adjusted model (VICET).

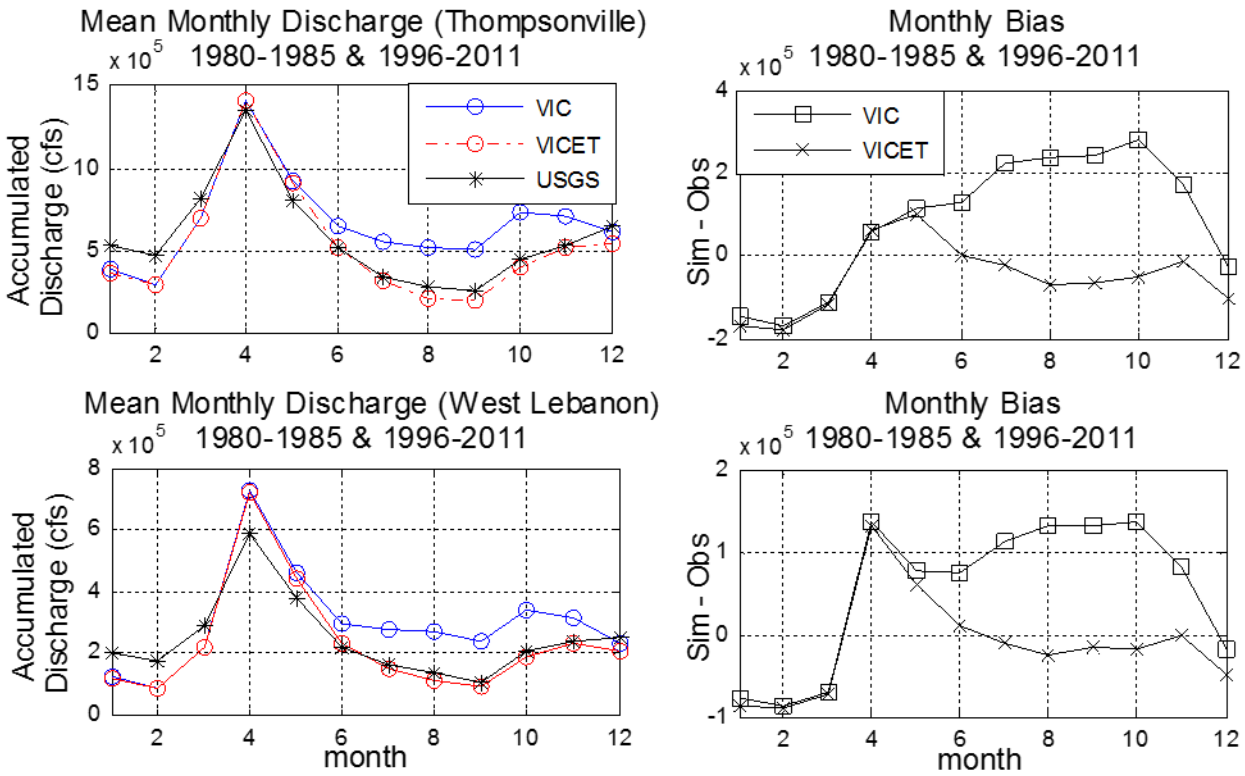

Fig. 4.4: The mean accumulated monthly discharge (left) and the monthly bias from USGS observation (right) for the Thompsonville, CT station (top) and the West Lebanon station (bottom) for the period of simulation excluding the availability of the ET data. The accumulated discharge is measured as the sum of all daily average cfs rates rather than converting to cubic feet.

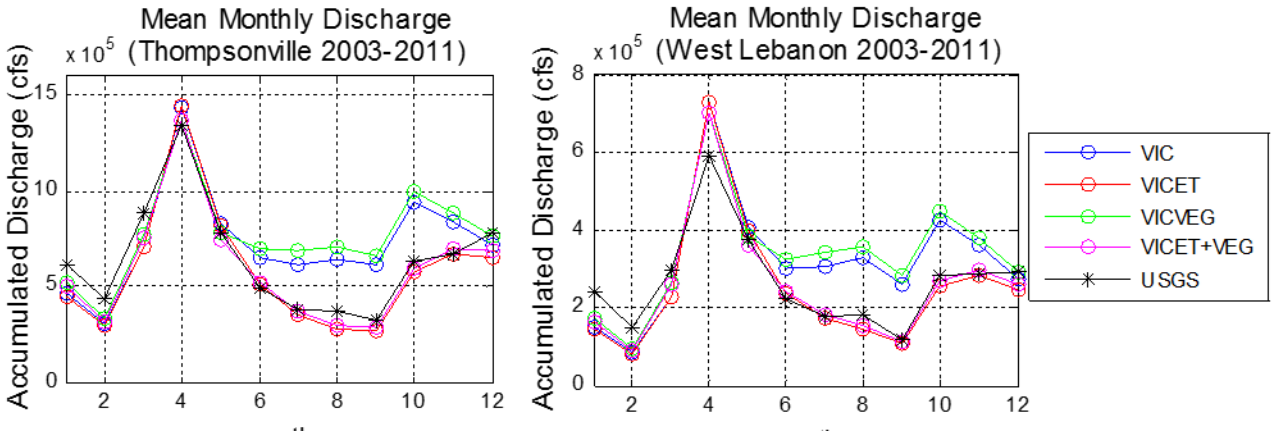

Fig. 4.5: The mean accumulated monthly discharge (left) for both discharge stations for each model version. The period of analysis is the period of simulation shared by all data sets (2003-2011).

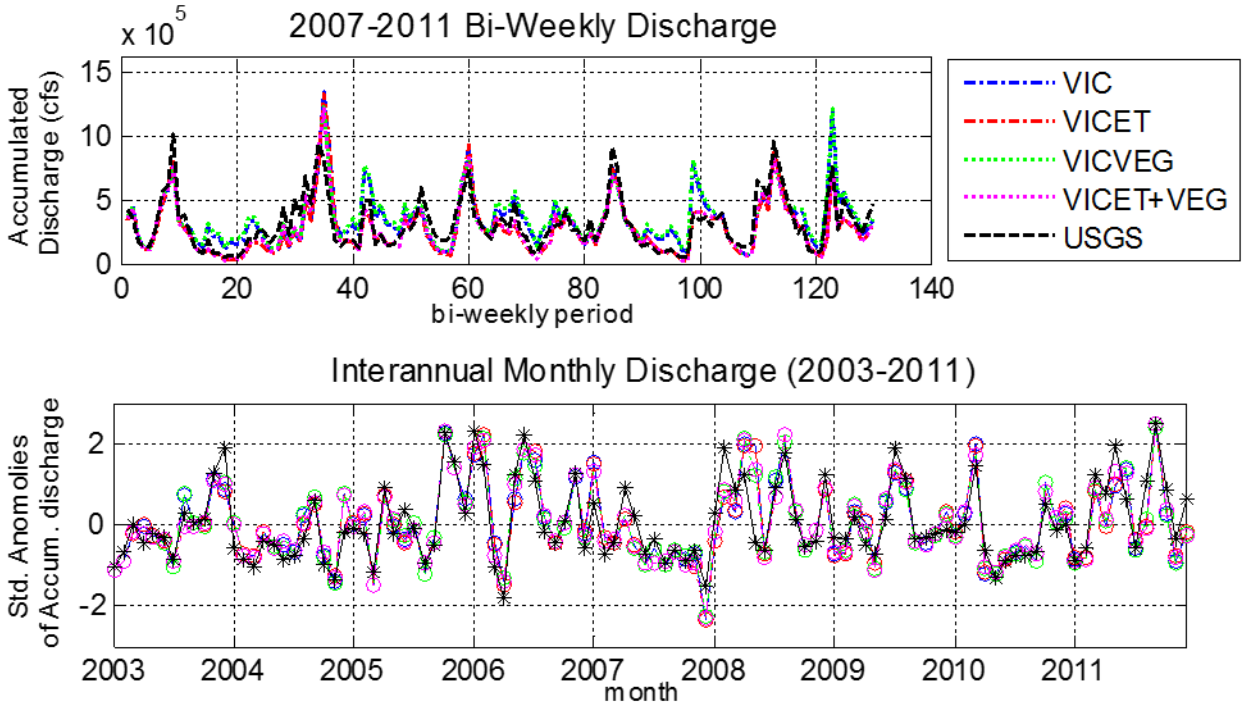

Fig. 4.6: The accumulated bi-weekly discharge for 2007-2011 and the standardized anomalies of inter-annual monthly discharge (2003-2011) for each model version for Thompsonville, CT.

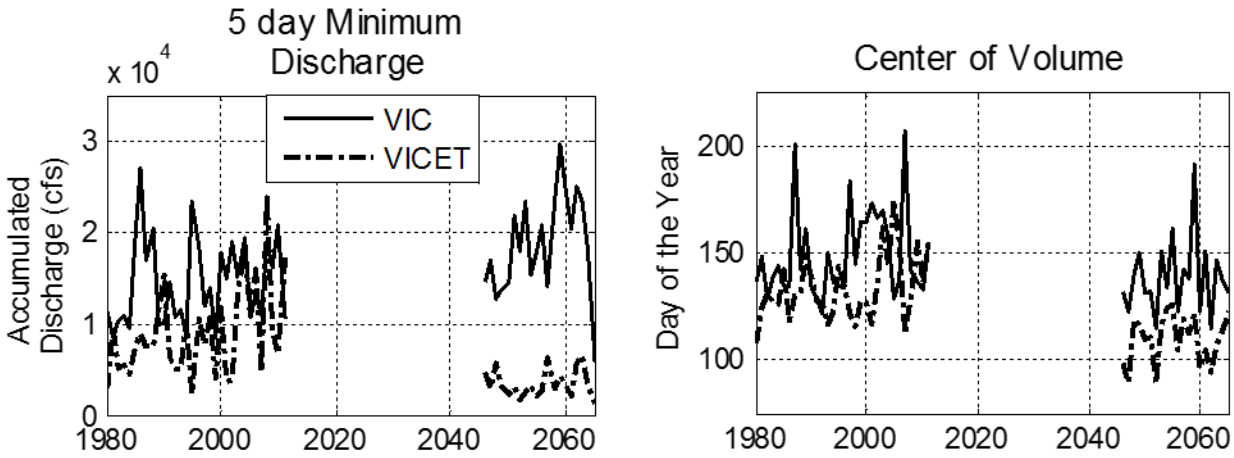

Fig. 4.7: The 5 day minimum accumulated discharge (left) and center of volume date (right) are both analyzed at Thompsonville, CT. The past (1980-2011) and future (2046-2065) for both the default and ET-adjusted model versions are included.

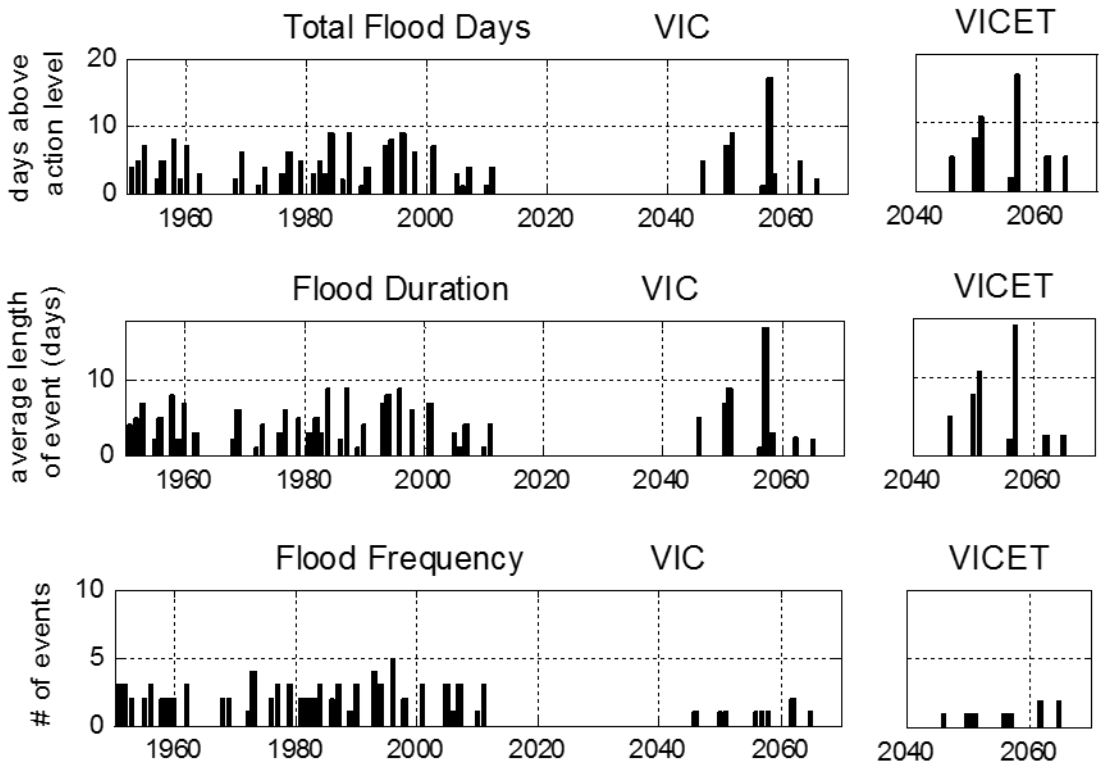

Fig. 4.8: The number of flood days, mean length of flood events, and # of events are analyzed for both the past (1980-2011) and future (2046-2065). Displayed for the future is the mean of all three future data sets for the default and ET adjusted model versions.

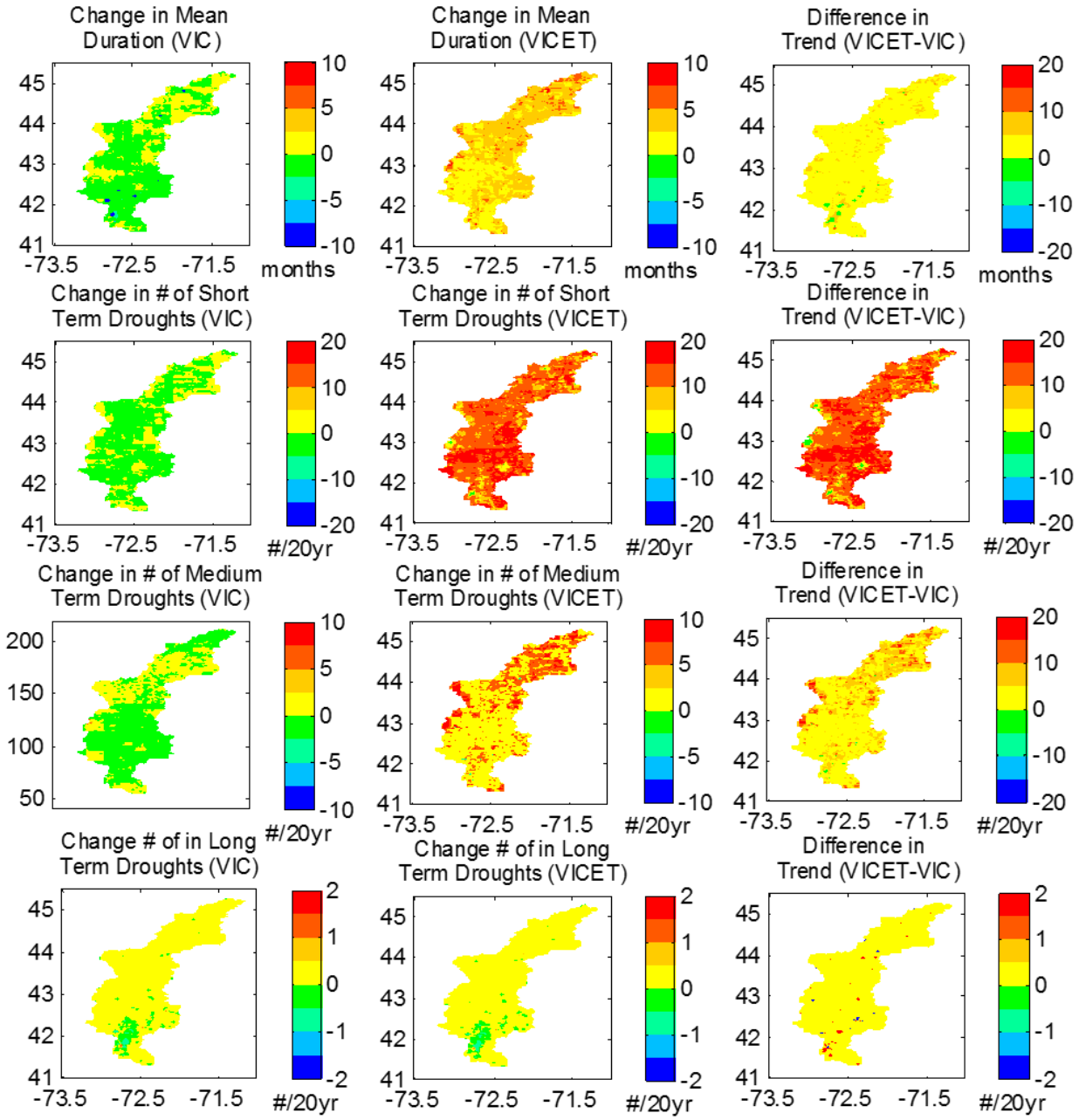

Fig. 4.9: Analysis of drought trends between future (2046-2065) and past (1980-2011) based upon soil moisture. Top row is the mean duration of droughts (months), second row is change in short term droughts (#), third row is change in medium term droughts (#), and bottom row is change in long term droughts (#). The left column is change (future-past) for the default model, the middle column is for the ET adjusted model, and the right column is the difference between model versions.

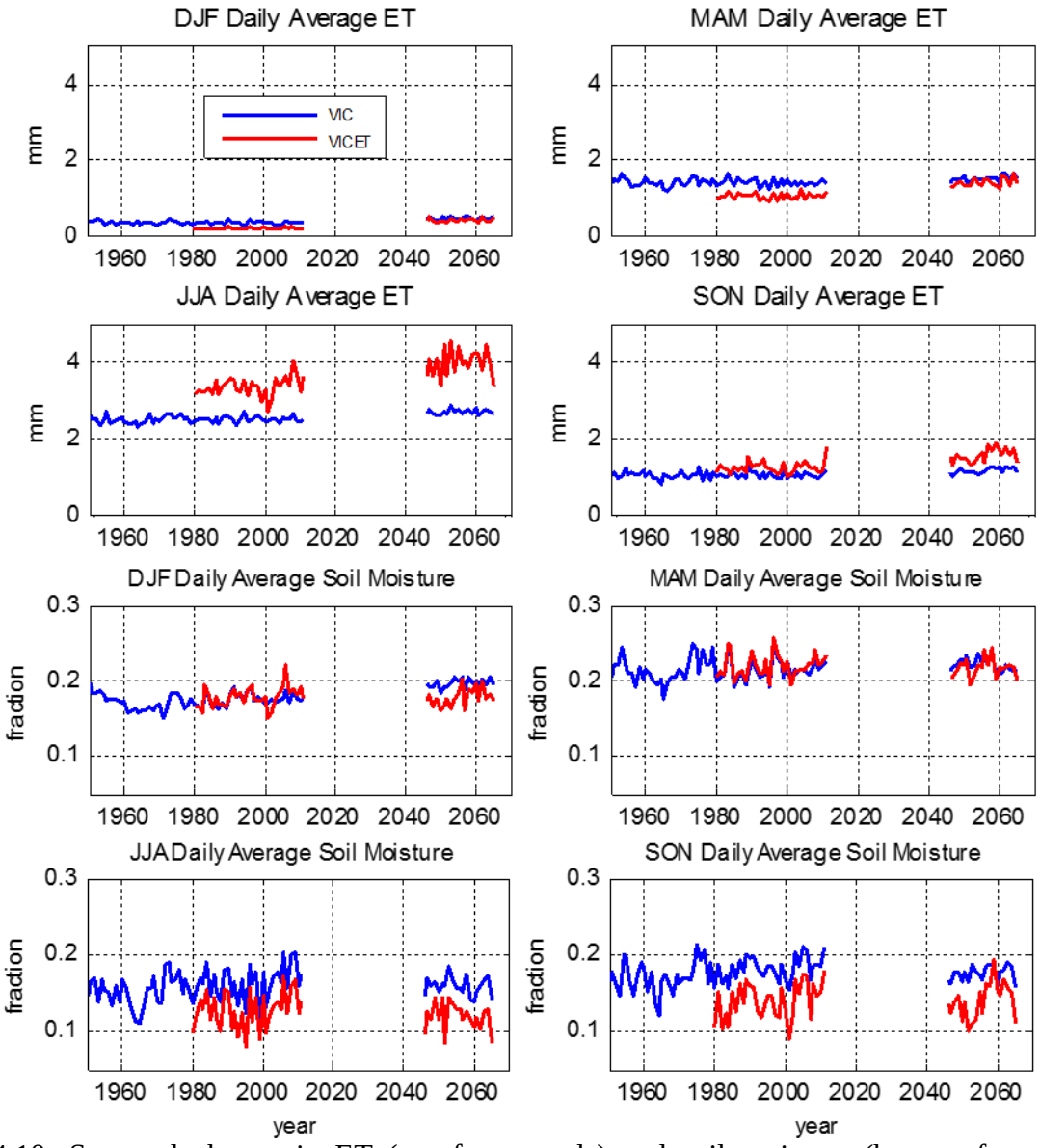

Fig. 4.10: Seasonal change in ET (top four panels) and soil moisture (bottom four panels) between past (1980-2011) and future (2046-2065) for both default and ET adjusted model versions.

Chapter 5

Understanding Evapotranspiration Trends and their Driving Mechanisms

This Chapter is in preparation for submission

5.1 Introduction

A major concern related to the global climate change is its impact on the regional and global water cycle. As shown by many climate modeling studies, increasing global temperature and enhanced greenhouse gas concentration such as CO_2 have had major effects on the dynamics of the hydrologic cycle and the surface energy budget, in particular, on evapotranspiration (e.g., Teuling et al. 2009). Evapotranspiration (ET) is the combination of evaporation from the land surface and bodies of water, sublimation from snow or ice, and transpiration from vegetation. ET is a critical process to the climate system greatly affecting both precipitation and runoff as it is at the core of the water, energy, and carbon cycles (Jung et al. 2010) as well as a key driver of droughts.

Most past studies support the notion that the hydrological cycle will intensify in response to warming (Trenberth 1998; Huntington 2006; Allen and Ingram 2002; Miralles et al. 2013). As atmospheric temperatures rise, so does the atmosphere's capacity to hold water vapor; therefore, the atmospheric demand for water vapor is expected to rise with warming. For this reason, climate models often predict an increase in global evaporation along with the subsequent intensification of precipitation (Miralles et al. 2013). However, despite the general consensus that warming tends to intensify the hydrological cycle and increase evaporative demand, there is much uncertainty as to the magnitude and spatial distribution of the response (Douville et al. 2012). Moreover, the variation and change of actual ET is subject to the influence of other

processes and therefore involves more complexities (e.g., Jung et al., 2010). Since moisture and energy availability also dictates terrestrial ET in addition to atmospheric demand, and the intensity of the terrestrial hydrological cycle can influence moisture availability, ET variation and changes are results of complex interactions between soil moisture, vegetation, ET, and precipitation (Miralles et a. 20113). The global ET trend has been the focus of several recent studies (e.g., Wang et al. 2010a, Jung et al. 2010). In performing the trend analysis, Wang et al. (2010a) used the ET data estimated with a modified Penman-Monteith approach (Wang et al., 2010b) at 1120 stations worldwide, and Jung et al. (2010) used a global ET dataset that was empirically derived from in situ FLUXNET data combined with satellite remote sensing and surface meteorological data. Both studies found a global increase in annual mean ET around 7mm per year per decade from 1982 to the late 1990s. These results correspond with what is expected from an intensification of the hydrological cycle. However, the increasing ET trend did not continue after 1998 and from 1998-2008 this global trend was replaced with a decreasing trend of similar magnitude (Wang et al. 2010, Jung et al. 2010). More recently, Mueller et al. (2013) using a merged data set derived from satellite and in situ observations, and Miralles et al. (2013) using satellite data, confirmed the overall positive mutli-decadal trend from the 1980's to the late 1990's and the declining trend starting around 2000. Miralles et al (2013) also found a recovery of an increasing ET trend since 2007. In addition, it has been shown with the use of hydrological models that changes to ET from 1951-2000 have been in large part due to anthropogenic causes (Douville et al. 2012). This poses an important question from a scientific standpoint, specifically, what is the driving mechanism behind this change in trend?

The primary climatic factors influencing ET are precipitation, radiation flux, air temperature, humidity, and wind speed. Climate conditions play an integral role in determining

the relationship between these parameters and ET making these relationships region and/or season dependent (Wang et al. 2010). Whereas air temperature may be more dominant in a cold climate, moisture supply may be more dominant in an arid region. Jung et al. (2010) suggested that the cessation of the increasing global trend was due to the fact that ET had previously increased to such an extent that it affected the surface moisture supply by limiting the available water and thereby limiting ET. This suggestion was backed by a strong correlation in the spatial variation of ET and soil moisture supply, especially in the southern hemisphere where most of the decrease of ET trend was found.

Precipitation is an important driving factor and input to simulated ET data sets. It is particularly influential to ET in water limited regimes. Terrestrial precipitation amount has been shown by observations to have increased by about 2.4 mm per decade from 1900 to 1988 which ceases around the same time as the increasing global ET trend (Dai et al., 1997). It has been determined that the trends in precipitation agree with the signs of the ET trends, with the exceptions of the polar climates, but that the period after 1997 exhibits a much stronger decreasing ET trend than global precipitation (Mueller et al. 2013). This likely indicates that ET is not constrained by precipitation alone but also by other factors.

The intensification or acceleration of the hydrological cycle does not just refer to evapotranspiration. Instead, it is most often associated with changing precipitation characteristics, particularly the increased frequency and magnitude of heavy and very heavy precipitation events (Groisman et al. 2004; Allan and Soden 2008; Tebaldi et al. 2006; Frich et al. 2002). These changes towards more precipitation extremes could very well lead to a decrease in the fraction of precipitation that infiltrates and is subsequently evaporated. In fact, Walter et al. (2004) linked increasing evapotranspiration to the acceleration of the hydrological cycle and

showed an imbalance in the increasing trends of precipitation and river discharge with discharge showing a stronger signal. Another study conducted on Korean basins found the total annual ET decreased in years with abnormally extreme precipitation (Song et al. 2014).

Other than precipitation and temperature, wind and radiation are also important ET forcings. Wind affects aerodynamic conductance, a critical factor in ET parameterization as well as influencing convection. There have been recent reports of negative trends in wind speed (Vautard et al. 2011; McVicar et al. 2012) which correspond with the change towards a decreasing global ET trend; however, spatially these changing ET and wind trends have not yet been shown to correlate. Incident shortwave radiation has been shown to primarily control variations of ET in humid regions while dry regions demonstrate an opposite negative dependence of ET on shortwave radiation. This is connected to changes in cloudiness and aerosols. A studying using the Community Land Model version 4 from 1982 onward also revealed a high correlation between net radiation and ET for global land and specifically in Africa, and North America (Shi et al. 2013). It is also important to note that land cover type, especially in areas with high transpiration is another important factor towards the parameterization of ET (Mueller et al. 2013). However, limited availability of reliable land use data hampers more detailed analysis on the impact of land cover changes on ET variations.

Lastly, large scale atmospheric circulation patterns could play an important role in these changing ET trends as the El Niño/Southern Oscillation (ENSO) can dominate the multi-decadal variability of evapotranspiration. Miralles et al. (2013) claims that the changing ET trends are recurrent oscillations that most likely reflect the transitions of El Niño conditions rather than being a consequence of a reorganization of the terrestrial water cycle. Still, ENSO's effect on ET is weaker in the northern latitudes of 30N to 90N and North America did not display

characteristics of being affected by ENSO mechanisms as much as Australia, Southern Africa, and eastern South America (Miralles et al. 2013).

Although there is still much uncertainty as to the spatial distribution of the global response to warming and possible hydrological cycle intensification, all analyses have shown that ET has significant decadal variations. This study makes use of a land surface model to investigate the variation and changes of the ET trend over the continental U.S. and to examine the potential causes of the ET trend changes. In the following, section 5.2 provides a description of the land surface model and data sets utilized as well as the methods of analysis. Section 5.3 evaluates the model performance against existing data. Section 5.4 reports the results from numerical experiments that are designed to isolate the effects of the most influential factors on ET. Discussion and conclusions are presented in Section 5.5.

5.2 Data and Methodology

The model used is the Community Land Model version 4.5 (CLM 4.5) (Oleson et al. 2013), and the NASA Land Data Assimilation System phase-2 (NLDAS-2) (Xia et al. 2012a; Xia et al. 2012b) forcing data is used to drive the model for the period 1980-2014. The domain of the simulations covers the Continental US (CONUS) and part of northern Mexico at a spatial resolution of 0.25°. Simulations included spin-up years in order for soil moisture to reach a state of relative equilibrium.

Within CLM, heterogeneity in the land surface is represented as a nested subgrid hierarchy where each grid cell can contain multiple land units types each of which can contain a different number of snow and soil columns, and each column can contain multiple plant functional types (PFTs) chosen from fifteen different categories (Oleson et al. 2013). The soil texture data is

taken from Bonan et al. 2002 which was created using the International Geopshere-Biosphere Programme (IGBP) soil data (Global Soil Data Task 2000). Both the percentage of PFTs within each grid cell and the prescribed leaf area index are derived from Moderate Resolution Imaging Spectroradiometer (MODIS) satellite data (Lawrence and Chase 2007). Slope and elevation are obtained from the USGS HYDRO1K 1-km dataset (Verdin and Greenlee 1996). Compared with other hydrological models such as Noah, Noah-MP, and VIC, CLM when driven with NLDAS-2 atmospheric forcing data has been shown to have the best performance in simulating ET compared with both FLUXNET and MODIS ET data (Cai et al. 2014).

In this study two sources of data are used to assess the CLM performance in simulating the recent decline of the terrestrial ET trend. There are currently output from four land-surface models available from the NLDAS phase-2 project (Xia et al 2012a): the Mosaic model (Koster and Suarez 1992), Noah version 2.8 (Xia et al 2012c), the Sacramento Soil Moisture Accounting Model (SAC) (Koren et al. 2000), and the Variable Infiltration Capacity Hydrological Model (VIC) version 4.0.3 (Liang et al. 1994). These data serves as the basis for a model inter-comparison and reveals whether CLM is capable of reproducing similar trends as these other popular hydrological models driven with the same forcing data. The second source of data for comparison is taken from Jung et al. 2010, which was derived from meteorological and remote sensing observations and FLUXNET. This comparison will affirm whether or not the modeled ET is capable of reproducing the spatial pattern and inter-annual changes found in previously mentioned studies.

In addition to the control simulation driven with the original NLDAS-2 forcing data, a number of experiments are performed to isolate the impact of some of the most potentially influential factors on the changing ET trends. These experiments involve altering a particular

variable within the forcing data such that its trend is removed. Details of these experiments can be found in *Table 5.1*. The removal of trends is conducted based on 5-year accumulations such that the accumulated amount over 1980-1984 and the accumulated amount over each of the subsequent 5 year periods is consistent. This was done by scaling the data for each time step with ratios found from 5-year accumulations. For experiments P2 and P3, the cumulative distribution function (CDF) of daily precipitation values for 1980-1989 and 1990-2014 are calculated, and then the distribution of precipitation values were adjusted such that the distribution of later years was fitted to the distribution of 1980-1989. This was done using a quantile mapping approach: for precipitation amount in any time step, finding its CDF value in 1990-2014, and then finding the precipitation amount that corresponds with the same CDF value in 1980-1989. Lastly, P-3 was further altered such that the annual amount of precipitation in any given year is equal to that of the original NLDAS-2 data, employing a similar ratio technique as before. All calculations and adjustments are made at the grid cell level.

5.3 Model Evaluation

The first step of the model evaluation is to determine whether the model can reproduce the ET trend and its changes that motivated this study. *Figure 5.1* shows the ET trend change comparison between CLM, the Jung et al. data, and the four other LSMs used in NLDAS-2. The first period indicated, 1982-1997, is the time period in which Jung et al. 2010 and Wang et al. 2010 found an increase in global land ET of about 7mm per year per decade and 1998-2008 was the time period in which this trend was found to reverse with similar magnitude. Similar temporal periods were examined by Mueller et al. 2013 and Miralles et al. 2013 which confirmed these trends. Although inconsistencies exist particularly with the Noah Model and in the eastern

U.S., the spatial patterns of change are quite similar throughout the models. The strongest signals of change including strong patterns of negative change within the Missouri River Basin and California and a strong positive changing trend in northern Mexico are present in each simulation, and it is in these regions of strong change in which many of our analyses are conducted as will be shown later. The Jung et al. data also portrays the same signals of change in these particular regions. Although the Jung et al. data shows slightly weaker signals of change, it is in part due to the data containing lower magnitudes of ET compared to the models. The majority of inconsistencies between the modeled and Jung et al. ET data exist in the eastern half of the U.S. Overall, CLM reproduces similar spatial patterns and magnitudes of changing trend as the Jung et al. data and other hydrological models, particularly in the regions which are investigated in this study.

The spatial and temporal variability of the model ET from CLM4.5 is compared in more detail with the Jung et al. 2010 data. The spatial distribution and seasonal variation of ET from the model and from the Jung et al. data as well as the temporal correlation between the two are exhibited in *Figure 5.2* for the time period of 1982-2008. Although CLM portrays some minor overestimates in some seasons compared with the Jung et al. data, the model performs well in capturing the overall spatial pattern of ET including that over the complex terrain of the Rocky Mountains. The lower inter-annual correlations are primarily in the eastern U.S. which corresponds with the differing signals for this region in *Figure 5.1*, while the regions in the western U.S., which many of our analyses focus on, have much stronger correlations. The modeled ET data correlates sufficiently well with the Jung et al. data such that it is capable of reproducing similar changing trends as exiting data and shows very similar patterns of change as

other LSMs, and can be used to examine the mechanics of the evapotranspiration process as well as its variations and interactions.

5.4 Results

5.4.1 ET Trend and its Changes

Since terrestrial evapotranspiration is a process at the core of the water, energy, and carbon cycles, its effects and influences are far reaching and complex, making its interactions difficult to study. For this reason, experimental simulations were conducted in order to isolate the effect of one potentially influential variable at a time (*Table 5.1*). The particular climatic factors focused on are precipitation amount, the intensity or probability distribution of precipitation, wind speed, and near-surface air temperature. In addition to studying the effects of these variables on ET trend changes across the entire study domain, three specific regions were chosen to conduct more detailed analysis. These regions were chosen for the strong signal of ET trend changes (*Figure 5.3*) in order to gain a better understanding as to what may have caused these more drastic changes. Region 1 and region 2, located within the Missouri River Basin and California respectively, experienced strong decline of the ET trend, similar to the global ET trend found by Jung et al. (2010); on the contrary, region 3, located in Northern Mexico, experienced a strong increase of the ET trend. Regions with both signs of change were chosen to provide further insight as the causes for a trend change of one sign may differ considerably from that of another sign.

As precipitation is the main driver of all hydrological processes, in addition to precipitation amount, a topic of particular interest is the extent to which the distribution or intensity of precipitation has on these trends. If precipitation has grown more intense due to warming, runoff

ratios might increase leading to lower soil moisture, which reduces ET through moisture limitation thus resulting in a change of ET trend. The three experiments P1, P2, and P3 are designed to illustrate the impact of precipitation characteristics changes on the ET. *Figure 5.4* shows the annual amount of precipitation in each experimental simulation involving changes to precipitation. As can be seen, P1 removes the trend in precipitation amount such that each five year interval has the same total precipitation. This alteration still captures the inter-annual variability while removing long term trend in precipitation amount. P2 features an alteration of the absolute distribution, with the precipitation distribution of 1990-2014 matching the distribution of 1980-1989, which affectively changes the amount of precipitation. In order to study the influence of distribution changes without changes in precipitation amount, P3 features a constant relative distribution of precipitation while the precipitation amount is kept the same as in the control simulation.

ET trends from each experiment were compared to those from the control simulation. This comparison was made for the 1982-1997 and 1998-2008 ET trends as well as the change in trend across the study domain. The removal of the wind and air temperature trends from the forcing data caused no noticeable differences in the ET trends during both time periods. In addition, keeping the relative distribution of precipitation unchanged as in P3 resulted in little observed difference between P3 and the control simulation. P1 and P2 experiments produced the most significant differences from the Control. *Figure 5.5* presents a detailed comparison of the changes to ET trends across the entire study domain for the control as well as experiments P1, P2, and P3. In region 3, a considerable amount of the change is dictated by a decreasing trend in the first period of 1982-1997, but the change in regions 1 and 2 are mostly dependent on changes in the later period. The P1 experiment eliminates the decreasing trend in region 3 as well as

nearly the entire study domain for the earlier period, and the P2 experiment removes much of the strong increasing trend in region 3 for the later period. P1 has the greatest success at removing the trends signals, not only extinguishing the earlier period's trends, but also removing the majority of the trends in regions 1 and 2 for the later period; however in terms of the magnitude of difference compared with the control, P2 has a comparable impact on the trends as can be seen in the lower panels of *Figure 5.5*.

Although the extensive influence of precipitation amount on these trends is not surprising, the lack of influence from removing wind and air temperature trends is unforeseen. It should also be noted that the majority of ET changes in any experiment happen near the turn of the millennia as the 1998-2008 ET trend is dominant towards the changing trends with the exception of region 3. *Figure 5.6* shows the correlation between precipitation and ET across CONUS throughout various seasons. All three regions of focused analysis chosen for this study are highly dependent on precipitation, as ET is water limited in these regions. A clear division can be seen between the Western and Eastern U.S. which illustrates the fact that the influences and constraining factors toward ET may fundamentally differ between these two halves.

5.4.2 Correlation between ET and Other Forcings

The correlations between ET and a large variety of forcing factors were examined for the 1980-2014 period, and the correlation coefficients are listed in *Table 5.2*. As precipitation has a great affect over ET change, and precipitation amount portrays such high correlations, a variety of different precipitation indicators were chosen for analysis. Three indicators were adopted from Frich et al. (2002): number of days with greater than or equal to 10mm (R10), maximum number of consecutive dry days of less than 1mm (CDD), and the simple daily intensity index, defined

by the annual total amount divided by the number of days with greater than or equal to 1mm (SDII). In addition, the accumulated amount of precipitation that falls on days in the top 1 percentile of daily precipitation as well as the fractional amount of the total are examined as well. The top 1% threshold value of precipitation is based on daily means from 1980-1989 using the original NLDAS-2 data and is defined for any day with rainfall.

It can be seen that for all three regions, the most influential precipitation factors are amount and R10 days. The intensity of precipitation does not correlate with ET as strongly as the amount or frequency. The amount of precipitation over the 1% percentile threshold has positive correlations in each region, although not as influential in region 3, which may indicate that having more precipitation occurring, no matter the intensity, contributes more to the amount of ET. *Figure 5.7* shows the temporal plots of variation for precipitation, soil moisture, and shortwave radiation plotted along with ET for each region. As concluded by Jung et al. 2010, the soil moisture and therefore water availability plays a very important role as well. This is especially the case in region 2 (California). Air temperature correlations are negative most likely due to the effects of evaporative cooling and so are correlations for shortwave radiation, indicating that these are regions where ET is limited by moisture rather than energy. Shortwave radiation indicates strong negative correlations, likely a reflection of cloud impact related to precipitation events. Longwave radiation has a positive correlation with ET, which may result from the ET-induced increase of atmospheric moisture and/or even cloudiness acting as a greenhouse gas. From *Figure 5.7*, it is also clear that although the 1982-1997 ET trend displayed in *Figure 5.5* is not a strong increasing trend in Region 1 or 2, this is in part due to higher ET values in the early years of this trend analysis.

It is apparent from *Figure 5.5* and *Table 5.2* that changes in precipitation amount are more influential to the ET trends than precipitation intensity changes. A further examination was conducted to identify how the P2 and P3 experiments affected the surface hydrology. *Figure 5.8* shows a comparison of the runoff ratios between these experiments and the control. Relative to the Control, both P2 and P3 produce lower runoff ratios in each of the three regions especially in region 2 and 3. On average, the absolute distribution changes have a greater impact on the runoff ratios. During the alteration of the forcing data, many of the most extreme precipitation days were cut back on and altered to more moderate events, due to the cumulative distribution of 1980-1989 possessing fewer extreme values. The modifications result in a partitioning of precipitation with a lower percentage of runoff and therefore a greater percentage of infiltration and moisture storage.

Despite the changing characteristics of precipitation affecting the surface hydrology, these effects do not impact the changes in annual amounts of ET nearly as significantly as precipitation amount does. However, there is evidence that the characteristics of precipitation are still playing a crucial role towards variations of ET. *Table 5.3* contains the correlations between ET and the number of days with rainfall exceeding a certain threshold. An interesting pattern emerges throughout all regions where days with greater than or equal to 4 or 5 mm of rain show the strongest correlations and as the "R days" diverge from this medium, the relations grow weaker steadily in both directions.

5.5 Conclusions and Discussion

This study quantifies the recent ET trend and its changes over the NLDAS-2 domain based on simulations using CLM4.5. The CLM4.5 ET, which compares well with both the Jung et al.

ET data and the NLDAS-2 models output, reveal both regions with strong positive changes of ET trend and regions with strong negative changes. These regions of strong signal are primarily located in a dry regime where ET is limited by water rather than energy. Results from numerical experiments and statistical analysis on various factors influencing ET variability and changes indicate that trends in wind and air temperature are not the root cause for the ET trend change in our study domain, and identified changes of precipitation characteristics to be the main cause. Precipitation characteristics changes dominate the ET trend change signal primarily through the amount of water reaching the ground surface and to a lesser extent through the intensity and frequency of precipitation influencing the partitioning of water between infiltration and runoff. As shown in *Figure 5.5*, the absolute distribution alteration involved with the P2 experiment does produce different ET trends across most of CONUS. These changes are due primarily to changes in precipitation amount resulting from the distribution alteration more than due to the distribution changes themselves. Relative distribution changes without precipitation amount changes as shown by the difference between experiment P3 and Control contributes to a much smaller portion of the ET trend changes.

It was suggested in Jung et al. 2010 that the primary cause of the global change of trend of terrestrial ET was that ET had intensified to such an extent during the period of the positive trend, that soil moisture was depleted, thereby restraining ET and reversing this trend. Although this logic is somewhat cyclical, the fact that soil moisture plays a critical role in ET trends cannot be ignored. Within the drier regions of the Western U.S. as well as Mexico which are examined in this study, ET is restricted by the amount of available water much more so than by energy. It is therefore not surprising that soil moisture correlations with ET are the strongest among all non-precipitation based factors.

Consistent with the intensification of the hydrological cycle, in the past several decades, extreme precipitation has increased across the U.S. (Groisman et al., 2004). The observed increase of precipitation extremes has significant implications on the surface water budget and ET trend. Mechanistically, if the distribution of precipitation changes results in a greater percentage of heavy rain rather than light or moderate, then runoff ratios would increase as infiltration rates may not keep up with the rainfall rate, thus reducing soil moisture and slowing down ET where it is water limited. This characteristic change could potentially lead to a reversal of an increasing ET trend. Note that the variation of very heavy precipitation (defined by the amount above the top 1 percentile of daily values) has a positive correlation with ET throughout all regions, and the same is true for simple daily intensity and other indicators of precipitation characteristic change. These positive correlations do not contradict the findings from the P3 experiment. Instead, they indicate that the variables used for the analysis are still dominated by precipitation amount. The analysis on the number of days with a certain threshold of precipitation (*Table 5.3*) does reveal that frequency of precipitation is a very important factor to consider and that having a large number of days with steady and fairly moderate rainfall is favorable towards ET.

Total precipitation amount is the principle influence over the ET trends and their variation during 1980-2014 across the NLDAS-2 domain. The variations of ET trends correspond directly with precipitation amount displaying stronger correlations than any other factor for any simulation in each region of strong ET trend changes. As precipitation drives hydrological processes and provides the input of water for the surface, this may seem predictable, but the extent to which precipitation amount dominates the ET trends in the absence of impact from other factors is an important conclusion. In addition, the manner in which both precipitation and

ET vary within our regions appears to be on a decadal scale as can be seen in *Figure 5.4*. In region 1 and 2 the late 1990's define a period of peak precipitation and ET, the period at the turn of the trend changes. This pattern of change may point to large scale atmospheric circulation patterns such as ENSO controlling the precipitation and thus ET regimes. Miralles et al. (2013) suggested the possibility that the changing ET trends may not be a result of a fundamental change in the mechanics of the water cycle, but rather are due to recurrent oscillations caused by transitions of El Niño conditions.

This study has investigated how evapotranspiration across CONUS and northern Mexico has changed in accordance with the recently discovered global change in trend of terrestrial ET and what are the driving mechanisms behind the changes in ET trend in the recent past. The finding that the ET variation is dominated by precipitation amount may be region dependent, and may or may not hold in the future. Due to the lack of high quality gridded meteorological forcing data elsewhere, this study focuses on the NLDAS-2 domain. Elsewhere, especially in the southern hemisphere where the strongest ET trend change was found (Jung et al., 2010), the relative importance of various driving factors may be different. In addition, as the warming-induced hydrological changes continue in the future, it is possible that the impact of the precipitation extremes may become more dominant than in the past, with ramifications for how ET might change in the future. These will be tackled in our follow-up study.

Summary of Experiments and Acronyms	
Acronym	**Experiment**
C	CLM 4.5 model forced by the original NLDAS-2 data (control)
P1	Precipitation Amount trend removed
P2	1990-2014 precipitation distribution matching the 1980-1989 distribution
P3	1990-2014 precipitation distribution matching the 1980-1989 distribution- further adjusted such that the annual amount is equal to the original simulation 'C'
W	Wind trend removed
A	Air Temperature trend removed

Table 5.1: Summary of experimental simulations and the acronyms used to describe each.

Correlations Coefficients of Annual Means with ET (1980-2014)																		
Variable	**Region 1**						**Region 2**						**Region 3**					
	C	**P1**	**P2**	**P3**	**W**	**A**	**C**	**P1**	**P2**	**P3**	**W**	**A**	**C**	**P1**	**P2**	**P3**	**W**	**A**
Precipitation	0.9524	0.9350	0.9508	0.9507	0.9510	0.9525	0.9245	0.8480	0.9080	0.9264	0.9242	0.9257	0.9567	0.9225	0.9615	0.9623	0.9565	0.9561
Amount of Precipitation above 1% threshold	0.7840	0.6583	0.7740	0.7796	0.7821	0.7836	0.7175	0.4990	0.6844	0.7874	0.7177	0.7187	0.4777	0.5362	0.7247	0.6870	0.4770	0.4743
Fractional Amount above 1% threshold	0.5401	0.3902	0.6644	0.5700	0.5381	0.5390	0.3990	0.2104*	0.4816	0.4574	0.3999	0.3993	0.2216*	0.3152	0.5547	0.5398	0.2210*	0.2179*
R10 Days	0.9007	0.8566	0.9026	0.9128	0.8992	0.9012	0.8732	0.7712	0.8532	0.8901	0.8726	0.8741	0.7663	0.7884	0.7873	0.7903	0.7658	0.7642
Simple Daily Intensity Index	0.6255	0.5103	0.7389	0.6939	0.6233	0.6249	0.4147	0.1861*	0.5082	0.4628	0.4144	0.4145	0.3569	0.3395	0.5620	0.6135	0.3563	0.3535
Consecutive Dry Days	-0.4401	-0.4618	-0.5491	-0.4809	-0.4389	-0.4382	-0.5215	-0.4250	-0.3732	-0.4820	-0.5214	-0.5190	-0.6810	-0.6321	-0.7026	-0.6454	-0.6812	-0.6819
Soil Moisture	0.8376	0.7572	0.8765	0.8279	0.8517	0.8463	0.9134	0.8445	0.9188	0.9030	0.9120	0.9176	0.8970	0.8415	0.9390	0.8732	0.8966	0.9087
Net Radiation	0.7959	0.6444	0.8393	0.7648	0.8036	0.6651	0.8319	0.6898	0.8633	0.8315	0.8346	0.5886	0.8767	0.8105	0.9153	0.8777	0.8757	0.5537
Shortwave Radiation	-0.5116	-0.4719	-0.2776	-0.5112	-0.5098	-0.5111	-0.8755	-0.6736	-0.8975	-0.8661	-0.8748	-0.8766	-0.6549	-0.3058	-0.8547	-0.6536	-0.6551	-0.6556
Longwave Radiation	-0.0729*	-0.1268*	-0.1578*	-0.0805	-0.0722*	-0.0720*	0.5758	0.4202	0.5830	0.5658	0.5757	0.5763	0.4406	0.1360*	0.6316	0.4418	0.4408	0.4411
10-m Wind	-0.4241	-0.3229	-0.6467	-0.4223	-0.3642	-0.4322	-0.2456*	-0.4165	-0.2091	-0.2648	-0.4151	-0.2798	-0.6108	-0.3675	-0.6178	-0.6164	-0.4429	-0.6261
Air Temperature	-0.4796	-0.4406	-0.4980	-0.4830	-0.4781	-0.3312	-0.6141	-0.4908	-0.6424	-0.6093	-0.6140	-0.4261	-0.6807	-0.4693	-0.8371	-0.6780	-0.6805	-0.4438

Table 5.2: Annual correlations between ET and various climatic factors in each of the three regions. Experiment acronyms can be found in *Table 5.1* and region numbers in *Fig. 5.3*. A "*" indicates that the correlation is not significant at the p=0.05 level.

Correlations Coefficients with ET (1980-2014 Inter-annual)			
Variable	**Region 1**	**Region 2**	**Region 3**
R1 Days	0.8201	0.8973	0.8583
R2 Days	0.8878	0.8981	0.9263
R3 Days	0.9229	0.8990	0.9516
R4 Days	0.9420	0.8932	0.9576
R5 Days	0.9455	0.8859	0.9488
R10 Days	0.9007	0.8732	0.7663
R15 Days	0.8546	0.8726	0.5569
R20 Days	0.8007	0.8371	0.4457
R25 Days	0.7333	0.7968	0.4289

Table 5.3: Correlations between ET and number of days with a certain amount of precipitation. R“x” represents the number of days in a year with greater than or equal to “x” mm of precipitation.

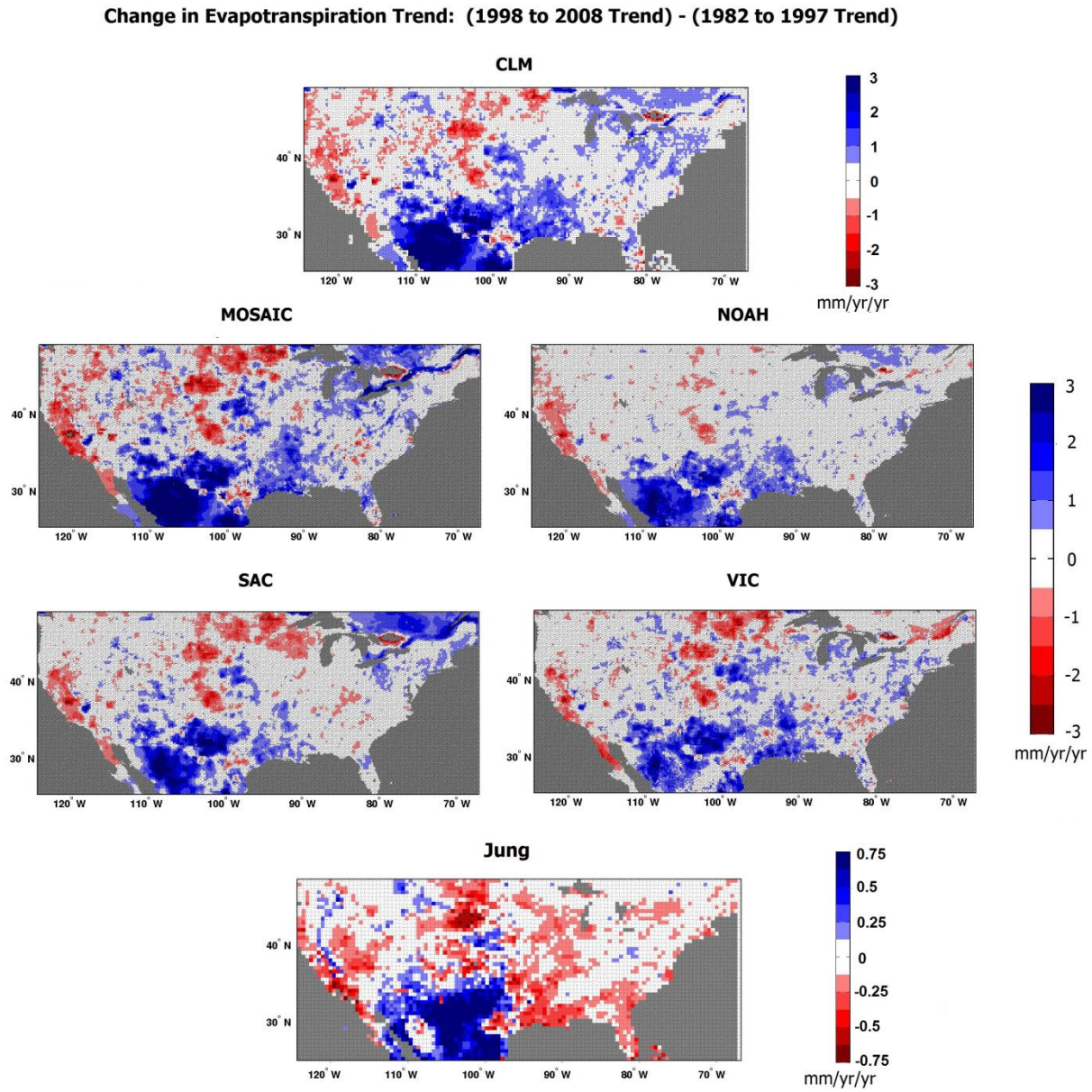

Fig. 5.1: Changes in evapotranspiration trend (mm/yr/yr) for the CLM 4.5 model used in this study, the data used in Jung et al. 2010, as well as each of the four land surface model outputs provided by NLDAS-2 over the study domain. The change in trend is defined by subtracting the ET trend calculated for 1982 -1997 from that of 1998-2008.

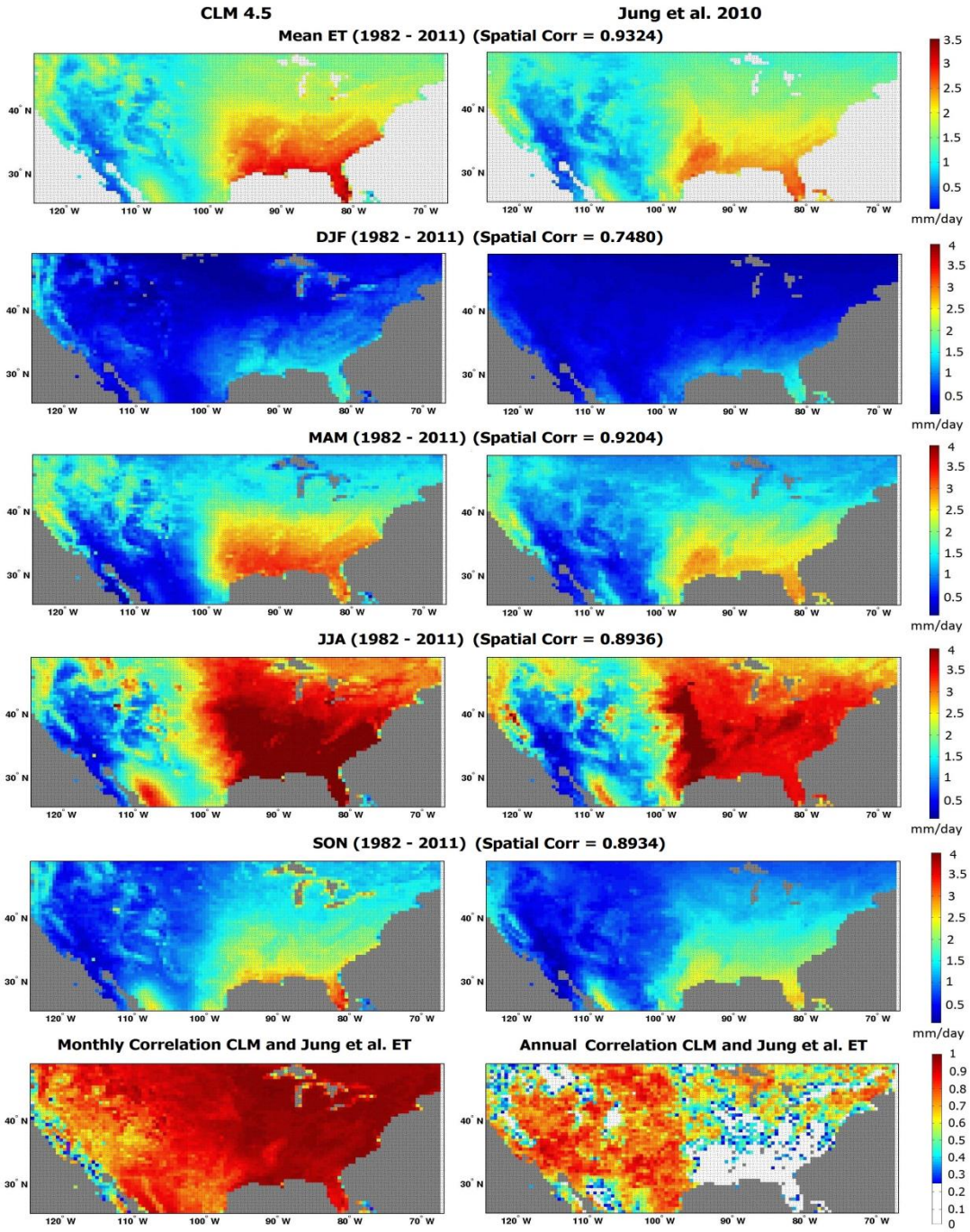

Fig. 5.2: An ET comparison of modeled data and Jung et al. (2010) data over the study domain. Included are the spatial patterns averaged over all seasons as well as for each individual season. The last row displays inter-annual ET correlations between modeled and Jung et al. data on the monthly scale (left) and annual scale (right) for 1982-2011. All values are significant ($p = 0.1$) on the monthly scale but insignificant values on the annual scale are left white.

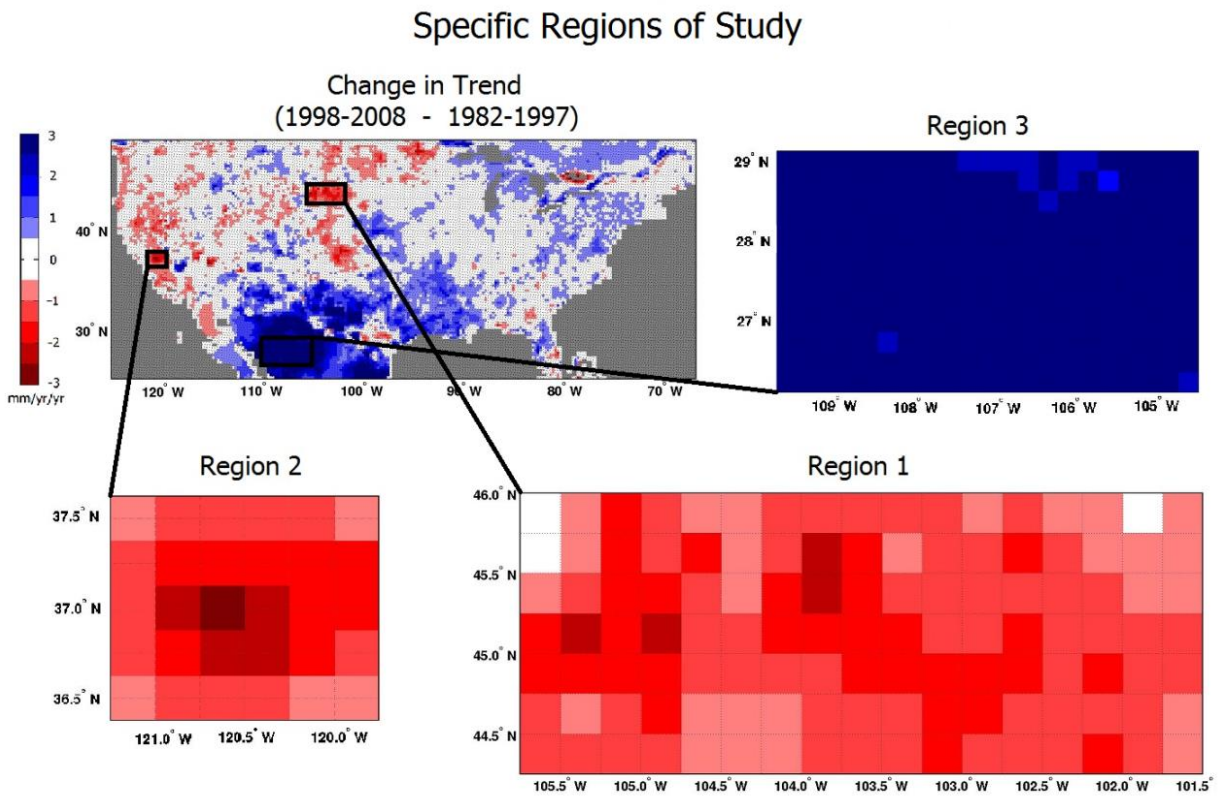

Fig. 5.3: The three regions chosen for a more in depth analysis based on the strength of the change in trend.

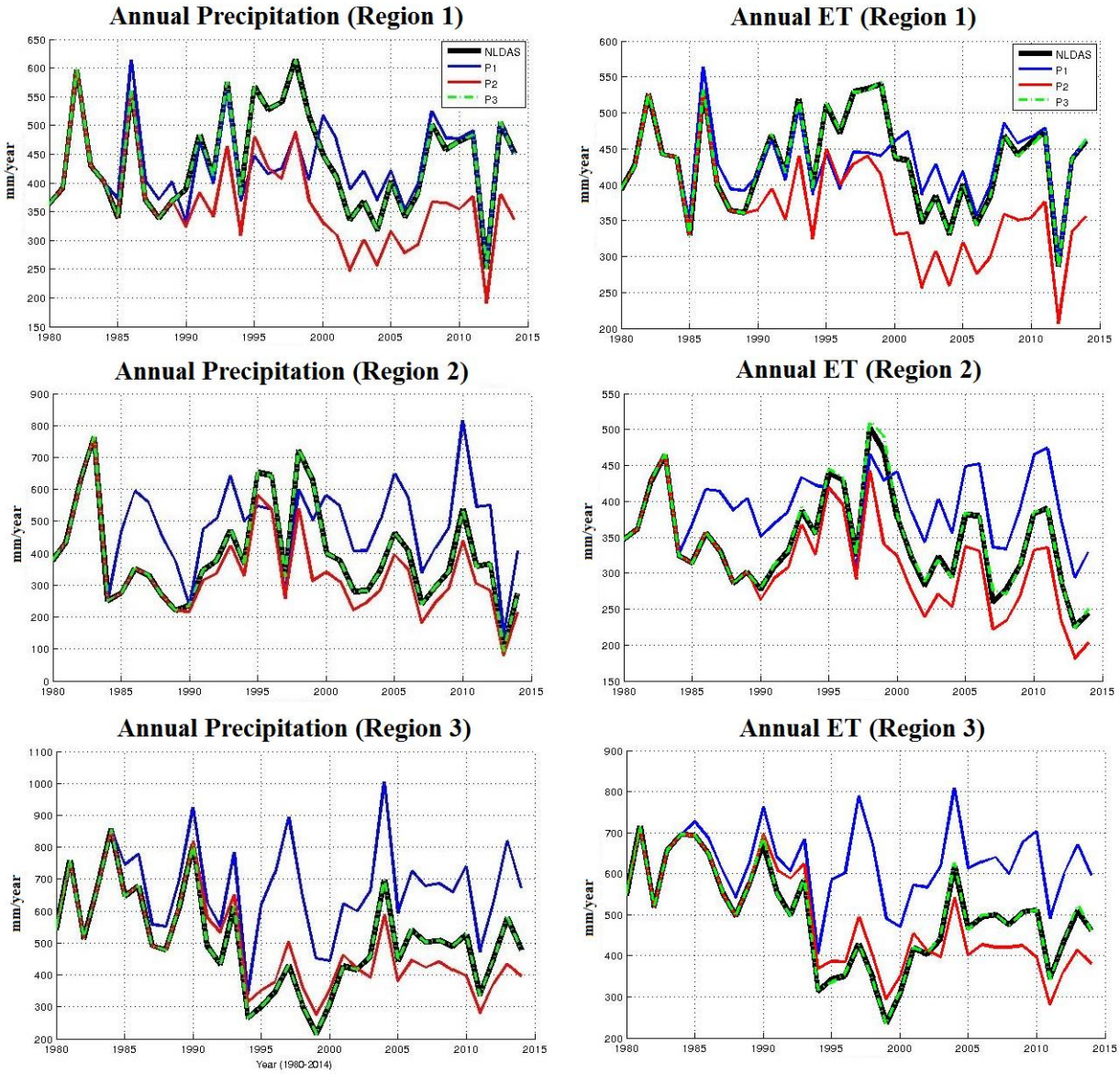

Fig. 5.4: The annual amount of precipitation and ET in each of the three regions for different experimental simulations including the original NLDAS (black), P1 (blue), P2 (red), and P3 (green).

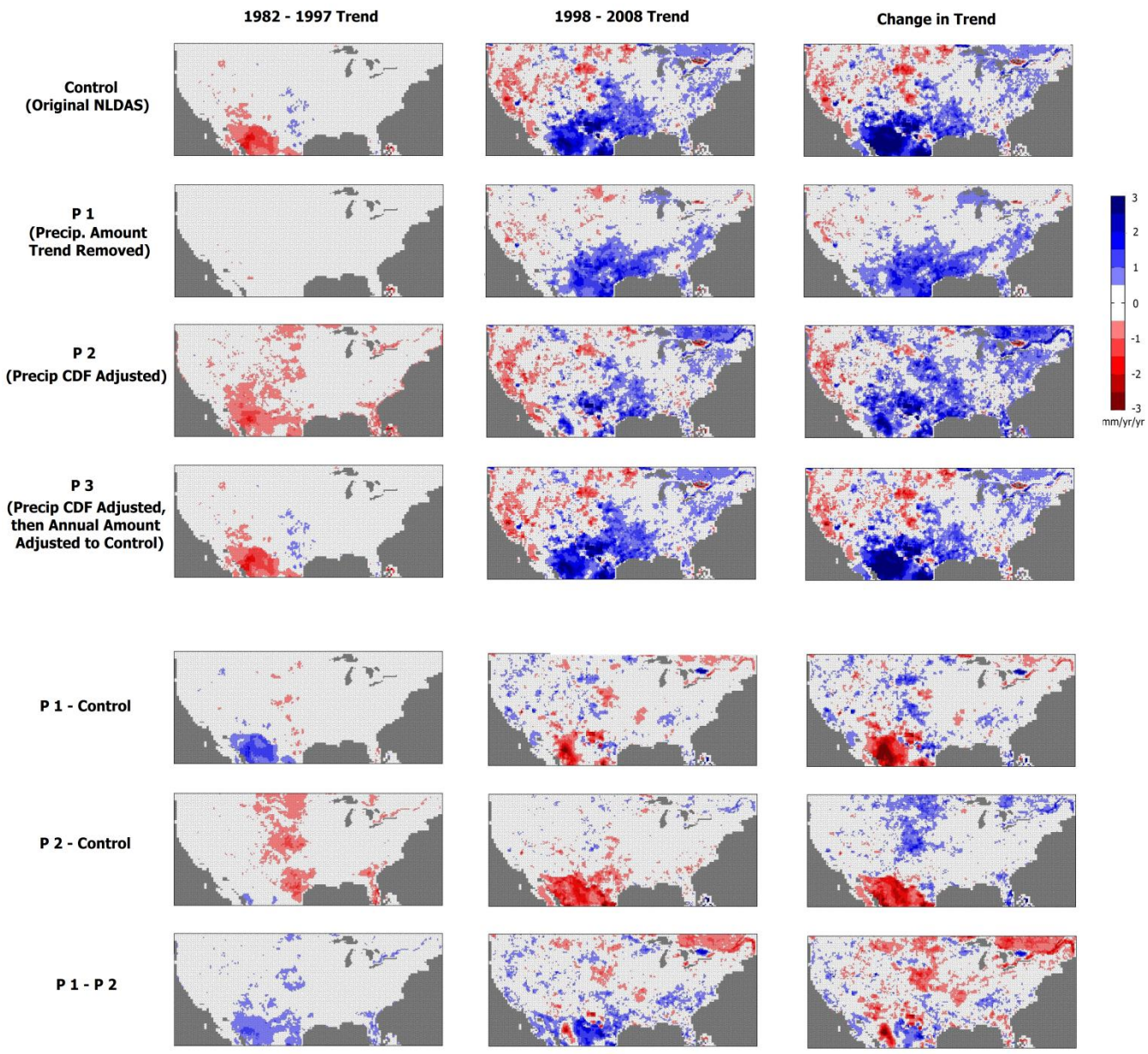

Fig. 5.5: Trend comparison of the control NLDAS simulation along with P1, P2, and P3. The top section contains the 1982-1997 trend, the 1998-2008 trend, and the change in trend (mm/yr/yr) for each experiment. The bottom section shows the difference between various simulation combinations.

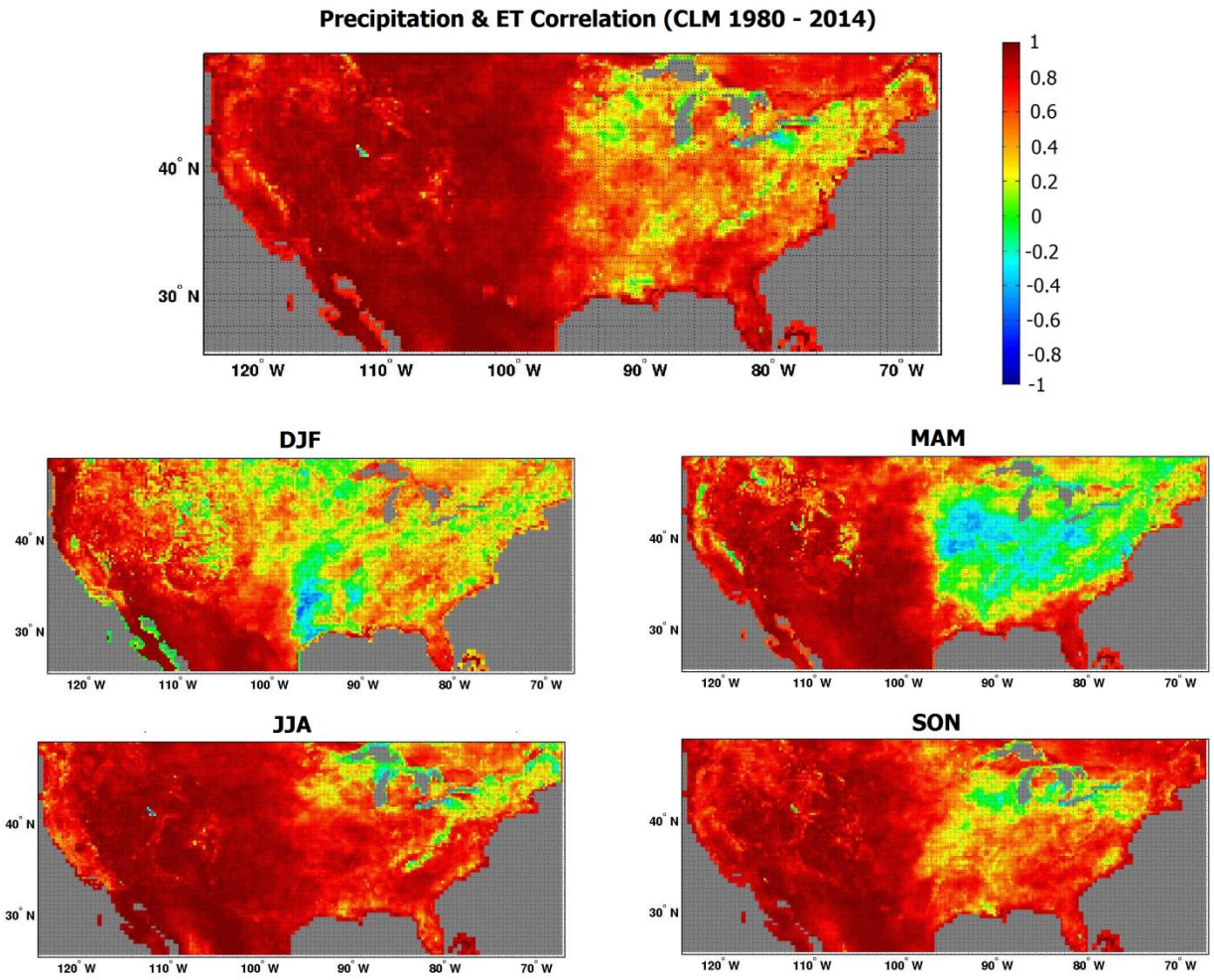

Fig. 5.6: Annual correlation between CLM 4.5 modeled evapotranspiration and NLDAS-2 precipitation. Contains correlations for the total annual mean as well as for each specific season.

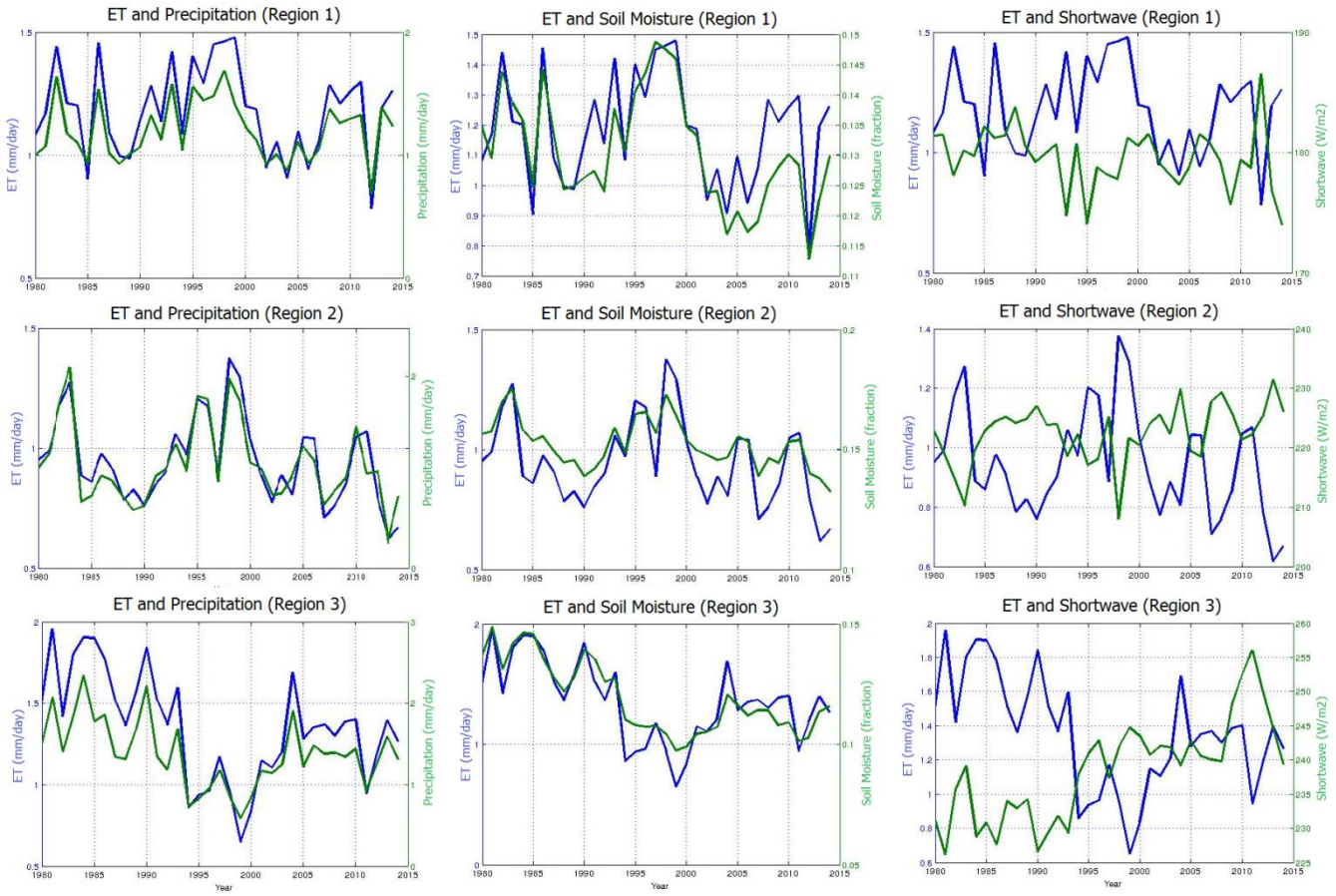

Fig. 5.7: Inter-annual changes in ET and Precipitation (left), Soil Moisture (middle), and Shortwave Radiation (right) for the three regions from 1980-2014. In all cases, ET is in blue and the other variable in green.

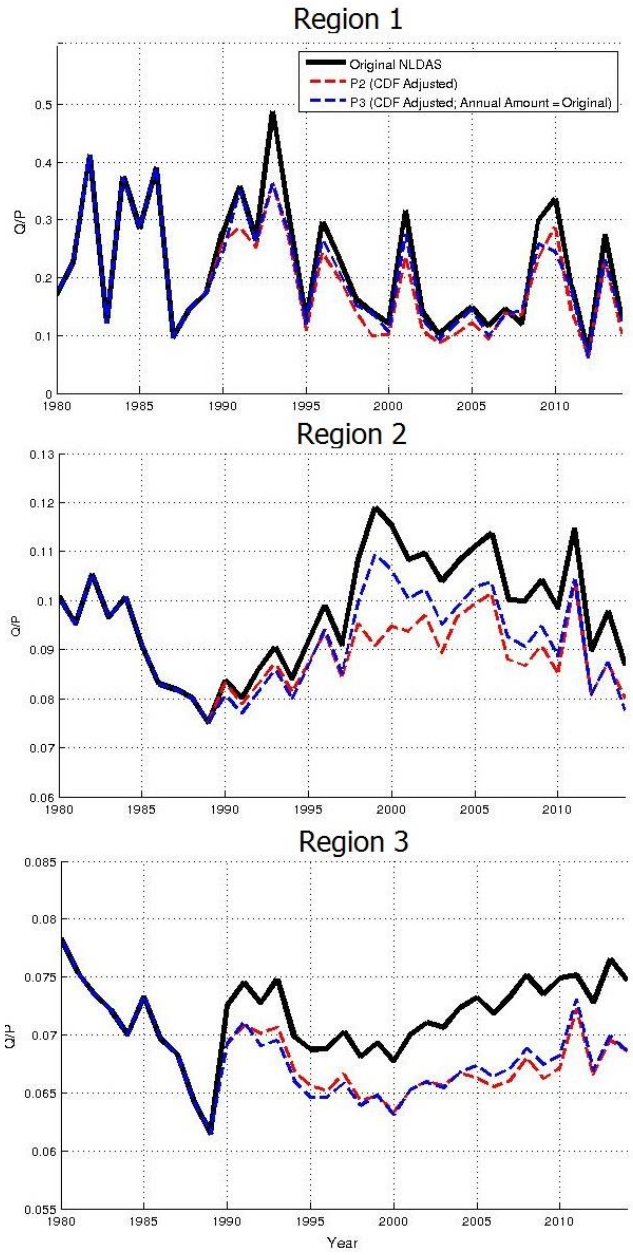

Fig. 5.8: The runoff ratios (runoff / precipitation) for each region. The P2 (red), and P3 (blue) simulations are analyzed due to their changes in the distribution of precipitation

Chapter 6

Summary and Conclusions

This chapter summarizes the main results and conclusions of this thesis, and suggests future research.

6.1 Summary and Conclusions of the Results

6.1.1 Modeling and Analysis of the Past

The historic analysis examines the impact of climate changes during 1950-2011 on hydrological processes in the Northeast using the Connecticut River Basin as a case study. It is concluded that the CRB experienced an increasingly wet regime with significant increases in precipitation extremes. Results show an increase in both the number of days with greater than 10mm precipitation and the simple daily intensity index. In addition, from 1950 to 2011, extreme precipitation amount (which is the total amount of precipitation from the upper 1% of daily precipitation) increased substantially, by 240% relative to the 1950 level. The weight of extreme precipitation as a fraction of total precipitation also increased, from about 10.6% in the 1950s to 30.4% in the 2000s. Despite the increase of precipitation extremes, the consecutive dry days experienced a slight decrease. Mean trend analysis shows indications of increasing precipitation amount, increasing discharge, increasing runoff ratios, increasing soil moisture, and a negligible evapotranspiration trend. There is no sign of an earlier snow melt season or timing of peak discharge. VIC simulations indicate that the basin is more subject to meteorological flood conditions than to drought conditions. In addition, comparison between VIC's two modes of operation shows that the full mode does a better job of simulating cold season fluxes and discharge due to its more robust treatment of energy budget allowing for a better simulation of

snow pack and melting. However, VIC in the water-only mode is considered sufficient for analyzing past variability, changes, and trends as both modes perform well in reproducing the observed inter-annual variation of the hydrological variables, and closely match each other.

6.1.2 Projections of the Future

The future analysis focuses on whether or not the recent warming-induced hydrologic changes in the U.S. Northeast will continue in the future (2046-2065) and how future changes of precipitation characteristics may influence other hydrological processes in the Connecticut River Basin. Future precipitation extremes show a decreased amount compared to the early 21st Century, but increased when compared to our entire historic period or the late 20th Century, as well as a consistently increasing mean intensity throughout the past and future. Projections indicate wetter winters including significantly greater precipitation, runoff, and soil moisture, as well as decreases to spring runoff. A critical change in future climate as compared to past climate is the replacement of the negligible ET trend with significant increases throughout all seasons indicating a 14% relative increase averaged throughout the seasons. Compared to the historic analysis, simulations suggest future decreases in snow pack and a shift of peak timing to an earlier date for SWE and discharge. Despite the decreases in the amount of snow melting in spring, there are indications of a faster spring melting which is linked to large flood events. Analyses of extreme hydrologic events reveal a change to the characteristics of flooding, including an increasing duration but decreasing frequency of events, which suggests that events will be rarer but potentially more economically and ecologically damaging. In addition, there is evidence supporting a reduction of drought risk, but the increased ET and drier summer soil moisture indicate that greater drought risk may manifest in a more distant future.

6.1.3 Integrating Remotes Sensing with Hydrological Modeling

In this part of the thesis, inter-annual LAI data derived from satellite remote sensing is incorporated into VIC (VICVEG), and ET data based on remote sensing was combined with ET from a default VIC simulation to develop a simple bias correction algorithm, and the simulation was then repeated with the bias-corrected ET replacing the simulated ET in the model (VICET). VICVEG better captures the inter-annual variability of discharge, particularly in the winter and spring and shows slight improvements to soil-moisture estimates. However, more notable are the VICET model version improvements to stream flow which occur on daily, biweekly, monthly and seasonal time scales. VICET produces this improved accuracy during time periods without ET observational data available indicating that the bias correction can be applied to other time periods. The methodology of incorporating ET data into VIC as a bias-correction tool also influences the model future hydrological trends. Compared to the default VIC, VICET portrays a future characterized by greater drought risk and a stronger decreasing trend of minimum river flows; little difference is found in flooding characteristics or maximum discharge. It is concluded that integration of remotely sensed data is capable of creating statistically measureable model improvements particularly towards the estimations of river flow. Therefore, the incorporation of remote sensing information into hydrologic models can improve model accuracy and insight into current and future hydrologic processes, as well as help characterize the model-related uncertainties in hydrological predictions.

6.1.4 Understanding Evapotranspiration Trends and their Driving Mechanisms

The final study uses CLM4.5 to quantify the recent (1980-2014) ET trend and its changes over the NLDAS-2 domain. Simulated ET, which compares well with NLDAS-2 output and ET data used in a similar prominent study conducted on the global scale, reveals that the regions with the strongest signals of positive and negative changes are dry and limited by water rather than energy. Of the various factors which influence ET, numerical experiments indicate that trends in wind and air temperature are not the direct driving mechanisms of change in these regions, but rather that changes of precipitation characteristics are the main cause. Total precipitation amount is the principle influence over the ET trends and their variations with intensity and frequency characteristics influencing the signal of change to a lesser extent by affecting the partitioning of water between infiltration and runoff. The manner in which precipitation and ET vary within our regions appears to be on a decadal scale which may point to large scale atmospheric circulation patterns such as ENSO controlling the precipitation and thus ET regimes rather than a fundamental change in the mechanics of the water cycle.

6.2 Future Research

In this thesis, the historic analysis documents the impacts of climate change and, in particular, increasing intensity of precipitation on hydrological processes. Although future projections indicate that the strong increase of extreme precipitation amount at the beginning of the 21st century is likely a reflection of a positive phase of natural decadal fluctuations superimposed to milder increases related to continuous climate changes, future projections are for mid-21st Century. It is still relatively uncertain to what extent these very heavy precipitation events will increase or fluctuate in the more near future which, as results have shown, is a dominate factor of change to the hydrology of the region. It is therefore recommended that the

relationship between temperature and various degrees of precipitation intensity be further studied on a regional basis. Comparing the amount of precipitation for various degrees of intensity to the temperatures at which they occur in the past, present, and future may provide insight as to the extent to which changes in extreme precipitation can be expected during continued warming.

The flood analysis conducted in the future projection study indicated a clear increase in the duration of flood events, and the majority of these events occur in years with anomalously high snow pack. Further analysis conducted in years to come should help to verify or disprove these projected characteristics and the link between them as major flood events account for a large proportion of climate-related damages in this region. In addition, a negligible trend in ET was found for the historic time period, but this is unlikely to remain the case in a warming world characterized by increasing intensification and atmospheric demand; also, contrary to prior work, there were no detectable changes in the seasonality of snow melt or peak discharge. Future projections suggest that these factors will change, but determining when and how these changes begin to manifest remains for future research.

Although the methodology developed in chapter 4 to incorporate remote sensing data into physically based hydrological models focuses solely on the Connecticut River Basin and the VIC model, it is applicable to other regions as well as other hydrological or land surface models. The concepts involved in the methodology are simple, easily adaptable, and resulted in clear statistically measureable improvements. Depending on the deficiencies any particular model may have in a particular region, the incorporation of remote sensing data could provide a variety of different kinds of improvements. Integration of remote sensing data into models is a promising area of study and should be subject to further examination and experimentation especially as more accurate and comprehensive data sets become available. Similar techniques could help to

better improve our understanding of climatic or hydrologic change and perhaps even improve upon our future predictions.

Lastly, the investigation of ET trends focuses on the NLDAS-2 domain due to the lack of high quality gridded meteorological forcing data elsewhere, but other regions, particularly in the southern hemisphere where the strongest changing terrestrial ET trend has been found, will likely reveal different relative importance of the various driving mechanisms. Also, under continued warming and intensification, it is possible that the impact of the precipitation intensity rather than simply precipitation amount may become a more dominant influence in the future. Therefore, future studies should be conducted as to how ET might change in the future in this NLDAS-2 domain as well as other regions of the world with different hydrological characteristics.

References:

Ahmed, K., Wang, G., Silander, J., Wilson, A. Allen, J., Horton, R., Anyah, R. 2013. Statistical downscaling and bias correction of climate model outputs for climate change impact assessment in the U.S. northeast. *Global and Planetary Change*, 100, 320-332.

Allan, R., Soden, B. 2008. Atmospheric Warming and Amplification of Precipitation Extremes. *Science*, 321, 1481-1484.

Anagnostou, E.N., V. Maggioni, E. Nikolopoulos, T. Taye, F. Hossain, 2010: Benchmarking High-resolution Global Satellite Rain Products to Radar and Rain gauge Rainfall Estimates, IEEE Transactions on Geosciences and Remote Sensing, Vol. 48, No 4, pp. 1667-1683.

Bjerklie, D., Trombley, T., Viger, R. 2011 Simulations of historical and future trends in snowfall and groundwater recharge for basins draining to Long Island Sound. *Earth Interactions*, 15, 1-35.

Bjerklie, D.M., Mullaney, J.R., Stone, J.R., Skinner, B.J., and Ramlow, M.A. 2012. Preliminary investigation of the effects of sea-level rise on groundwater levels in New Haven, Connecticut. U.S. Geological Survey Open-File Report 2012–1025, 46 p., at http://pubs.usgs.gov/of/2012/1025/.

Bonan, G. B., Oleson, K.W., Fisher, R.A., Lasslop, G., and Reichstein, M. 2012. Reconciling leaf physiological traits and canopy flux data: Use of the TRY and FLUXNET databases in the Community Land Model version 4. *Journal of Geophysical Research*, 117, G02026. DOI:10.1029/2011JG001913.

Bormann, Helge. 2011. Sensitivity analysis of 18 different potential evapotranspiration models to observed climatic change at German climate stations. *Climatic Change* 104.3-4, 729-753.

Cai, X., Yang, Z.L., Xia, Y., Huang, M., Wei, H., Leung, R., Ek, M. 2014. Assessment of simulated water balance from Noah, Noah-MP, CLM, and VIC over CONUS using the NLDAS test bed. Journal of Geophysical Research: Atmospheres, 10.1002/2014JD022113, 13751-13770.

Caya, D., Laprise R. 1999: A Semi-Implicit Semi-Lagrangian Regional Climate Model: The Canadian RCM. *Monthly Weather Review*, 127, 341-362.

Clay, C., Deininger, M., Hafner, Hafner, J. The Connecticut River Watershed: Conserving the Heart of New England. The Trust for Public Land, viii+56 pages.

Collins, M.J. 2009. Evidence for changing flood risk in New England since the late 20th century. *Journal of the American Water Resources Association*, 45, 279-290.

Connecticut River Watershed Council. Watershed facts. CRWC. Retrieved February 1, 2013 from http://www.ctriver.org/our_region_and_rivers/river_facts/index.html.

Dai, A., Fung, I., DelGenio, A. 1997. Surface observed global land precipitation variations during 1900-88, *Journal of Climate*, 10, 2943–2962.

Dai, A., Qian, T., Trenberth, K. 2009. Changes in continental freshwater discharge from 1948-2004. *Journal of Climate*, 22, 2773-2792.

Dorigo, W. A., Scipal, K., Parinussa, R. M., Liu, Y. Y., Wagner, W., de Jeu, R. A. M., and Naeimi, V. 2010. Error characterisation of global active and passive microwave soil moisture data sets. *Hydrology and Earth System Sciences*, 14, 2605-2616.

Douville, H., Ribes, A., Decharme, B., Alkama, R., Sheffield, J. 2012 Anthropogenic influence on multidecadal changes in reconstructed global evapotranspiration. *Nature Climate Change*, 3, 59-62.

Easterling, D., Meehl, G., Parmesan, C., Changnon, S., Karl, T., Mearns, L. Climate Extremes: Observations, Modeling, and Impacts. Science, 289, 2068-2074.

Eitzinger, J., Marinkovic, D., Hösch, J. 2002. Sensitivity of different evapotranspiration calculation methods in different crop-weather models. *Integrated Assessment and Decision Support, Proceedings of the First Biennial Meeting of the International Environmental Modelling and Software Society*. Vol. 1.

Fischer, J. Landflux.org: Remote Sensing of Ecosystem-Atmosphere, Carbon, Water & Energy Exchange. Retrieved May 15, 2012 from http://landflux.org/Data.php.

Fischer, J. and Tu, K, Baldocchi, D. 2008. Global estimates of the land-atmosphere water flux based on monthly AVHRR and ISLSCP-II data, validated at 16 FLUXNET sites. *Remote Sensing of Environment*, 112(3), 909-919.

Fisher, J., Malhi, Y., Bonal, D., DaRocha, H., De Araujo, A., Gamo, M., Hirano, G., et al. 2009. The land atmosphere water flux in the tropics. *Global Change Biology*, 15, 2694-2714.

Flato, G. M., cited 2012. The third generation Coupled Global Climate Model (CGCM3). Environment Canada Canadian Centre for Climate Modelling and Analysis. [Available online at www.ec.gc.ca /ccmac-cccma/default.asp?lang=En&n=1299529F-1.]

Ford, T., Quiring S. 2013. Influence of MODIS-Derived Dynamic Vegetation on VIC-Simulated Soil Moisture in Oklahoma. *Journal of Hydrometeorology*, 14, 1910-1921.

Franchini, M., Pacciani, M. 1991. Comparative analysis of several conceptual rainfall-runoff models. *Journal of Hydrology*, 122, 161-219.

Frich, P., Alexander, L.V., Della-Marta, P. Gleason, B., Haylock, M., Klein Tank, A.M.G. & Peterson, T. 2002. Observed coherent changes in climatic extremes during the second half of the twentieth century. *Climate Research*, 19,193-212.

Gao, H., Tang Q., Shi X., Zhu C., Bohn T., Su F., Sheffield, J., Pan, M., Lettenmaier, D., & Wood, E. 2009. *Water Budget Record from Variable Infiltration Capacity (VIC Model).* Seattle: University of Washington, 120-173.

GFDL Global Atmospheric Model Development Team, 2004. The new GFDL global atmospheric and land model AM2-LM2: Evaluation with prescribed SST simulations. *Journal of Climate*, 17, 4641–4673.

Global Soil Data Task. 2000. Global soil data products CD-ROM (IGBP-DIS). International GeosphereBiosphere Programme-Data and Information Available Services [Available online at http://www.daac.ornl.gov].

Gerten, D., Rost, S., von Bloh, W., Lucht, W. 2008. Causes of change in 20th century global river discharge. Geophysical Research Letters, 35, DOI: 10.1029/2008GL035258.

Giorgi, F., Marinucci, M.R., Bates, G.T. 1993a. Development of a second-generation regional climate model (RegCm2). Part I: Boundary-layer and radiative transfer processes. *Monthly Weather Review*, 121, 2794-2813.

Giorgi, F., Marinucci, M.R., de Canio, D., Bates, G.T. 1993b. Development of a second-generation regional climate model (RegCM2). Part II: Convective process and assimilation of lateral boundary conditions. *Monthly Weather Review*, 121, 2814-2832.

Groisman, P., Knight, R., Karl, T. 2001. Heavy Precipitation and High Streamflow in the Contiguous United States: Trends in the Twentieth Century. American Meteorological Society, 82, 219-246.

Groisman, P., Knight, R., Easterling, D., Karl, T., Hegerl, G., & Razuvaev, V. 2005. Trends in Intense Precipitation in the Climate Record. *Journal of Climate*, 18, 1326-1350.

Groisman, P., Knight, R., Karl, T., Easterling, D., Sun, B., Lawrimore, J. 2004. Contemporary Changes to the Hydrological Cycle over the Contiguous United States: Trends Derived from In Situ Observations. *American Meteorological Society*, 5, 64-85.

Hayhoe, K., Wake, C., Huntington, T. 2006. Past and future changes in climate and hydrological indicators in the US Northeast. *Climate Dynamics*, 28, 381–407.

Hodgkins G.A., Dudley, R.W., Huntington, T.G. 2003. Changes in the timing of high river flows in New England over the 20th Century. *Journal of Hydrology*, 278, 244-252.

Huntington, T. G. 2003. Climate warming could reduce runoff significantly in New England, USA. *Journal of Agricultural and Forest Meteorology*, 117, 193-201.

Huntington, T. G. 2006. Evidence for intensification of the global water cycle: Review and synthesis. *Journal of Hydrology*, 319, 83-95.

Huntington, T. G., Richardson, A.D., McGuire, K.J., & Hayhoe, K. 2009. Review: climate and hydrological changes in the northeastern United States: recent trends and implications for forested and aquatic ecosystems. *Canadian Journal of Forest Research*, 39, 199-212.

Immerzeel, W.W., Bold, P. 2008. Calibration of a distributed hydrological model based on satellite evapotranspiration. *Journal of Hydrology*, 349, 411-424.

Jimenez, C., et al. 2011. Global intercomparison of 12 land surface heat flux estimates, *Journal of Geophysical Research-Atmospheres*, 116, D02102, doi:10.1029/2010JD014545.

Jung, M., Reichstein M., Ciais, P., Seneviratne, S., Sheffield, J., et al. 2010. Recent decline in global land evapotranspiration trend due to limited moisture supply. *Nature*. 467, 951-954.

Karl, T.R., Melillo, J., & Peterson, R. D. (Eds.). 2009. *Global Climate Change Impacts in the United States*. Cambridge: Cambridge University Press.

Koren, V.I., Smith, M., Wang, D., Zhang, Z. 2000. Use of Soil Property Data in the Derivation of Conceptual Rainfall-Runoff Model Parameters Proceedings of the 15th Conference on Hydrology. AMS, Long Beach, CA, pp. 103–106.

Koster, R., Suarez, M. 1992. Modeling the Land Surface Boundary in Climate Models as a Composite of Independent Vegetation Stands. *Journal of Geophysical Research*, 97, 2697-2715.

Kite, G.W., Droogers, P. 2000. Comparing evapotranspiration estimates from satellites, hydrological models, and field data. *Journal of Hydrology*, 229, 3-18.

Labat, D., Godderis, Y., Probst, J., Guyot, J. 2004. Evidence for global runoff increase related to climate warming. *Advances in Water Resources,* 27, 631-642.

Lawrence, P.J., and Chase, T.N. 2007. Representing a MODIS consistent land surface in the Community Land Model (CLM 3.0). *Journal of Geophysical Research*, 112 : G01023. DOI:10.1029/2006JG000168.

LDAS Land Data Assimilation Systems. NASA: LDAS Retrieved October 1, 2011 from http://ldas.gsfc.nasa.gov/nldas/NLDAS2forcing.php.

Lettenmaier, D.P., Ford, D., Fisher, S.M., Hughes, J.P., Nijssen, B. 1996. Water management implications of global warming. 4. The Columbia River Basin. Report to Interstate Commission on the Potomac River Basin and Institute for Water Resources. US Army Corps of Engineers, University of Washington, Seattle, WA.

Lettenmaier, D. Variable infiltration capacity (VIC) macroscale hydrologic model. Retrieved August 1, 2011 from http://www.hydro.washington.edu/Lettenmaier/Models/VIC/.

Liang, X., D. P. Lettenmaier, E. F. Wood, and S. J. Burges, 1994: A Simple hydrologically Based Model of Land Surface Water and Energy Fluxes for GSMs, *Journal of Geophysical Research*, 99(D7), 14,415-14,428.

Liu, Y.Y., Dorigo, W. A., Parinussa, R.M., de Jeu, R.A.M., Wagner, W., McCabe, M.F., Evans, J.P. & van Dijk, A.I.J.M. 2012. Trend-preserving blending of passive and active microwave soil moisture retrievals. *Remote Sensing of the Environment*, 123, 280-297.

Lu, J., Sun, G., McNulty, S. G. and Amatya, D. M. 2005. A Comparison of Six Potential Evapotranspiration Methods for Regional Use in the Southeastern United States. JAWRA. *Journal of the American Water Resources Association*, 41, 621–633. doi: 10.1111/j.1752-1688.2005.tb03759.x

Maggioni, V., H. J. Vergara, E. N. Anagnostou, J. J. Gourley, Y. Hong, D. Stampoulis. 2013a. Investigating the Applicability of Error Correction Ensembles of Satellite Rainfall Products in River Flow Simulations, Journal of Hydrometeorology, doi: http://dx.doi.org/10.1175/JHM-D-12-074.1

Maggioni, V., R. Reichel, E.N. Anagnostou. 2013b. The Efficiency of Assimilating Satellite Soil Moisture Retrievals in a Land Data Assimilation System Using Different Rainfall Error Models, Journal of Hydrometeorology, Volume 14, Issue 1 (February 2013) pp. 368-374.

Manning R. 1891. On the flow of water in open channels and pipes. *Transactions of the Institution of Civil Engineers of Ireland*, 20, 161-207.

Mauer, E. Ed Maurer Home Page: Gridded Observed Meteorological Data. Retrieved September 1, 2011 from http://www.engr.scu.edu/~emaurer/data.shtml.

Marshall, E., Randhir, T. 2008. Effect of climate change on watershed system: a regional analysis. *Climate Change*, 89, 263-280.

McVicar, T. R. et al. 2012. Global review and synthesis of trends in observed terrestrial near-surface wind speeds: Implications for evaporation. *Journal of Hydrology*, 416-417, 182-205.

Mearns, L., Arritt, R., Biner, S., Bukovsky, M., McGinnis, S., Sain, S., Caya, D., Correia Jr., J., Flory, D., Gutowski, W., Takle, E., Jones, R., Leung, R., Moufouma-Okia, W., McDaniel, L., Nunes, A., Qian, Y., Roads, J., Sloan, L., and Snyder, M. 2012. The North American Regional Climate Change Assessment Program: Overview of Phase I Results. *Bulletin of the American Meteorological Society*, 93, 1337–1362.

Melillo, J. M., Terese (T.C.) Richmond, and Gary W. Yohe, Eds., 2014: Climate Change Impacts in the United States: The Third National Climate Assessment. U.S. Global Change Research Program, 841 pp. doi:10.7930/J0Z31WJ2.

McKenney, Mary S., and Norman J. Rosenberg. 1993. Sensitivity of some potential evapotranspiration estimation methods to climate change. *Agricultural and Forest Meteorology*, 64.1, 81-110.

Miralles, D., van den Berg, M., Gash, J., Parinussa, R., de Jeu, R., Beck, H., Holmes, T., Jimenez, C., Verhoest, N., Dorigo, W., Teuling, A., Dolman, J. 2013. El Nino-La Nina cycle and recent trends in continental evaporation. *Nature Climate Change*, 4, 122-126.

Mishra, V., Dominguez, F., Lettenmaier, D. 2013. Urban precipitation extremes: How reliable are regional climate models? Geophysical Research Letters, Vol 39, L03407, doi:10.1029/2011GL050658.

Mu, Q., Heinsch, F., Zhao, M., Running, S. 2007. Development of a global evapotranspiration algorithm based on MODIS and global meteorology data. *Remote Sensing of the Environment*, 111, 519-536.

Mueller, B., Hirschi, M., Jimenez, C., Ciais, P., Dirmeyer, P., Dolman, A., Fisher, J., Jung, M., Ludwig, F., Maignan, F., Miralles, D., McCabe, M., Reichstein, M., Sheffield, J., Wang, K., Wood, E., Zhang, Y., Seneviratne, S. 2013. Benchmark products for land evapotranspiration: LandFlux-EVAL multi-data set synthesis. *Hydrology and Earth System Sciences*, 17, 3707-3720.

Naeimi, V., Scipal, K., Bartalis, Z., Hasenauer, S., and Wagner, W. 2009. An Improved Soil Moisture Retrieval Algorithm for ERS and METOP Scatterometer Observations. *IEEE Transactions, Geoscience Remote Sensing*, 47, 1999-2013.

Nohara, D., Kitoh, A., Masahiro, H., Oki, T. 2006. Impact of Climate Change on River Discharge Projected by Multimodel Ensemble. *Journal of Hydrometeorology*, 7, 1076-1089.

National Oceanic and Atmospheric Administration. Advanced Hydrologic Prediction Service hydrographs. Retrieved September 12, 2013 from http://water.weather.gov/ahps2/hydrograph.php?wfo=box&gage=tmvc3&hydro_type=2.

Oleson, K.W., D.M. Lawrence, G.B. Bonan, B. Drewniak, M. Huang, C.D. Koven, S. Levis, F. Li, W.J. Riley, Z.M. Subin, S.C. Swenson, P.E. Thornton, A. Bozbiyik, R. Fisher, E. Kluzek, J.-F. Lamarque, P.J. Lawrence, L.R. Leung, W. Lipscomb, S. Muszala, D.M. Ricciuto, W. Sacks, Y. Sun, J. Tang, Z.-L. Yang. 2013. Technical Description of version 4.5 of the Community Land Model (CLM). Ncar Technical Note NCAR/TN-503+STR, National Center for Atmospheric Research, Boulder, CO, 422 pp, DOI: 10.5065/D6RR1W7M.

Pal, J.S., Small, E.E., Eltahir, A.B. 2000. Simulation of regional-scale water and energy budgets: Representation of subgrid could and precipitation processes within RegCM. *Journal of Geophysical Research*, 105 (D24), 29 579 - 29 594.

Pal, J.S., and Coauthors. 2007. Regional climate modeling for the developing world: The ICTP RegCM3 and RegCNET, *Bulletin of American Meteorological Society*, 88, 1395-1409.

Parr DT, Wang GL. 2014. Hydrological Changes in the U.S. Northeast Using the Connecticut River Basin as a Case Study: Part 1. Modeling and Analysis of the Past. *Global and Planetary Change*, 122, 208-222.

Parr DT, Wang GL, Ahmed, KF. 2015a. Hydrological changes in the U.S. Northeast using the Connecticut River Basin as a case study: Part 2. Projections of the Future. *Global and Planetary Change*, doi:10.1016/j.gloplacha.2015.08.011.

Parr DT, Wang GL., Bjerklie, D. 2015b. Integrating Remote Sensing Data on Evapotranspiration and Leaf Area Index with Hydrological Modeling: Impacts on Model Performance and Future Predictions. *Journal of Hydrometeorology*, doi: http://dx.doi.org/10.1175/JHM-D-15-0009.1

Oki, T., Kanae, S. 2006. Global Hydrological Cycles and World Water Resources. *Science*, 313, 1068-1072.

Park, D., Markus, M. 2014. Analysis of a changing hydrologic flood regime using the Variable Infiltration Capacity model. *Journal of Hydrology*, 515, 267-280.

Renard, B., Kavetski, D., Kuczera, G., Thyer, M., Franks, S. 2010. Understanding predictive uncertainty in hydrologic modeling. The challenge of identifying input and structural errors. *Water Resources Research*, 46, W05521, doi:10.1029/2009WR008328.

Reynolds, C.A., Jackson, T.J., Rawls, W.J. 1990. Estimated available water content from the FAO soil map of the world, global soil profile databases, pedo-transfer functions. USDA Agricultural Research Service: NOAA National Geophysical Data Center Boulder, CO. Retrieved February 6, 2013 from http://www.ngdc.noaa.gov/sef/fliers/se02006.shtml.

Scinocca, J.F., McFarlane, N.A. 2004. The variability of modeled tropical precipitation. Journal of Atmospheric Science, 61, 1993-2015.

Shaw, S. B., Royem, A.A., Riha, S. J. 2011. The relationship between extreme hourly precipitation and surface temperature in different hydroclimatic regions of the United States. *Journal of Hydrometeorology*, 12, 319-325.

Sheffield, J., Wood, E. 2007. Characteristics of global and regional drought, 1950-2000: Analysis of soil moisture data from off-line simulation of the terrestrial hydrological cycle. *Journal of Geophysical Research: Atmospheres*, 112, D17115.

Sheffield, J., Wood, E. 2008. Global trends and variability in soil moisture and drought characteristics, 1950-2000, from observation-driven simulations of the terrestrial hydrologic cycle. *Journal of Climate*, 21, 432-458.

Sheffield, J., Wood, E. 2008. Projected changes in drought occurrence under future global warming from multi-model, multi-scenario, IPCC AR4 simulations. *Climate Dynamics*, 31, 79-105.

Sheffield, J., Livneh, B., Wood, E. 2012. Representation of terrestrial hydrology and large-scale drought of the continental U.S. from the North American regional reanalysis. *Journal of Hydrometeorology*, 13, 856-876.

Shi, X., Mao, J., Thornton, P., Huang, M. 2013. Spatiotemporal patterns of evapotranspiration in response to multiple environmental factors simulated by the Community Land Model. *Environmental Research Letters*, 8, doi:10.1088/1748-9326/8/2/024012.

Singh, D., Tsiang, M., Rajaratnam, B., Diffenbaugh, N. 2013. Precipitation extremes over the continental United States in a transient, high resolution, ensemble climate model experiment. *Journal of Geophysical Research: Atmospheres*, 118, 7063-7086.

Song, Y., Ryu, Y., Jeon, S. 2014. Interannual variability of regional evapotranspiration under precipitation extremes: A case study of the Youngsan River basin in Korea. *Journal of Hydrology*, 519, 3531-3540.

Stampoulis, D., E.N. Anagnostou, 2012: Evaluation of Global Satellite Rainfall Products over Continental Europe, Journal of Hydrometeorology, Volume 13, Issue 2, pp. 588-603.

Tang, Q, T., Vivoni, E., Munoz-Arriola, F., Lettenmaier, D. 2012. Predictability of Evapotranspiration Patterns Using Remotely Sensed Vegetation Dynamics during the North American Monsoon. *Journal of Hydrometeorology*, 13, 103-121.

Tebaldi, C., Hayhoe, K., Arblaster, J., & Meehl, G. 2006 Going to the Extremes. *Climatic Change*, 79, 185-211.

Teuling, A.J., Hirschi, M., Ohmura, A., Wild, M., Reichstein, M., Ciais, P., Buchmann, N., Ammann, C., Montagnani, L., Richardson, A.D., Wohlfahrt, G., Seneviratne, S. 2009. A Regional perspective on trends in continental evaporation. *Geophysical Research Letters*. L02404, doi:10.1029/2008GL036584

Trenberth, K. (1999). Conceptual Framework for Changes of Extremes of the Hydrologic Cycle with Climate Change. *Climate Change*, 42, 327-339.

Trenberth, K., Dai, A., Rasmsussen, R., Parsons, D. 2003. The Changing Character of Precipitation. *American Meteorology Society*, 84, 1205-1217.

Trenberth, K., Smith, L., Qian, T., Dai, A., Fasullo, J. 2006. Estimates of the Global Water Budget and its Annual Cycle Using Observational and Model Data. *Journal of Hydrometeorology*, 8, 758-769.

Trambauer, P., et al. 2014. Comparison of different evaporation estimates over the African continent. *Hydrology and Earth System Sciences,* 18.1, 193-212.

USGS. *HYDRO1k Documentation – USGS Planetary GIS Web Server – PIGWAD*. Retrieved September 30, 2011 from Earth Resources Observation and Science (EROS) Center from http://eros.usgs.gov.

USGS. USGS Water Data for the Nation. Retrieved January 30, 2012 from USGS Surface-Water Monthly Statistics for Connecticut from http://waterdata.usgs.gov/ct/nwis.

Utsumi, N., Seto, S., Kanae, S., Maeda, E., Oki, T. 2011. Does higher surface temperature intensify extreme precipitation? Geophysical Research Letters, 38, L16708, doi:10.1029/2011GL048426.

Vano, J., Das, T., Lettenmaier, D. 2012. Hydrologic sensitivities of Colorado River runoff to changes in precipitation and temperature. *Journal of Hydrometeorology*, 13, 932-949.

Vano, J., Das, T., Lettenmaier, D. 2014. A sensitivity-based approach to evaluating future changes in Colorado River discharge. *Journal of Climatic Change*, 122, 621-634.

Vautard, R., Cattiaux, J., Yiou, P., Thépaut, J.-N. and Ciais, P. 2011. Northern Hemisphere atmospheric stilling partly attributed to an increase in surface roughness. *Nature Geoscience*, 3, 756-761.

Vinukollu, R., Wood, E., Ferguson, C., Fisher, J. 2011. Global estimates of evapotranspiration for climate studies using multi-sensor remote sensing data: Evaluation of three process-based approaches. *Remote Sensing of Environment*, 155, 801-823.

Verdin, K. L., and S. K. Greenlee. 1996. Development of continental scale digital elevation models and extraction of hydrographic features, paper presented at the Third International Conference/Workshop on Integrating GIS and Environmental Modeling, Santa Fe, New Mexico, 21–26 January, Natl. Cent. for Geogr. Inf. and Anal., Santa Barbara, California.

Wagner, W., Dorigo, W. de Jeu, R., Fernandez, D., Benveniste, J., Haas, E., Ert, M. 2012. Fusion of active and passive microwave observations to create an essential climate variable data record on soil moisture. *Remote Sensing and Spatial Information Sciences*, 1-7, XXII ISPRS Congress. Melbourne: Australia.

Wake, C. P., Markham, A. 2005. Indicators of climate change in the Northeast 2005. *Clean Air—Cool Planet.* The Climate Change Research Center, University of New Hampshire, Portsmouth, NH. Retrieved February 16, 2013 at http://www.tribesandclimatechange.org/documents/nau/res_NortheastCCIndicators2005.pdf.

Walter T., Wilks, D., Parlange, J., Schneider, R. 2004. Increasing Evapotranspiration from the Conterminous United States. *Journal of Hydrometeorology*, 5, 405-408.

Wang, K., Dickinson, R., Wild, M., Liang, S. 2010. Evidence for decadal variation in global terrestrial evapotranspiration between 1982 and 2002: 2. Results. *Journal of Geophysical Research*, 115, D20113, doi:10.1029/2010JD013847.

Wattenbach, M., Franz, D., Liang, W., Schmidt, M., Seitz, F., Guntner, A. 2012. Integration of MODIS LAI products into the hydrological model WGHM indicate the sensitivity of

total water storage simulations to vegetation cover dynamics. *Geophysical Research Abstracts,* 14, EGU2012-10116.

Weiß, M. and Menzel, L. 2008. A global comparison of four potential evapotranspiration equations and their relevance to stream flow modelling in semi-arid environments, Adv. Geosci., 18, 15-23, doi:10.5194/adgeo-18-15-2008.

Wittenberg, A.; Rosati, Anthony; Lau, Ngar-Cheung; Ploshay, Jeffrey J. (2006). GFDL's CM2 global coupled climate models – Part 3: Tropical Pacific Climate and ENSO. *Journal of Climate*, 19 (5): 698–722.

Wood AW, Maurer EP, Kumar A, Lettenmaier DP. 2002. Long-range experimental hydrologic forecasting for the eastern United States. Journal of Geophysical Research, 107:Art. No. 4429.

Wood A, Leung LR, Sridhar V, Lettenmaier DP. 2004. Hydrological implications of dynamical and statistical approaches to downscaling climate model surface temperature and precipitation fields. *Climatic Change,* 62, 189-216.

Xia, Y., Mitchell, K., Ek, M., Sheffield, J., Cosgrove, B., Wood, E., Luo, L., Alonge, C., Wei, H., Meng, J., Livneh, B., Lettenmaier, D., Koren, V., Duan, Q., Mo, K., Fan, Y., Mocko, D. 2012a. Continental-scale water and energy flux analysis and validation for the North American Land Data Assimilation System project phase 2 (NLDAS-2): 1. Intercomparison and application of model products. *Climate and Dynamics*, 117, DOI: 10.1029/2011JD016048.

Xia, Y., Mitchell, K., Ek, M., Sheffield, J., Cosgrove, B., Luo, L., Alonge, C., Wei, H., Meng, J., Livneh, B., Duan, Q., Lohman, D.. 2012b. Continental-scale water and energy flux analysis and validation for the North American Land Data Assimilation System project

phase 2 (NLDAS-2): 2. Validation of model-simulated streamflow. *Journal of Geophysical Research*, 117, DOI: 10.1029/2011JD016051.

Xia, Y., et al. 2012c. NCEP/EMC (03.01.2012), *NLDAS Noah Land Surface Model L4 Hourly 0.125 x 0.125 degree,version 002*, Edited by David Mocko, NASA/GSFC/HSL., Greenbelt, Maryland, USA:Goddard Earth Sciences Data and Information Services Center (GES DISC), Accessed November 1, 2014 at doi:10.5067/47Z13FNQODKV

Xia, Y., Ek, M., Wei, H. 2012. Comparative analysis of relationships between NLDAS-2 forcings and model outputs. *Hydrological Processes*, 26, 467-474.

Xia, Y., Hobbins, M., Mu, Q., Ek, M. 2014. Evaluation of NLDAS-2 evapotranspiration against tower flux site observations. *Hydrological Processes*, DOI: 10.1002/hyp.10299.

Zhang, XJ, Tang, Q., Pan, M., Tang, Y. 2014. A Long-Term Land Surface Hydrologic Fluxes and States Dataset for China. *Journal of Hydrometeorology*, doi: 10.1175/JHM-D-13-0170.1.

Zhang, Y.Q., Viney, N.R., Chiew, F.H.S., van Dijk, A.I.J.M., Liu, Y.Y. 2011. 2011. Improving hydrological and vegetation modelling using regional calibration schemes together with remote sensing data. 19th International Congress on Modelling and Simulation, Perth, Australia, 12–16 December 2011. http://mssanz.org.au/modsim2011

Zhou, S., Liang, X., Chen, J., Gong, P. 2004. An assessment of the VIC-3L hydrologic model for the Yangtze River basin based on remote sensing: a case study of the Baohe River Basin. *Canadian Journal of Remote Sensing*, 30, 840-853.

Zhou, Y., Zhang, Y., Vaze, J., Lane, Patrick, Xu, S. 2013. Improving runoff estimates using remote sensing vegetation data for bushfire impacted catchments. *Agricultural and Forest Meteorology*, 182-183, 332-341.